ISTANBUL TECHNICAL UNIVERSITY ★ GRADUATE SCHOOL

SYNTHESIS OF BORON CONTAINING PHTHALOCYANINES

PhD THESIS

Nilgün ÖZGÜR

Department of Chemistry

Chemistry Programme

APRIL 2021

ISTANBUL TECHNICAL UNIVERSITY ★ GRADUATE SCHOOL

SYNTHESIS OF BORON CONTAINING PHTHALOCYANINES

PhD THESIS

Nilgün ÖZGÜR
(509122006)

Department of Chemistry

Chemistry Programme

Thesis Advisor: Prof. Dr. Esin HAMURYUDAN

APRIL 2021

ISTANBUL TEKNİK ÜNİVERSİTESİ ★ LİSANSÜSTÜ EĞİTİM ENSTİTÜSÜ

BOR İÇEREN FTALOSİYANİNLERİN SENTEZİ

DOKTORA TEZİ

Nilgün ÖZGÜR
(509122006)

Kimya Anabilim Dalı

Kimya Programı

Tez Danışmanı: Prof. Dr. Esin HAMURYUDAN

NİSAN 2021

Nilgün Özgür, a Ph.D. student of ITU Graduate School student ID 509122006, successfully defended the thesis entitled "SYNTHESIS OF BORON CONTAINING PHTHALOCYANINES", which she prepared after fulfilling the requirements specified in the associated legislations, before the jury whose signatures are below.

Thesis Advisor : **Prof. Dr. Esin HAMURYUDAN**
İstanbul Technical University

Jury Members : **Prof. Dr. Ahmet GÜL**
Istanbul Technical University

Prof. Dr. Zehra BAYIR
Istanbul Technical University

Prof. Dr. Sabiha MANAV YALÇIN
Yıldız Technical University

Prof. Dr. Yasemin KURT
Istanbul University

Date of Submission : 06 March 2021
Date of Defense : 21 April 2021

To my family,

FOREWORD

Firstly, I would like to express my greatest gratitude to my supervisor Prof. Dr. Esin HAMURYUDAN, for her continuous encouragement, support and help during the course of my work, and the preparation of my thesis.

My thesis committee guided me through all these years. I give great thanks to the members of Ph.D. examining committee, Prof. Dr. Ahmet GÜL for his support, guidance and valuable suggestions and Prof. Dr. Sabiha MANAV YALÇIN, for their time and deliberative consideration of this work.

Besides, I owe a debt of gratitude to the Chemistry Department staff for their kind guidance during the experiments and measurement of the samples and want to express my deep gratitude to those. My deep appreciation goes out to Dr. Ilgın NAR. His excellent support has made an invaluable contribution to my Ph.D. I am also grateful to Dr. Hande R. PEKBELGİN KARAOĞLU and Dr. Armağan ATSAY for their friendship and the warmth they extended to me during my time at ITU.

Last but not least, I thank my family for their confidence and support. They have continuously taken interest in my goals, supported them, and made sure I achieved them to my fullest potential. They have always been there for me, no matter what, and I know they always will.

April 2021

Nilgün ÖZGÜR
(M.Sc. Chemist)

TABLE OF CONTENTS

Page

ABBREVIATIONS

δ	**:** Chemical shift
br	**:** Broad
^{11}B NMR	**:** Boron 11 nuclear magnetic resonance
$BF_3.OEt_2$	**:** Boron trifluoride dietherate
BNCT	**:** Boron neutron capture therapy
CsCl	**:** Cesium chloride
d	**:** Doublet
DBU	**:** 1,8-diazabicyclo[5.4.0]-undec-7-ene
DHB	**:** 2,5-Dihydroxybenzoic acid
DMF	**:** Dimethylformamide
DMSO	**:** Dimethylsulfoxide
DPBF	**:** 1,3-diphenylisobenzofuran
^{1}H NMR	**:** Proton nuclear magnetic resonance
KOH	**:** Potassium hydroxide
MALDI	**:** Matrix assisted laser desorption/ionization
MeOH	**:** Methanol
MPc	**:** Metallophthalocyanine
MS	**:** Mass spectrometry
m/z	**:** Mass to charge ratio
N_2	**:** Nitrogen
NaOH	**:** Sodium hydroxide
Pc	**:** Phthalocyanine
PDT	**:** Photodynamic therapy
ppm	**:** parts per million
s	**:** Singlet
t	**:** Triplet
THF	**:** Tetrahydrofuran

LIST OF TABLES

Page

LIST OF FIGURES

Page

SYNTHESIS OF BORON CONTAINING PHTHALOCYANINES

SUMMARY

Phthalocyanines, which is a kind of tetrapyrrole derivatives, constitute one of the important topics for both basic science and applied studies in recent years. 2-dimensional π-electron delocalization on phthalocyanines causes a large increase in their rare physical properties, resulting in many different applications from industry (batteries, inks) to medicine (BNCT, PDT). In recent years, the use of asymmetric or low-symmetry phthalocyanines, which are named in this way due to the difference of the substituted groups in the peripheral and non- peripheral position, in areas such as nonlinear optics (NLO), PDT, BNCT has led to intense research on this subject.

The lack of solubility of Pcs without substituents in common solvents prevents the investigation of the properties of them and their use for different applications. Therefore, the most important goal of research has been to obtain soluble products.

Phthalocyanines (Pc) and their metal complexes (MPc) can be readily modified by adding metal atoms to the central space and various groups on the peripheral and nonperipheral positions. Thus, they offer a wide range of uses from molecular science to medicine. The low solubility of phthalocyanine derivatives in water makes the purification and characterization stages difficult and provides disadvantages in biological applications. The inability of phthalacyanins to show high affinity to tumor cells due to their lipophilic properties necessitates the synthesis of their water-soluble derivatives.

Although many procedures were discovered for the preparation of symmetric substituted Pcs, a few procedures can be used to synthesize asymmetric Pcs. These methods also differ according to the type of product targeted for synthesis. For the synthesis of A_3B type asymmetric phthalocyanine containing two different substituents, the most applicable method is the cyclotetramerization of the starting materials containing these substituents. The most important problem in this procedure is the difficulty in separating the targeted Pcs from the isomer mixture that has exactly similar physicochemical properties. Although the widely used statistical condensation method is not a selective synthesis method for the target Pc, the yield of the desired asymmetric compound can be increased with the proportional change of the starting materials.

BNCT, developed by taking advantage of boron properties, is a two parts cancer treatment method. The first of these parts is the stable boron isotope (^{10}B) accumulating in tumor cells and the second is the low-energy neutron source. In this treatment method, non-radioactive ^{10}B atoms are bombarded with thermal neutrons to form a high-energy α particle and an ^{11}B isotope that breaks down into lithium ion. Research on BNCT has shown that high boron-containing compounds selectively accumulate in tumor cells, so the focus has been on the synthesis of these agents. Carboranes are rich in boron atoms as well as their characteristic features, which allows them to be used in BNCT applications.

Compounds in which polyhedral boron structures are covalently bonded to metal phthalocyanines are potential products that can be used in areas such as PDT and BNCT. While examples of porphyrins containing polyhedral boron are frequently encountered in the literature, phthalocyanine derivatives are limited to a small number of examples. Generally, two methods are used in the preparation of carborane containing phthalocyanines. In the first method, after the phthalocyanine synthesis is completed, the carborane unit is attached to the structure, while in the second method, phthalocyanine synthesis is carried out based on the phthalonitrile derivative containing carborane.

Within the scope of this thesis, it is aimed to investigate the synthesis, characterization, and properties of carborane groups that have the potential to be used in BNCT and asymmetrical phthalocyanines substituted with groups that provide solubility and interaction with target cells.

The studies consist of four parts. The first part covers the synthesis of phthalonitrile derivatives and carborane derivatives as starting materials, while the second part covers the synthesis of new unsymmetrical metal-free and metallophthalocyanines with an A_3B-type structure as a result of cyclotetramerization of dinitrile derivatives by statistical condensation method. The third part includes the preparation of phthalocyanine derivatives functionalized with carborane and metallocarborane groups and in the last part, electrochemical studies of some selected compounds are displayed.

In the first part, phthalonitriles which are starting molecules in the synthesis of the targeted phthalocyanine compounds are 4,5 di(hexylthio) phthalonitrile (**1**), 4 - [(2-hydroxyethyl) thio] phthalonitrile (**2**), 4- [3- (diethylamino) phenoxy] phthalonitrile (**3**) and cobaltocarborane compound which is a metallocarborane derivative with oxonium functional group was synthesized, and their structures were defined by spectrometric techniques and elemental analysis.

In the second part, for the synthesis of unsymmetrical metal-free and metallo phthalocyanine derivatives, it was firstly started with the synthesis of two A_3B type hexylthio-hydroxyethylthio (**7**) and diethylaminophenoxy-hydroxyethylthio substituted (**10**) unsymmetrical metal-free phthalocyanines, continued with multi-step reaction sequences and the structures were elucidated with spectroscopic methods. In the preparation of unsymmetrical metal-free Pc **7**, primarily dilithium phthalocyanine was prepared by lithium template cyclotetramerization of hexylthio and hydroxyethylthio substituted phthalonitriles. After that, dilithium phthalocyanine was acidified with acetic acid to transform into metal-free phthalocyanine Pc **7**. Column chromatography was used for the isolation of the product in 26% yield. Metallo phthalocyanine Pc **8** was prepared by refluxing Pc **7** in 1-pentanol with zinc(II) acetate under N_2 atmosphere (94% yield). Newly synthesized phthalocyanine derivatives Pc **7** and Pc **8** were characterized by their spectral data and elemental analysis. Also, aggregation behavior of Pc **7** and Pc **8** was analyzed at different concentrations in chloroform. According to these results, Pc **7** and Pc **8** have monomeric structure and obey the Beer-Lambert law in this concentration range.

Similarly, Pc **10** was prepared by cyclotetramerization of diethylaminophenoxy substituted phthalonitrile and hydroxyethylthio substituted phthalonitrile in 1-pentanol. Pc **11** was obtained by refluxing Pc **10** in dry pentanol with Zinc(II) acetate under N_2 atmosphere. As a result, Pc **10** and Pc **11** were obtained in 21% and 89% yield, respectively.

Steglich esterification is a general method of preparation of ester functional group under very mild conditions. By using this method, esterification of Pc **9** and Pc **13** was achieved by reacting the 4-pentynoic acid with Pc **8** and Pc **11** in the presence of DCC and DMAP. The urea derivatives formed during the reaction were easily removed by precipitation and column chromatography. Pc **9** and Pc **13** were obtained in 60% and 67% yield, respectively.

Different methodologies to synthesize carborane containing phthalocyanines have been reported. One of them is the decaborane insertion to alkynyl units of the phthalocyanine derivatives. Therefore, Pc **12** including terminal alkynyl group was obtained from the reaction of propargyl bromide and Pc **11** with NaH in toluene. The purity of the Pc **12** was verified by spectroscopic and elemental analyses.

In the third part, phthalocyanine derivatives **14** and **15** were synthesized by covalently linking the carborane units to unsymmetrically alkynyl substituted phthalocyanine complexes. Decaborane insertion to Pc **14** was carried out by reaction of Pc **9** and decaborane in a mixture of dry C_2H_3N and dry C_7H_8. By using the same method, Pc **15** containing mono *o*-carboranyl unit was prepared in 68% yield. Characterization of the products was carried out by elemental and spectral analysis, and mass spectroscopy. Spectral analyses for novel phthalocyanines were compatible with the targeted structures.

One of the most important necessity for BNCT agents is the water solubility of the synthesized compounds. For this purpose, tricationic water soluble Pc **16** was obtained by quaternarization of diethylamino substituted Pc **15**. The reaction was carried out by heating Pc **15** with methyl iodide for 2 days in chloroform at 50 ° C in 84% yield. The characterization and purity of the resulting water-soluble compound has been demonstrated by techniques including ^{1}H NMR, ^{11}B NMR and UV-Vis.

In addition, in this part, molecules bearing the "cobaltocarborane" group, which have similar properties to carborane but allow more boron atoms to be loaded in a single molecule, were also synthesized. Cobaltacarborane functionalized metallophthalocyanine complexes Pc **17** and Pc **18** were prepared from Pc **8** and Pc **11.** In these reactions, hydroxyl groups in Pc **8** and Pc **11** attacked to the oxonium units of cobalt bis(dicarbollide). A_3B-type Pc **17** and Pc **18** were purified by using DCM as mobile phase with 52% and 73% yields, respectively.

Electrochemistry provides important information on the redox behavior of phthalocyanine and carborane compounds. Lastly, the electrochemical properties of newly synthesized unsymmetrical phthalocyanine **8, 9, 14** and **17** were reported. The reduction and oxidation potentials of phthalocyanine complexes were studied by CV and SWV in dichloromethane using TBAP as supporting electrolyte system and platinum working electrode.

Consequently, within the scope of this doctoral thesis, the synthesis, characterization and research of the electrochemical features of phthalocyanine derivatives containing the substituent groups that provide both interaction with target cells and solubility in organic solvents and water and carborane units required for BNCT were carried out.

BOR İÇEREN FTALOSİYANİNLERİN SENTEZİ

ÖZET

Bir çeşit tetrapirol türevi olan ftalosiyaninler, son yıllarda hem temel bilimler hem de uygulamalı çalışmalar için önemli konulardan birini oluşturmaktadır. Ftalosiyaninler üzerindeki 2-boyutlu π-elektron delokalizasyonu ve ender fiziksel özellikleri sayesinde endüstriden (piller, boyalar) tıbba (BNCT, PDT) kadar bir çok farklı uygulama ile karşımıza çıkmaktadır. Son yıllarda periferik ve non-periferik konumlarda sübstitüe edilmiş grupların farklılığından dolayı asimetrik veya düşük simetrili ftalosiyaninler olarak isimlendirilen ftalosiyanin türevlerinin lineer olmayan optik (NLO), PDT, BNCT gibi alanlarda yoğun araştırmalara yol açmıştır.

Sübstitüent içermeyen ftalosiyaninlerin yaygın olarak kullanılan çözücülerde çözünürlüğünün düşük olması, bu bileşiklerin özelliklerinin incelenmesini ve farklı uygulama alanlarında kullanılmalarını engellemektedir. Bu nedenle araştırmaların en önemli hedefi çözünür ürünler elde etmek olmuştur.

Ftalosiyaninler (Pc) ve bunların metal kompleksleri (MPc), merkez boşluğa farklı metal iyonlarının, periferal ve non-periferal pozisyonlara ise çeşitli sübstitüentlerin eklenmesiyle kolayca modifiye edilebilirler. Böylece, moleküler bilimden tıbba kadar geniş bir kullanım alanı sunmaktadırlar. Ftalosiyanin türevlerinin sudaki çözünürlüklerinin düşük olması saflaştırma ve karakterizasyon aşamalarını zorlaştırırken biyolojik uygulamalarda da dezavantaj sağlamaktadır. Lipofilik özellikleri nedeniyle ftalasiyaninlerin tümörlü hücreye yüksek afinite gösterememesi suda çözünür türevlerinin sentezini zorunlu kılmaktadır.

Simetrik sübstitüe ftalosiyaninlerin hazırlanması için bir çok prosedür keşfedilmiş olmasına rağmen, asimetrik ftalosiyaninlerin sentezi için bir kaç yöntem uygulanabilmektedir. Bu sentez metotları sentezi amaçlanan ürün türüne göre de farklılaşmaktadır. A_3B tipi düşük simetrili ftalosiyanin eldesi için en uygulanabilir metot bu sübstitüentleri içeren başlangıç moleküllerinin siklotetramerisasyonudur. Bu metottaki en önemli sorun, hedeflenen ftalosiyaninlerin tamamen benzer fizikokimyasal özelliklere sahip izomer karışımından ayrılmasındaki zorluktur. Yaygın olarak kullanılan istatistiksel kondenzasyon yöntemi hedef ftalosiyanin için seçici bir sentez yöntemi olmamasına rağmen, istenen asimetrik bileşiğin verimi başlangıç maddelerinin orantılı değişimi ile arttırılabilir.

Borun özelliklerinden yararlanılarak geliştirilen bor nötron yakalama terapisi (BNCT) iki bileşenli bir kanser tedavi yöntemidir. Bu bileşenlerden birincisi tümör hücrelerinde biriken kararlı bor izotopu (^{10}B) ikincisi ise düşük enerjili nötron kaynağıdır. Bu tedavi yönteminde radyoaktif özellik göstermeyen ^{10}B atomu termal nötron ile bombardıman edilerek yüksek enerjili α parçacığı ve lityum iyonuna parçalanan ^{11}B izotopu oluşturulmaktadır. BNCT hakkında yapılan çalışmalar fazla miktarda bor içeren moleküllerin kanser hücrelerinde seçici olarak biriktiğini gösterdiğinden bu özellikteki ajanların sentezi üzerinde odaklanmıştır. Karboranlar,

BNCT uygulamalarında kullanılmalarına olanak sağlayan yüksek termal ve kimyasal kararlılıklarının yanı sıra bor atomları bakımından da zengindir.

Polihedral bor kafes yapılarının metalli ftalosiyaninlere kovalent bağlarla bağlı olduğu bileşikler fotodinamik terapi (PDT) ve bor nötron yakalama terapisi (BNCT) gibi alanlarda kullanılabilecek potansiyel ürünlerdir. Polihedral bor içeren porfirin örneklerine literatürde sıklıkla rastlanırken ftalosiyanin türevleri az sayıda örnekle sınırlıdır. Karboran sübstitüe ftalosiyanin sentezinde genellikle iki yöntem kullanılmaktadır. Birinci yöntemde ftalosiyanin sentezi tamamlandıktan sonra karboran ünitesi yapıya bağlanırken, ikinci yöntemde ise karboran içeren ftalonitril türevinden yola çıkılarak ftalosiyanin sentezi gerçekleştirilmektedir.

Bu tez kapsamında BNCT'de kullanılma potansiyeline sahip karboran grupları ile çözünürlüğü ve hedef hücrelerle etkileşimi sağlayan gruplarla sübstitüe edilmiş simetrik olmayan ftalosiyaninlerin sentezi, karakterizasyonu ve özelliklerinin incelenmesi amaçlanmıştır.

Yapılan çalışmalar dört kısımdan oluşmaktadır. Birinci kısım başlangıç maddeleri olarak kullanılacak ftalonitril türevleri ve karboran türevlerinin sentezini, ikinci kısım dinitril türevlerinin istatistiksel kondenzasyon yöntemi ile siklotetramerizasyonu sonucu A_3B yapısındaki simetrik olmayan yeni metalli ve metalsiz ftalosiyaninlerin sentezini içermektedir. Üçüncü kısım da, karboran ve metallokarboran grupları ile fonksiyonlaştırılmış türevlerinin hazırlanması son aşamada ise seçilen bazı bileşiklerin elektrokimyasal çalışmaları gösterilmiştir.

İlk kısımda hedeflenen ftalosiyanin bileşiklerinin sentezinde başlangıç maddesi olarak kullanılacak olan 4,5 di(hekziltiyo) ftalonitril (**1**), 4-[(2-hidroksietil) tiyo] ftalonitril (**2**) ve 4-[3-(dietilamino) fenoksi] ftalonitril (**3**) türevleri ile *o*-karborandan başlayarak bir metallokarboran türevi olan oksonyum fonksiyonel grubuna sahip kobaltokarboran bileşiği sentezlenmiş, tüm yapılar spektroskopik tekniklerle ve elementel analizi ile tanımlanmıştır.

İkinci kısımda, simetrik olmayan metalsiz ve metalli ftalosiyanin türevlerinin sentezi için öncelikle hekziltiyo-hidroksietiltiyo sübstitüe (**7**) ve dietilaminofenoksi-hidroksietiltiyo sübstitüe (**10**) olmak üzere iki A_3B tipi asimetrik metalsiz ftalosiyanin sentezi ile başlanmış, çok aşamalı reaksiyon dizileri ile devam edilmiş ve spektroskopik yöntemlerle yapılar aydınlatılmıştır. Asimetrik metal içermeyen ftalosiyanin türevi **7** nolu bileşiğin sentezinde, öncelikle dilityum ftalosiyanin, heksiltiyo ve hidroksietiltiyo sübstitüe ftalonitrillerin lityum etkili siklotetramerizasyonu ile hazırlandı. Daha sonra, dilityum ftalosiyanin asetik asit ile asitlendirilerek metal içermeyen ftalosiyanin **7**'ye dönüştürüldü. Ürünün %26 verimle izolasyonu için kolon kromatografisi kullanıldı. Pc **7**'nin 1-pentanol içinde çinko (II) asetat varlığında N_2 atmosferi altında reflux edilmesiyle %94 verimle metalli ftalosiyanin Pc **8** hazırlandı. Yeni sentezlenen ftalosiyanin türevleri **7** ve **8**, spektral veriler ve element analiz ile karakterize edildi. Ayrıca **7** ve **8**'in agregasyon davranışı kloroformda farklı konsantrasyonlarda incelenmiştir. Bu sonuçlara göre, **7** ve **8** monomerik yapıdadır ve bu konsantrasyon aralığında Beer-Lambert yasasına uymaktadır.

Benzer şekilde **10** nolu bileşik dietilaminofenoksi ve hidroksietiltiyo sübstitüe ftalonitrillerin 1-pentanol içinde siklotetramerizasyonu ile hazırlanmıştır. Pc **10**'un azot atmosferi altında $Zn(CH_3COO)_2$ varlığında kuru pentanol içinde reflux edilmesiyle Pc **11** elde edildi. Sonuçta, Pc **10** ve Pc **11** sırasıyla %21 ve %89 verimle elde edildi.

Steglich esterifikasyon, yumuşak koşullar altında ester fonksiyonel grubun hazırlanmasına yönelik genel bir yöntemdir. Bu yöntem kullanılarak Pc **9** ve Pc **13** esterleşmesi, disikloheksilkarbodiimid (DCC) / N, N dimetilaminopiridin (DMAP) varlığında 4-pentinoik asidin Pc **8** ve Pc **11** ile reaksiyona sokulmasıyla sağlanmıştır. Reaksiyon sırasında oluşan üre türevleri, çöktürme ve kolon kromatografisi yöntemleri ile kolayca uzaklaştırıldı. Pc **9** ve Pc **13** sırasıyla %60 ve %67 verimle elde edildi.

Karboran sübstitüe ftalosiyaninleri sentezlemek için farklı stratejiler bildirilmiştir ve bunlardan biri de ftalosiyanin türevlerinin alkinil birimlerine dekaboran eklemesidir. Bu nedenle, propargil bromür ve Pc **11**'in toluen içerisinde sodyum hidrür varlığında reaksiyonundan terminal alkinil grubu içeren Pc **12** %80 verimle elde edilmiştir. Yeni sentezlenen Pc **12**'nin saflığı, elementel ve spektroskopik analizlerle doğrulanmıştır.

Çalışmanın üçüncü kısımda, karboran birimleri, asimetrik olarak sübstitüe edilmiş ftalosiyanin komplekslerine kovalent olarak bağlanarak **14** ve **15** nolu ftalosiyanin türevleri sentezlendi. Pc **14**'e dekaboran eklenmesi, Pc **9** ve dekaboranın kuru asetonitril ve kuru toluen karışımı içinde reaksiyonuyla gerçekleştirildi. Aynı yöntem kullanılarak mono *o*-karboranil ünitesi içeren Pc **15** %68 verimle hazırlandı. Ürünlerin karakterizasyonu, elementel analiz, spektroskopik yöntemler ve kütle spektroskopisi ile yapılmaktadır. Tüm yeni ürünler için spektral araştırmalar, hedeflenen yapılarla tutarlıdır.

BNCT ajanları için önemli gerekliliklerden biri de sentezlenen bileşiklerin suda çözünürlükleridir. Bu amaçla, dietilamino sübstitüe Pc **15**'in kuaternerizasyonu ile trikatyonik suda çözünür Pc **16** elde edildi. Reaksiyon Pc **15**'in metil iyodür ile 2 gün boyunca karanlık ortamda kloroform içerisinde 50 °C'ye ısıtılmasıyla %84 verimle gerçekleştirildi. Elde edilen suda çözünür bileşiğin karakterizasyonu ve saflığı ^{1}H NMR, ^{11}B NMR ve UV-Vis gibi çeşitli karakterizasyon teknikleri ile doğrulanmıştır.

Ayrıca çalışmanın bu aşamasında karborana benzer özellikler gösteren ancak tek bir molekülde daha fazla bor atomu yüklenmesine imkân veren "kobaltokarboran" grubu taşıyan moleküller de sentezlenmiştir. Kobaltakarboran ile fonksiyonelleştirilmiş metaloftalosiyanin kompleksleri Pc **17** ve Pc **18**, kobalt bis (dikarbollid) oksonyum türevinin halka açma reaksiyonu yoluyla ftalosiyanindeki hidroksil grubunun nükleofilik saldırısı ile Pc **8** ve Pc **11** 'den hazırlanmıştır. A_3B tipi Pc **17** ve Pc **18** yürütücü olarak DCM kullanılarak saflaştırılmış ve sırasıyla %52 ve %73 verimle elde edilmiştir.

Elektrokimya ftalosiyanin ve karboran bileşiklerinin redoks davranışı hakkında önemli bilgiler vermektedir. Çalışmanın son aşamasında, yeni sentezlenen asimetrik ftalosiyanin türevlerinden **8**, **9**, **14** ve **17**'nin elektrokimyasal özellikleri rapor edilmiştir. Ftalosiyanin komplekslerinin indirgenme ve oksidasyon potansiyelleri, diklorometan içinde destekleyici elektrolit sistemi olarak tetrabutilamonyum perklorat (TBAP) ve çalışma elektrotu olarak platin kullanılarak döngüsel voltametri (CV) ve kare dalga voltametri (SWV) ile çalışılmıştır.

Sonuç olarak bu doktora tezi kapsamında, hem hedef hücrelerle etkileşmeyi hem de organik çözücülerde ve suda çözünürlüğü sağlayacak sübstitüent grupları ile BNCT için gereken karboran birimlerini birlikte içeren ftalosiyanin türevlerinin sentezi, karakterizasyonu ve elektrokimyasal özelliklerinin incelenmesi gerçekleştirilmiştir.

1. INTRODUCTION

1.1 History and Structure of Phthalocyanines

First time, the term ‘phthalocyanine’ was used in 1933 by Professor P. Linstead (Figure 1.1) (Linstead, 1934). The word ‘phthalocyanine’ is derived from naphta (rock oil) and cyanine (dark blue).

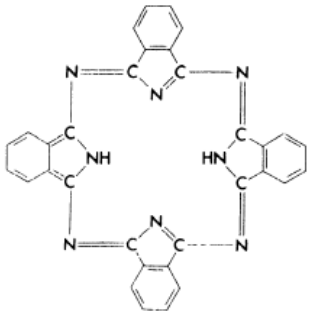

Figure 1.1 : Phthalocyanine.

The phthalocyanine class compounds are separated into two groups, namely metallo and metal-free phthalocyanines. Several thousands of different phthalocyanines have been synthesized by changing the two atoms of the phthalocyanine derivative with many metal atoms of the Periodic Table.

Phthalocyanines, which are an important class of organic materials, were discovered by accident. In the beginning of 1900s, Braun and Tscherniac serendipitously obtained first metal free phthalocyanine from o-cyanobenzamide as unidentified blue compound (Figure 1.2) (Braun et al., 1907).

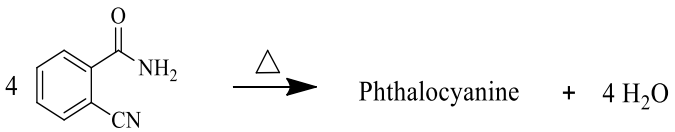

Figure 1.2 : Accidental discovery of metal free phthalocyanine from o-cyanobenzamide.

In a similar way, de Diesbach and von der Weid tried to synthesize dicyanobenzene by the reaction of $C_6H_4Br_2$ with CuCN in C_5H_5N. After the reaction, instead of dinitrile derivative, a blue product was obtained in 23% yield with $C_{26}H_{18}N_6Cu$ formula (Figure 1.3) (Diesbach et al., 1927).

Figure 1.3 : Accidental discovery of metallophthalocyanine from *o*-dibromobenzene.

In 1928, a blue impurity was attained from phthalimide which reacted with the iron lining in the glass-lined iron kettle by accident (Dandridge et al., 1929). The obtained compound was treated with H_2SO_4 in an attempt to examine the stability and it was seen that iron metal was not taken out. When the crude compound was examined, results indicated that it involved C, 62; H, 3; N, 19; and Fe, 13 per cent. So it meant that the ratio of carbon to nitrogen was 4 to 1 and two nitrogen atoms were boned with a phthalic residue. As to these experimental results, it was seen that blue sample had an isoindole unit (C_8H_7N) (Linstead, 1934). In 1934, a bright blue compound was prepared in 40% yield from o-cyanobenzamide and magnesium at 240-250 °C with $C_{32}H_{20}O_2N_8Mg$ or $(C_8H_4N_2)_4$ $Mg.2H_2O$ formulas (Figure 1.4) (Dent et al., 1934).

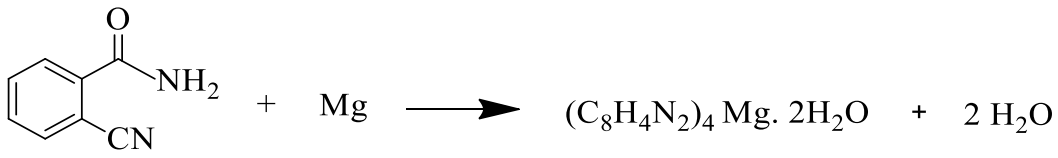

Figure 1.4 : Synthesis of magnesium phthalocyanine from *o*-cyanobenzamide.

When the blue solid was treated with cold concentrated H_2SO_4 or hot concentrated HCl, contrary to iron compound, magnesium metal was isolated from the structure. Magnesium and iron compounds undoubtedly were phthalocyanine but differed in their stability against to acids.

Prior to the end of the 1930s, the structure of these substances could not be clarified by researchers. In 1929, Imperial Chemical Industries (ICI) granted Reginald P.

Linstead to elucidate the formation of these substances. Linstead and his students prepared a range of papers that identified the structure of them and described the synthesis of novel metal compounds (Byrne et al., 1934; Dent et al., 1934; Linstead et al., 1934).

For the first time, Linstead used the name phthalocyanine in 1933, to identify totally synthetic compounds which resemble the naturally occurring porphyrins. Elemental analysis, ebullioscopy and oxidative degradation was used to clarify the molecular structure of phthalocyanine. Afterwards, in addition to chemical analysis, Robertson affirmed the exact structure via X-ray analysis (Robertson, 1935-1937; Fox, 1987).

Since the accidental discovery in the early 1900s, phthalocyanines widely used as coloring material due to their high stability, good color properties, and relatively low cost. In 1935, copper phthalocyanine that was named Monastral fast blue was started to produce as colorant at the Imperial Chemical Industries. Moreover, in 1936 I. G. Farbenindustrie and in the end of 1930's the DuPont Company started to manufacture copper phthalocyanine. Preliminary production method of phthalocyanines was improved by Wyler and it is still the most common process for industrial-scale manufacture of phthalocyanine dyes and pigments. In this method, phthalic anhydride and metal salt are heated in molten urea using ammonium molybdate as catalyst (Fox, 1987). In the 1950s and 1960s, sulfonated water-soluble phthalocyanine dyes and reactive dyes were widely used in textile industry as colorants.

The results of comparative experiments proved that unlike *o*-phthalonitrile, terephthalonitrile (I), homophthalonitrile (II), o-xylylene dicyanide (III), o-cyanocinnamonitrile (IV), and 2,2'- diphenonitrile (V) reagents did not give the same phthalocyanine products under the similar reaction conditions (Figure 1.5) (Robertson, 1935).

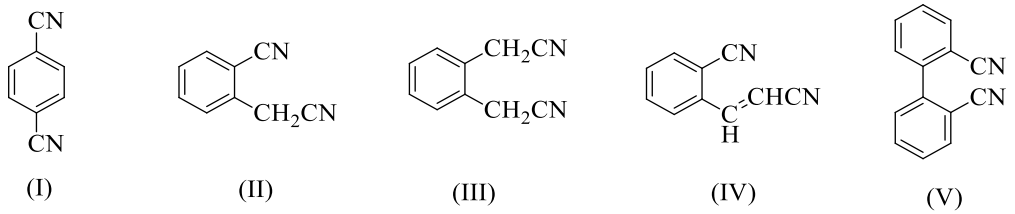

Figure 1.5 : Other dinitrile derivatives.

According to these experiments, the two -C≡N groups forming the skeleton of phthalocyanine should be attached to adjacent carbon atoms in aromatic structure and no other saturated atom or aromatic unit should be placed between the nitrile groups and the aromatic core. The available evidence is strongly in favor of the isoindole formula. Monoiminophthalimide (VI), and 1, 3-diiminoisoindoline (VII) which are contain the isoindole units, are the phthalocyanine precursors (Figure 1.6).

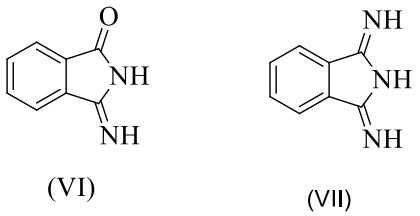

(VI) (VII)

Figure 1.6 : Isoindole derivatives.

It is clear that only one isoindole unit cannot provide the intense color of phthalocyanines. The further investigations which are made for both free and metallic phthalocyanines, prove that they have four C unit formula. The attachment of these isoindole units to one another in order to obtain strong colors will be through extra cyclic nitrogen atoms. These four C_8 components can be organized into a chain structure (VIII) or ring structures (IX) and (X) with $(C_8H_5N_2)_4$, $(C_8H_4N_2)_4H_2$ and $C_{32}H_{18}N_8$ formulas, respectively (Figure 1.7).

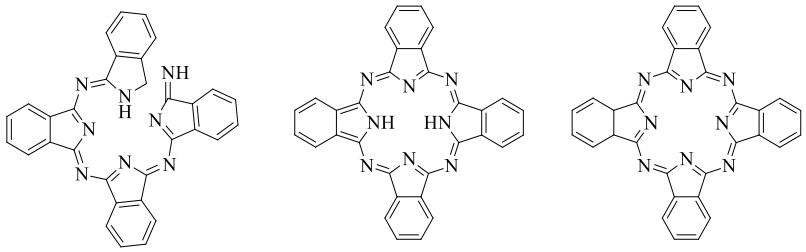

(VIII) (IX) (X)

Figure 1.7 : Chain structure (VIII) and ring structures (IX), (X).

Structure (X) does not have imino-hydrogen and all the aromatic rings are benzenoid structure; structure (IX) are slightly different in concerning with the attachment of the metal on the derivatives. Copper atom, in the structure (XI) which is the form of a metallo derivative of structure (IX) displaced two hydrogen atoms and bonds by covalencies to the nitrogen atoms of the two isoindole units and also is coordinated

with the other two nitrogen atoms. In addition, in the structure (XII), the metal is attached to the nitrogen atoms by coordination bonds (Figure 1.8).

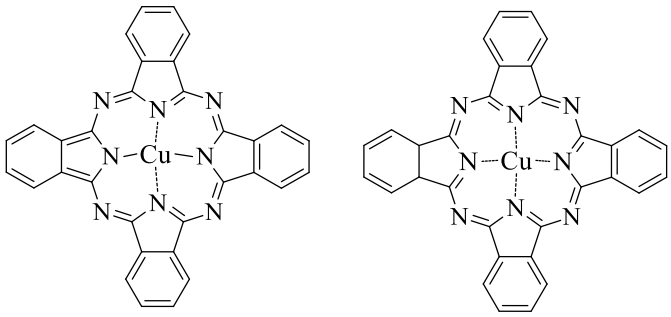

(XI) (XII)

Figure 1.8 : Copper phthalocyanines.

Some experiments have proved that the formulas (XIV) and (XVI) are preferred structures for phthalocyanines. The stability of copper phthalocyanine in the vapor phase at around 600 °C cannot be achieved if the metal atom was held only by co-ordinate bonds. Besides, the presence of oxidizable hydrogen atoms in the metal free phthalocyanines and its absence in the metallophthalocyanines shows that bivalent metal atom replaces with hydrogen atoms and bond by covalent bonds (Robertson, 1935).

Fully synthetic phthalocyanines can be prepared from phthalonitriles and metal atoms. Especially 90% of copper phthalocyanines produced are used as pigments. Around $8x10^7$ kg of phthalocyanines are produced every year around the world. 40% of them are used as printing inks, 30% are paints, 20% coloring plastics and 10% are color filters for LCD and TFT (Erk et al., 2003). In addition to them, phthalocyanine derivatives are used as catalysts, as organic semiconductors, as organic LED, as photovoltaics, as liquid crystalline, as photo active element in photo copiers, as photo sensitizers and for photo dynamic cancer therapy (Sorokin, 2013; Blochwitz et al., 1998; Bottari et al., 2010; Ayhan et al., 2009; Gregory, 2000).

1.2 Properties of Phthalocyanines

1.2.1 Physical and chemical properties

Phthalocyanine derivatives are widely utilized materials in various applications (Figure 1.9). Their widespread usage derives from their unique chemical and physical properties. Phthalocyanine macrocycle has a central cavity which can accommodate more than 60 different metal ions (metal-phthalocyanine (M-Pc)) and hydrogen atoms (metal-free phthalocyanine (H_2Pc)) (Sakamoto et al., 2009).

In terms of surface chemistry, phthalocyanines are more remarkable than other organic molecules. The planar structure of the phthalocyanines, ligand functionality, stability and reactivity are some of the important properties.

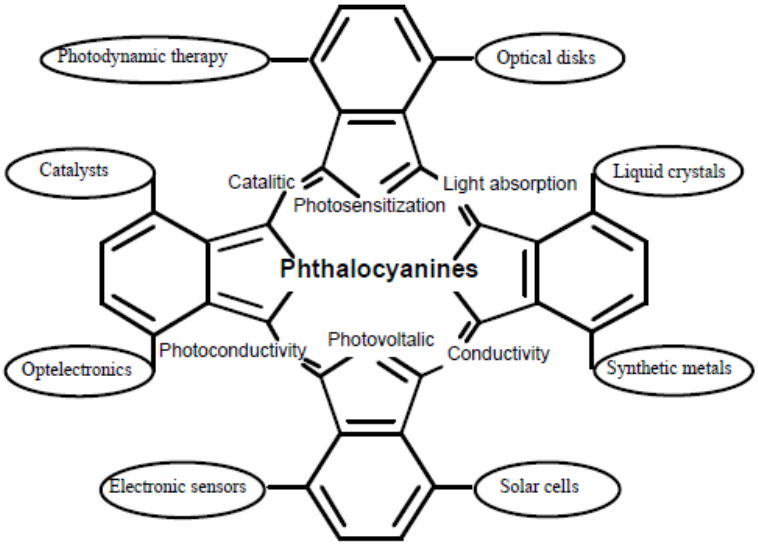

Figure 1.9 : Various applications of phthalocyanine derivatives.

Reactivity, electronic and magnetic properties of phthalocyanines can be different from according to metal atoms. Structural changes in the phthalocyanine macrocycle and different substituents in the peripheral substituents give them various features. When a wide variety of metal complexes come together with different substituents, supramolecular adjustments, and axial ligands, a tremendous diversity arises. The coordination chemistry of phthalocyanine derivatives is derived from the ability of phthalocyanines to complex with various elements in the periodic table (Figure 1.10) (Buchler, 1975).

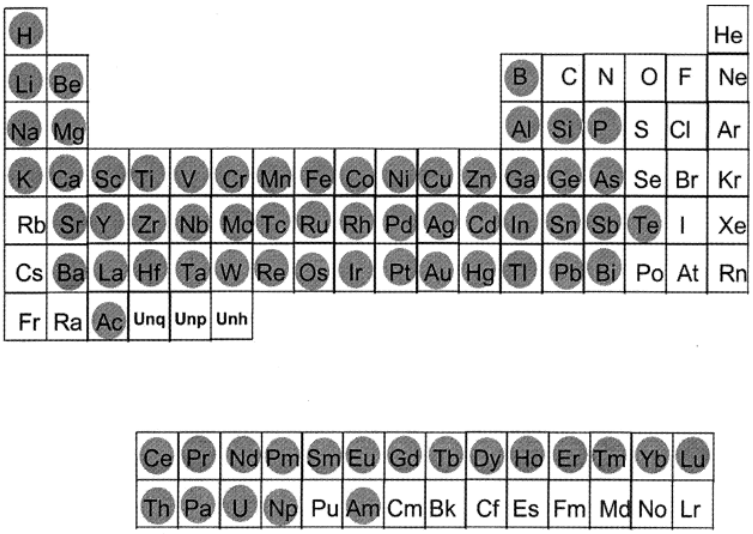

Figure 1.10 : The elements that form complexes with phthalocyanines.

Similar to porphyrins, the phthalocyanine derivatives are also completely conjugated planar sysytems and exhibit the same -NH- tautomerism (Figure 1.11) (Wöhrle et al., 1989).

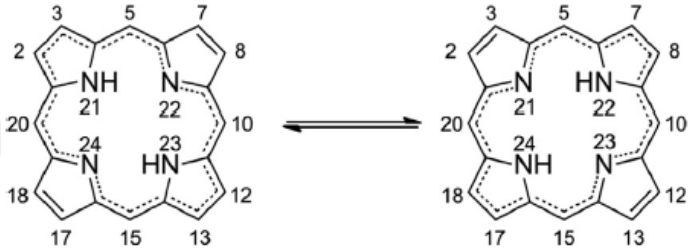

Figure 1.11 : Porphin (2HP).

Figure 1.11 also shows that, 18 π electron pathway on the cyclic polyene ring and tautomerism results in intramolecular double-proton transfer. According to IUPAC nomenclature, 2,3,7,8,12,13,17 and 18 positions are β-positions; 1,4,6,9,11,14,16 and 19 are α-positions and 5,10,15 and 20 are meso-positions on the Porphin ring.

Phthalocyanines contain extended conjugated π system that gives them strong light absorption properties in the UV-Vis area. Phthalocyanine derivatives with high photo stability and easy availability, are the most important organic colorants (Dini et al., 2003). Phthalocyanines, which are thermally stable, undergo sublimation at 500-800 K.

The most important reactions seen in phthalocyanines with such a balanced electronic configuration are the redox reactions that hydrogen atoms carry out with suitable reducing / oxidizing agents.

The diversity of shapes and sizes of PCs depends on three different effects: (1) disk shaped macrocyclic structure, (2) size of central metal atom and, (3) valence state thereof. The geometry of the unsubstituted Pc ring is D_{4h} and many metal atoms with ion radii ranging from 50 to 150 pm can be coordinated by the Pc ring inside the central cavity. This diversity results in various different geometries in the metallo phthalocyanine complexes. Oxidation state of Pc is -2. However, when the phthalocyanine is coordinated with the metal atom having a different oxidation state from +2, atomic aggregate MX_n is occured. From Figure 2.2 it can be seen that the oxidation state of the central atom ranges from + 1 (H, Li, Na, K) to + 5 (Mo, Ta, W, Re). The richness of the molecular structures of the complexes of general formula PcM_mX_n is partially shown in Figure 1.12.

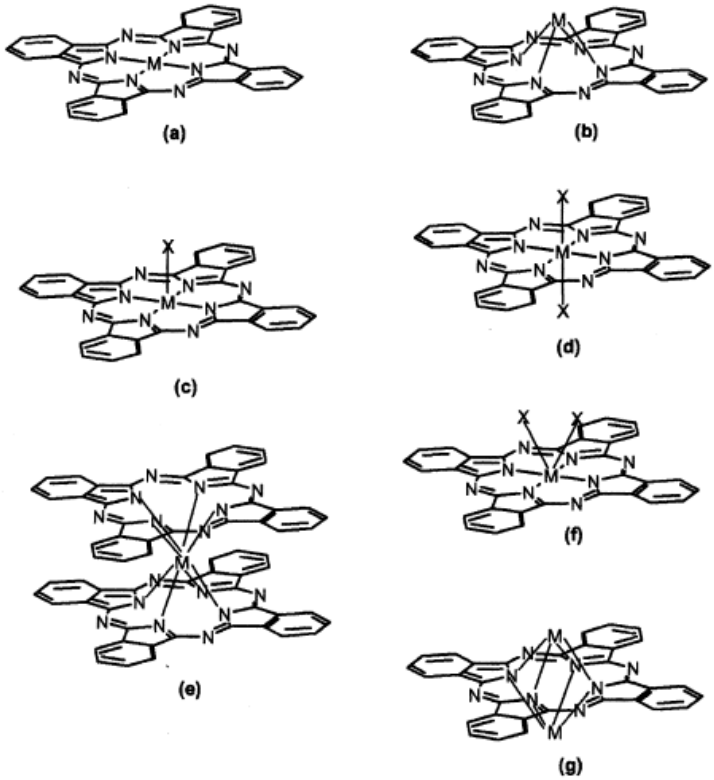

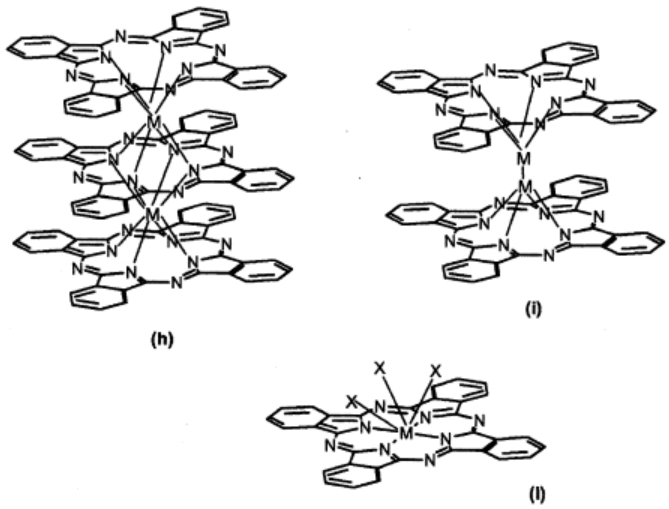

Figure 1.12 : PcMmXn molecules having M in various possible oxidation states [+1 in (g); +2 in (a), (b); +3 in (c), (h); +4 in (c), (d), (e), (f), (i); +5 in (c) and (I)].

In the PcM_2 structure, which contains monovalent metal atoms in the center, such as $PcLi_2$ and PcH_2, the metal atoms are coordinated by 4 pyrroline rings (Figure 1.12 (a)). In the PcTl2 structure, one metal atom is located above the phthalocyanine ring and other one is located under the ring (Figure 1.12 (g)). The PcM complexes are found in structure a or b in Figure 1.12, based on the magnitude of the divalent metal atom. While divalent central atoms like Beryllium, Magnesium, Chromium, Manganese, Iron, Cobalt, Nickel, Copper, Zinc give PcM complexes while larger divalent central atoms like Pb or Pt can give complexes with quasi-pyramidal geometry (Fielding et al., 1965). Trivalent metal atoms are coordinated with the ligand X to form Pc complexes with pyramidal geometry. PcAlF, PcGaCl and PcInCl are the most common examples with such a pyramidal geometry. Sandwiched type phthalocyanines are obtained with trivalent metal atoms and in the absence of ligand X (Figure 1.12 (h)) (Janczak et al., 1999).

First time, the crystal structures of Pc's were listed by Moser and Thomas in 1983 (Moser et al., 1983). These structures were named as α-, β-, γ-, δ-, ε-, μ-, X-, and R-forms. Later, η-, ρ-, τ-, and Y-forms were also defined.

The phthalocyanine molecules shown in Figure 1.12 are usually found in monoclinic, triclinic and orthorhombic crystal structures in space. In the following examples attempted to explain the crystal structures that might be interesting.

The orientations of Pc molecules in the monoclinic crystals of PcH_2, PcPb and PcTiO and their different forms are shown respectively in Figures 1.13-1.15.

It was observed that in both monoclinic β-form and X-form, adjacent PcH_2 macrocycles slightly slipped eachother and directed perpendicular to the macrocyclic plane (Hammond et al., 1996).

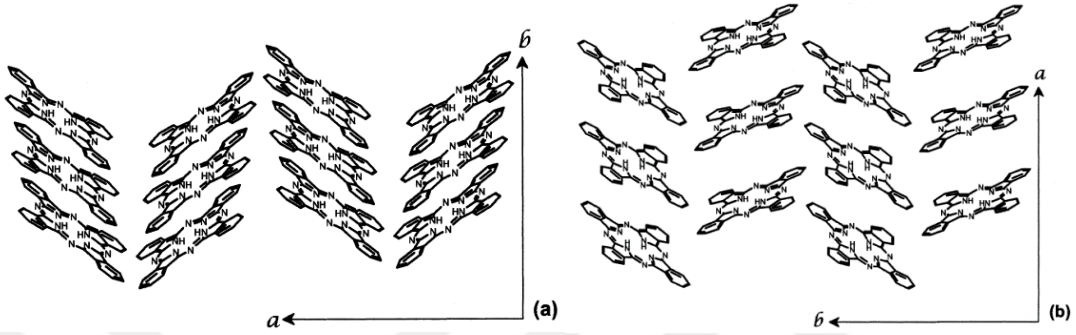

Figure 1.13 : Monoclinic (a) β-form and (b) X-form of PcH_2.

In the X-form of PcH_2 the inter-ring distance is higher than β-form. In that case, it is expected that electronic transport will be more efficient in β-form.

In monoclinic PcPb, macrocycles are oriented parallel to ring plane like a stacked structure (Figure 1.14).

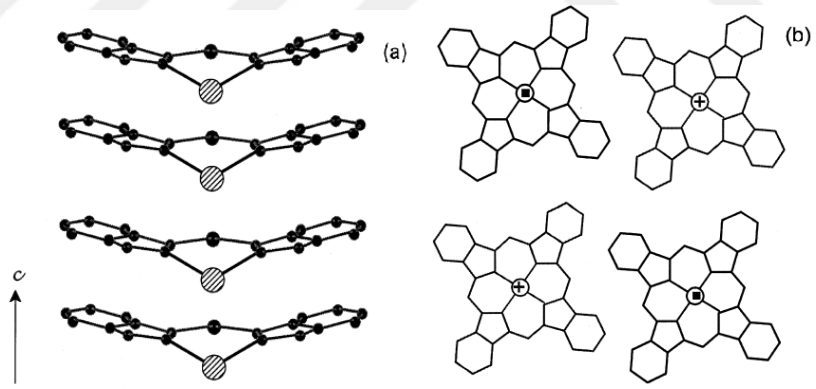

Figure 1.14 : Monoclinic PcPb viewed (a) through a section parallel to the c-axis and (b) along the c-axis.

The concave shape of PcPb forms by reason of the fact that Pb atoms are positioned outside the plane instead of the macrocyclic plane. This structure gives anisotropic character of the electroconductive properties to PcPb (Ukei, 1976).

PcTiO has a monoclinic structure by having the coordinated central metal with an axial substituent (Figure 1.15). The existence of the axial substituent on the central metal prevents adjacent PcTiO molecules to arrange in a stacked structure.

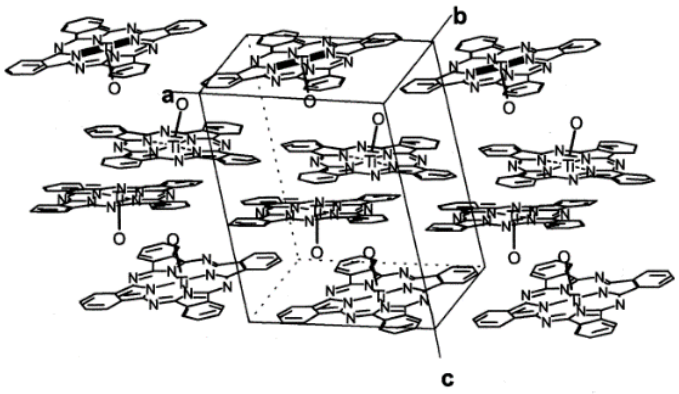

Figure 1.15 : Spatial arrangement of PcTiO molecules.

PcTiO molecule has square pyramidal structure and in the monoclinic structure, Pc rings observed parallel to the crystallographic ab plane. The pyramid vertices constituted by the O atoms are perpendicularly to the macrocycle rings. The Ti=O bonds are approximately parallel to the c direction. The ensemble of parallel Ti=O bonds belonging to side-sharing Pc rings form a layer which is upward and downward. By structure, PcTiO can resemble the structure of a Langmuir-Blodgett film whose chemical-physical properties are periodically stratified (Cook, 1999).

Many Pc-based materials such as PC_3Bi_2, PcSn, $PcTiCl_2$, PcTiO in phase II, PcGaOH, PcAlCl, PcTaC1 crystallize with triclinic symmetry. The orientations of Pc molecules in the triclinic crystals of PcPb, PcTiO (II phase) and PC_3Bi_2 are shown respectively in Figures 1.16-18. In contrast to monoclinic PcPb, triclinic PcPb shows a complex arrangement (Figure 1.16).

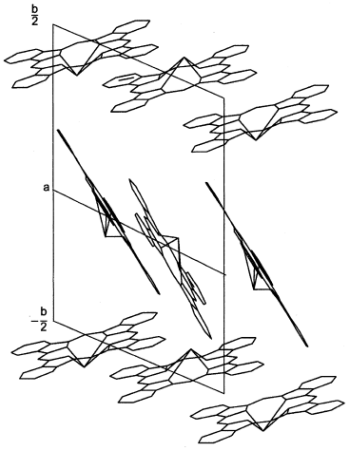

Figure 1.16 : Triclinic lead phthalocyanine structure.

This structure leads to the disruption of the column arrangement which aids electronic intermolecular hopping. Therefore, photoconductivity is effected by negatively in triclinic PcPb phase II.

In Figure 1.17, adjacent slipped PcTiO molecules which have axial O ligands oriented in opposite directions with alternating downward and upward.

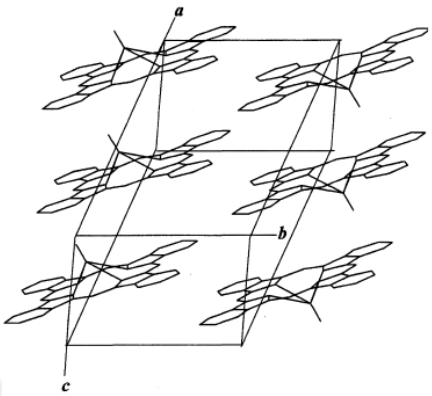

Figure 1.17 : PcTiO molecules in the triclinic structure.

Figure 1.18 shows a sandwiched type arrangement of Pc_3Bi_2 molecules. The minimization of the repulsive electrostatic energy originated by the high positive charge of Bi is a direct consequence of the distances between related elements of the structure (Janczak et al., 1999).

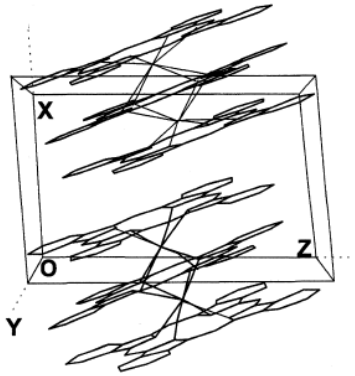

Figure 1.18 : Molecular packing of Pc_3Bi_2 in the triclinic crystal structure.

The molecular geometries of Pcs whose crystal structures have a orthorombic symmetry include the types depicted in Figure 1.19 $PcTl_2$ and in Figure 1.20 Pc_2In.

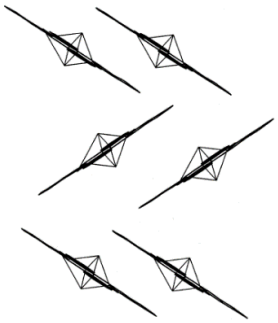

Figure 1.19 : Molecular packing of Pc_3Bi_2 in the triclinic crystal structure.

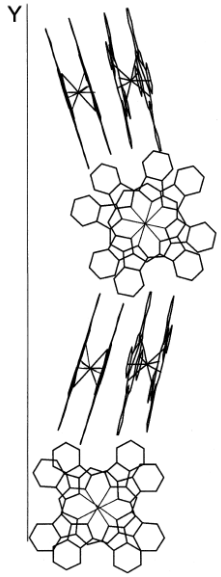

Figure 1.20 : Spatial arrangement of Pc_2In molecules in the orthorhombic structure.

1.2.2 Photochemical and photophysical properties

Photochemical analyzes involve quantitative measurement of the efficiency of photosensitizers and alteration of materials by light. Photophysical analyzes involve the time a fluorophore spends in the excited state before emitting a photon and returning to the ground state, and triplet quantum yields and lifetimes. Φ_T of the photosensitizer is expected to correlated with the Φ_Δ values. Therefore, the tendency in changing of Φ_Δ should be parallel to changes of Φ_T values. Φ_T, Φ_F and Φ_Δ of complexes can be found from photochemical and photophysical data.

In recent years, application areas of metallophthalocyanines have spread to fields such as electrocatalysts, photosensitizers in PDT, and photoconducting agents used in printers. MPc complexes comprising of non-transitional metal atoms are used as

photosensitizers. The existence of diamagnetic metals Zn, Al or Si e.g. into the Pc derivatives gives them higher Φ_T and longer triplet lifetimes (Nyokong, 2007). So, in this part, photophysical and photochemical features of MPc derivatives bearing diamagnetic central metal atoms wil be explained.

During photosensitization, at the first step metallophthalocyanine is excited to triplet state and then the energy is transferred to ground state oxygen, ($^3\Sigma_g$), in order to generate excited state oxygen, ($^1\Delta_g$). This mechanism is named as Type II (Bonnett, 2000; Patterson et al., 1990; Maree et al., 2002). On the other hand, triplet state oxygen interacts with triplet state ^{3}MPc* and singlet oxygen is generated. In this way, Φ_Δ can be compared with MPc triplet state quantum yields. The excited triplet state MPc can interact with ground state O_2 or substrates producing superoxide and hydroperoxyl molecules by Type I mechanism (Bonnett, 2000; Rosenthal et al., 1995).

Phthalocyanines are the second generation photosensitizers for photodynamic theraphy (PDT). Over the last few decades, especially silicon, zinc, and aluminum phthalocyanine derivatives have been synthesized. Also, their high Φ_T and long lifetimes of the excited triplet state have been investigated. Gül A. and his research group prepared a new ZnPc containing four borinic ester units (Figure 1.21). Furthermore, the effects of substituents are examined (Gül et al., 2014).

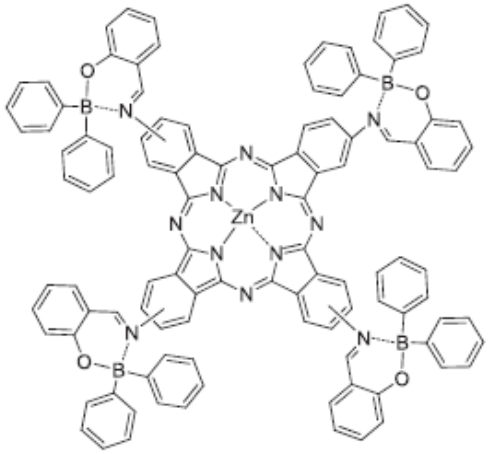

Figure 1.21 : Zinc phthalocyanine substituted with four borinic acid esters.

In this study, t_F is equal to the mean time of a particle stays in excited state before fluorescence. High fluorescence quantum yield with short fluorescence lifetime (t_F

=0.15 ns) and singlet oxygen quantum yield (Φ_{Δ}= 0.36) allow the useage of the new ZnPc as a PS in PDT.

The groups of Nagao Kobayashi and Tebello Nyokong synthesized water soluble unsymmetrical phthalocyanine derivative which conjugated with folic acid and investigated their physicochemical properties (Figure 1.22) (Matlou et al., 2017).

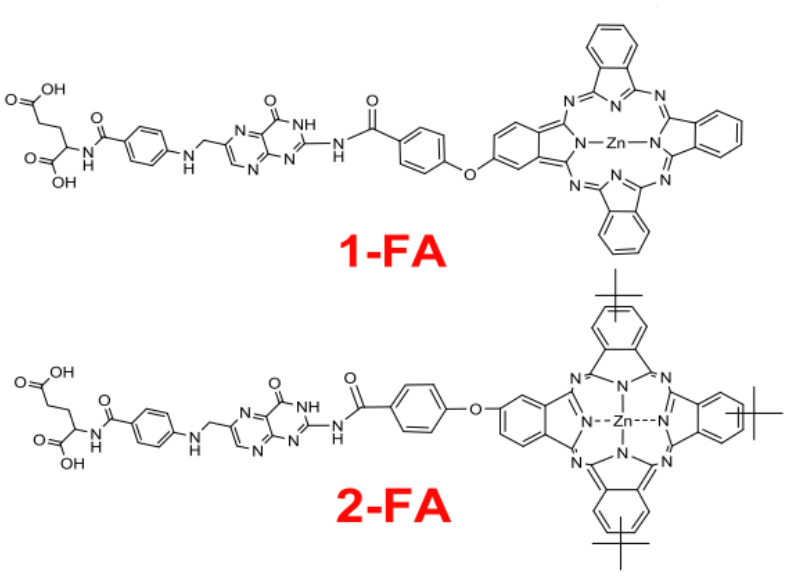

Figure 1.22 : Amide binding of unsymmetrical ZnPc complexes.

This work reported that photophysical and photochemical experiments of low symmetrical ZnPcs linked with folic acid (FA). By reason of the fact that the presence of FAs increased the water solubility and single oxygen quantum yields in the water could be studied for conjugates. It has been found that chemically bonded conjugates have better photosensitizing properties than physical mixtures. The 1-FA and 2-FA phthalocyanine derivatives have been shown to be effective singlet oxygen generators. Φ_{Δ} values of 1-FA and 2-FA are 0.61 and 0.47, and oxygen quantum yields are 0.17 and 0.12 in water solutions, respectively. Such a result is a direct consequence of the photosensitizing abilities of phthalocyanines.

In contrast to unmetallated phthalocyanine complexes, ZnPc complexes and their derivatives show efficient PDT effect and they are well known for their photosensitizing abilities. David A. Russell and coworkers investigated that gold

nanoparticles were functionalized with ZnPc and a lactose analogues (Figure 1.23) (Calavia et al., 2018).

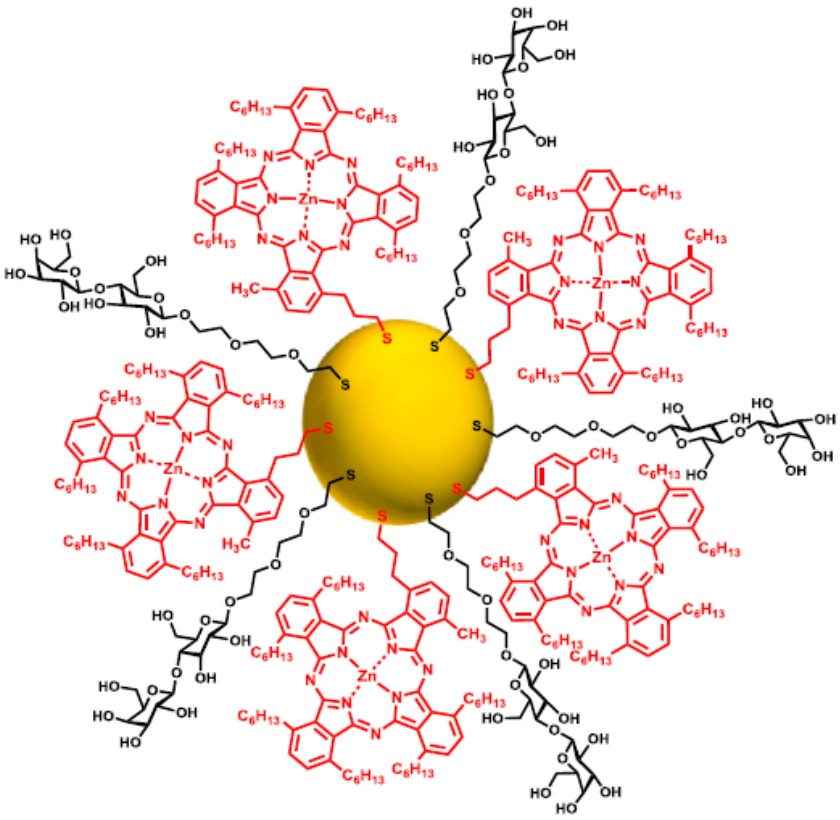

Figure 1.23 : Structure of the lactose-C3Pc-AuNPs.

In this study, the ability of lactose-phthalocyanine functionalized with gold nanoparticles to target the receptors overexpressed on some breast cancer cells was studied. In vitro PDT studies were carried out with lactose-C3Pc-AuNPs in both MDA-MB-231 and SK-BR-3 cells which receptors on the surface of breast cancer cells. It was determined that SK-BR-3 cells were killed more efficiently by lactose-C3Pc-AuNPs (97%). In conclusion, hydrophobic phthalocyanine photosensitizer on the gold nanoparticles has clear advantages for targeted photodynamic therapy.

M.A. Idowu et al. prepared unsymmetrical Mg(II) or Al(III) Pc derivatives which substituted with a carboxyl unit and 3 pyridylsulfanyl gropus was linked with a magnetic nanoparticle (Figure 1.24). The photophysical and photochemical behavior of the both Pc–AIMN conjugates and a mixture of phthalocyanine and AIMNs without a linkage were investigated (Idowu et al., 2018).

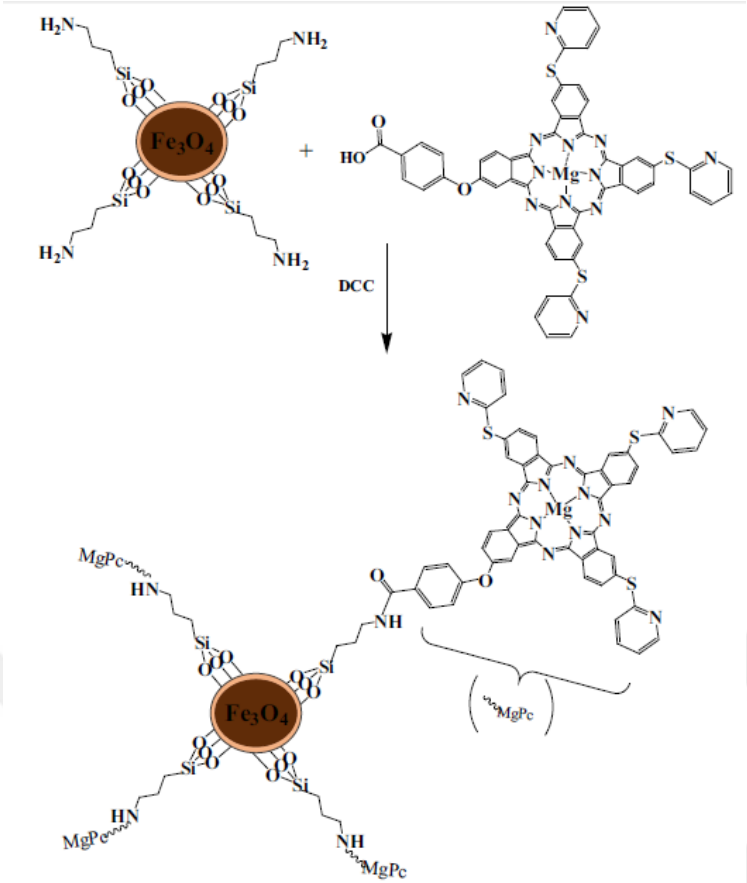

Figure 1.24 : Synthesis of the conjugation of the MgPc-AIMN.

The measured fluorescence quantum yields for MgPcs and AlPcs are 0.20 and 0.10 respectively. Due to the properties of the magnesium atom, MgPc derivatives had high fluorescence quantum yield values. Generally, it is observed that the Φ_F values are higher in the linked complexes than in mixed samples. It is known that aluminum complexes exhibit long triplet lifetimes. As expected that linked or mixed AlPc-AIMNs had longer triplet lifetimes than MgPc-AIMN complexes.

Silicon phthalocyanines show lower tendency to aggregation in solution than zinc phthalocyanines. Owing to their anticonvulsant and antimicrobial activities thiadiazole derivatives play an important role in medicinal chemistry. Especially, 1,3,4-thiadiazoles have antibacterial, pharmacological and antifungal properties. Recently, silicon phthalocyanine axially disubstituted with 1,3,4-thiadiazole group is prepared and its photophysical and photochemical parameters are also presented (Figure 1.25) (Güzel et al., 2017).

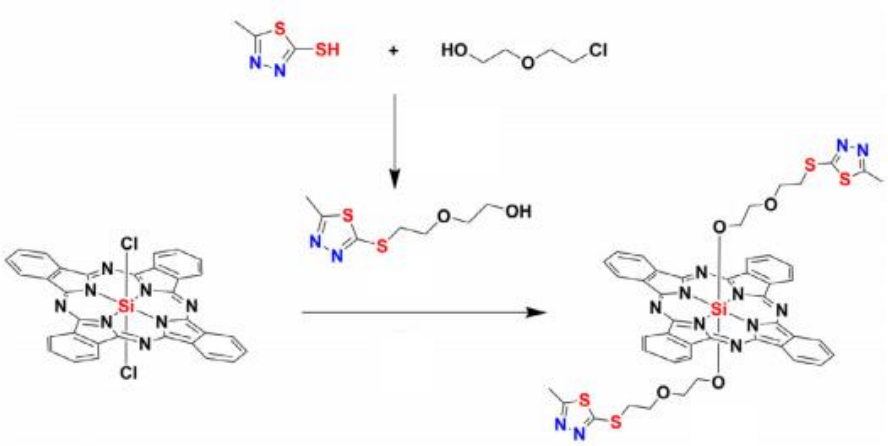

Figure 1.25 : Synthetic pathway of SiPc.

In this paper, fluorescence property of the SiPc was investigated in DMSO and the Φ_F value is found as 0.12 as expected (Figure 1.26 (a)). Besides, Φ_Δ was specified by quenching of DPBF chemically. In this study, SiPc showed very good Φ_Δ value (Φ_Δ = 0.86) (Figure 1.26 (b)).

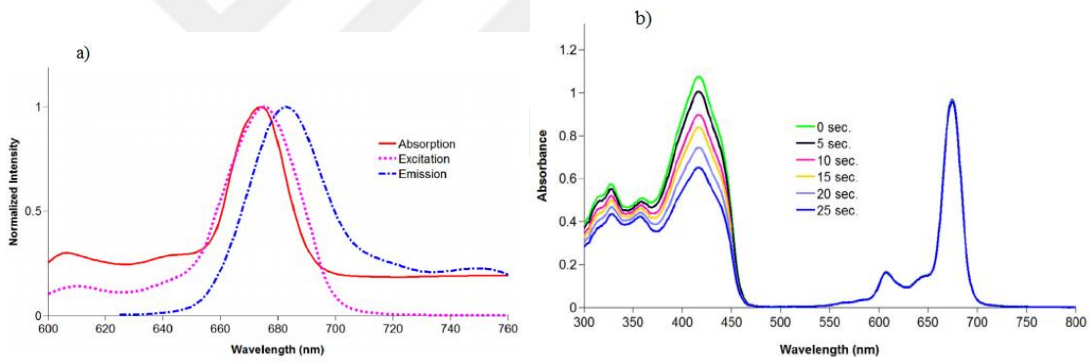

Figure 1.26 : a) Absorption, excitation and emission spectra of SiPc; b) Φ_Δ of SiPc in DMSO.

These results show that axially disubstituted silicon phthalocyanine can be a potential photosensitizer for photodynamic theraphy.

Substituents and central metal atoms significantly affect the triplet state, singlet oxygen, fluorescence quantum yields, and triplet lifetimes of MPc complexes. While the triplet quantum yields of phthalocyanines containing heavy central metal increases, their triplet lifetime is shortened.

1.2.3 Absorption spectra of phthalocyanines

Most of the organic coloring materials have been extracted from natural products. On the other hand, artificially designed dyes for various purposes have been synthesized (Kim, 2006). Phthalocyanines are aromatic macrocycles and they have symmetrical 18π electrons. Therefore, they are very similar to naturally occurring porphyrins (Figure 1.27(a)).

The molecular and electronic structure of the compounds is very effective on the spectral shape of the absorption spectrum. Therefore, UV-vis absorption is the foremost property of phthalocyanines. Figure 1.27(b) displays a characteristic UV absorption spectrum of metallo phthalocyanine.

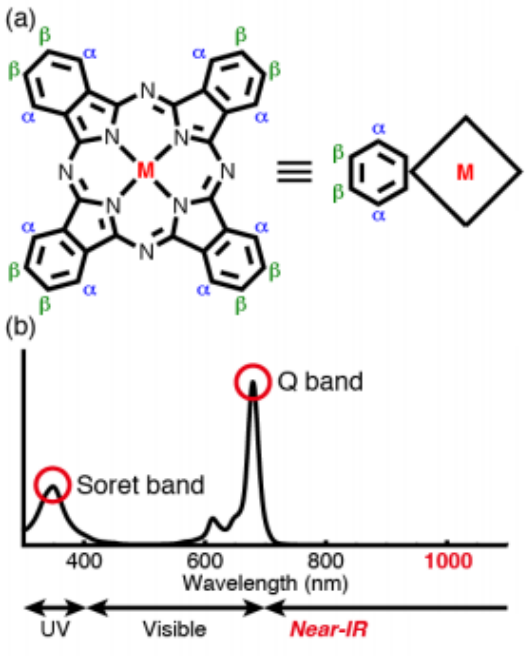

Figure 1.27 : (a) Structure of phthalocyanine. (b) Absorption spectrum of a metallated Pc.

On the other side, H_2Pc gives split Q band components. The decrease in molecular symmetry from D4h to D2h by diagonally positioning two protons on pyrrolic nitrogens causes this splitting. (Figure 1.28).

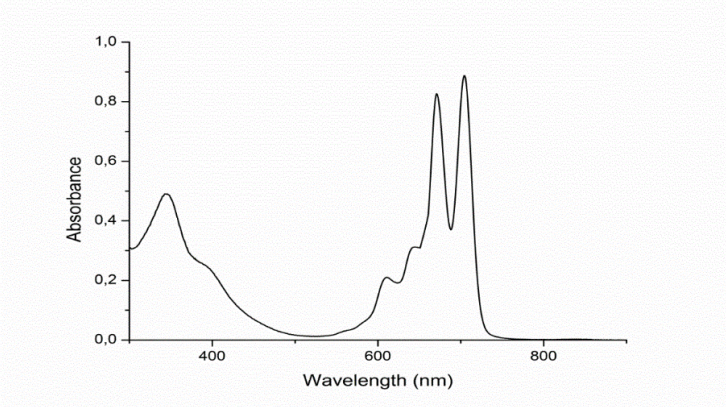

Figure 1.28 : Absorption spectra of a metal free Pc.

Typical metallo Pc which has D4h symmetry show an energy band in the 650–700 nm area (Q band) and B band in the 300–500 nm area (Soret band). The sharp and intense Q band is derived from π–π* transition.

Recently, I. Özçeşmeci et al synthesized metal-free Pcs substituted with 2,3-dihydroxyropoxy and [2,3,5,6- tetrafluoro-4-(2,3-dihydroxyropoxy)]benzyloxy units and carried out their electronic absortion studies (Figure 1.29) (Özçeşmeci et al., 2016).

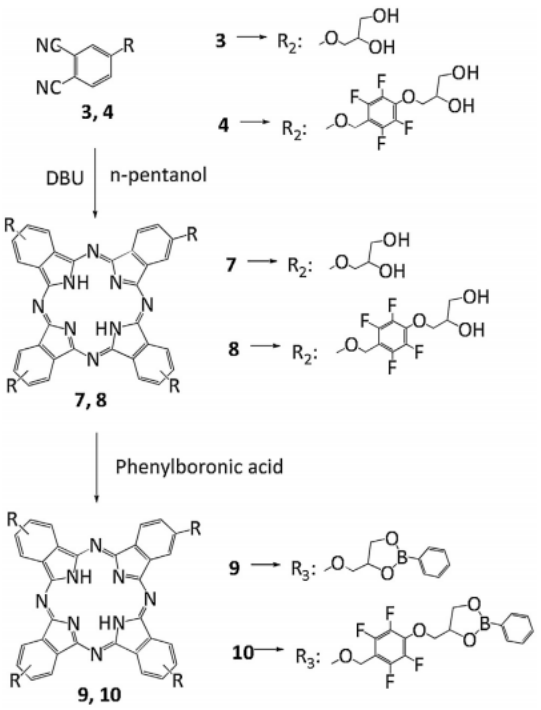

Figure 1.29 : Synthesis of metal-free phthalocyanine derivatives.

In this paper, metal-free phthalocyanine derivatives show characteristic UV-vis spectrum with two strong absorptions. One of them is B or Soret band is based on π levels → LUMO transition at around 300–400 nm. Other absorption is Q band arising from the π-π* transition from HOMO → LUMO of the Pc^{-2} ring (Figure 1.30).

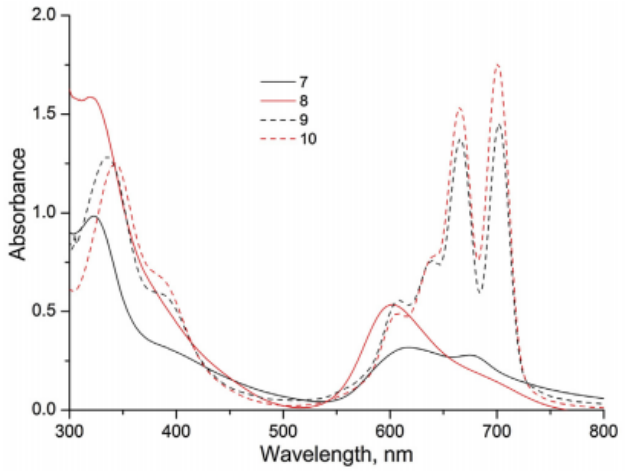

Figure 1.30 : Absorption spectra of (**7**–**8**) in C_2H_5OH and (**9**–**10**) in CH_2Cl_2.

The differences between the optical properties of **7**–**8** in ethanol and **9**–**10** in dichloromethane indicates the formation of aggregation. Pc **7** and Pc **8** displayed strong Q bands at 600-700 nm in C_2H_5OH without shoulder. According to this article, the presence of fluorinated groups and boron groups greatly reduces the aggregation of phthalocyanines, and boron groups cause batchromic shift.

Pcs which are used in organic solar cells, PDT, heat absorber, and near IR imaging absorb light in the near infrared area. The unique optical (especially Q band) features of phthalocyanines is gaining importance in these applications.

Basically, three approaches have been developed for phthalocyanines absorbing in the near IR area.

1. In order to decrease the separation between HOMO and LUMO energy stages, π conjugation could be extended by expansion of the macrocycle. In this way, spectra is red-shifted (Kobayashi et al., 2004; Furuyama et al., 2012).

2. As Fukuda's research group reported recently, in Pc oligomers electronic conjugation can be extended with orbital interactions between monomeric molecules.

In their work, they showed that the Q band of the oxidized units of a sandwich-type phthalocyanine shifted to the infrared area (Fukuda et al., 2012).

3. Q band can be splitted by lowering the molecular symmetry.

In addition to their useful properties, 'π electron conjugation modifications' have some negative effects. For instance, benzoannulated phthalocyanines tend to oxidation and become air-sensitive (Muranaka et al., 2010). Purification and separation of low symmetrical Pcs are rough processes and yield is very low. To overcome this problem, Nagao Kobayashi and coworkers suggested main-group elements as substituents (Furuyama et al., 2014). Due to their remarkable properties, for example influential orbital interplays, large electronegativity, and variety of coordination, it is expected that these groups can change the absorption spectra of Pcs dramatically. In this work, the synthesis and specialities of group 16 atoms (Sulfur, Selenium, and Tellurium) containing phthalocyanines were discused and phthalocyanines substituted with group 15 atoms (Phosphorus, Arsenic, and Antimony) in the central core were described (Figure 1.31,32).

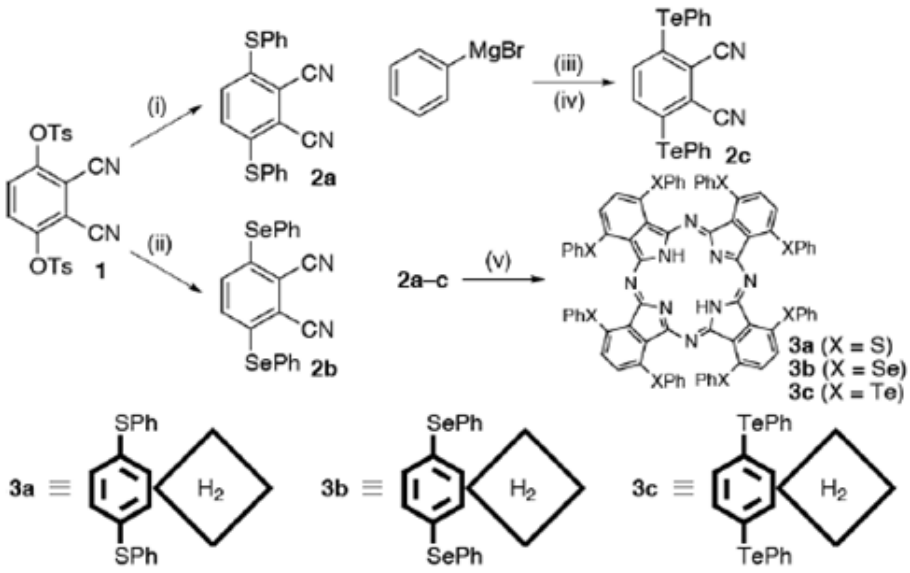

Figure 1.31 : Synthesis of group 16 substituted Pcs.

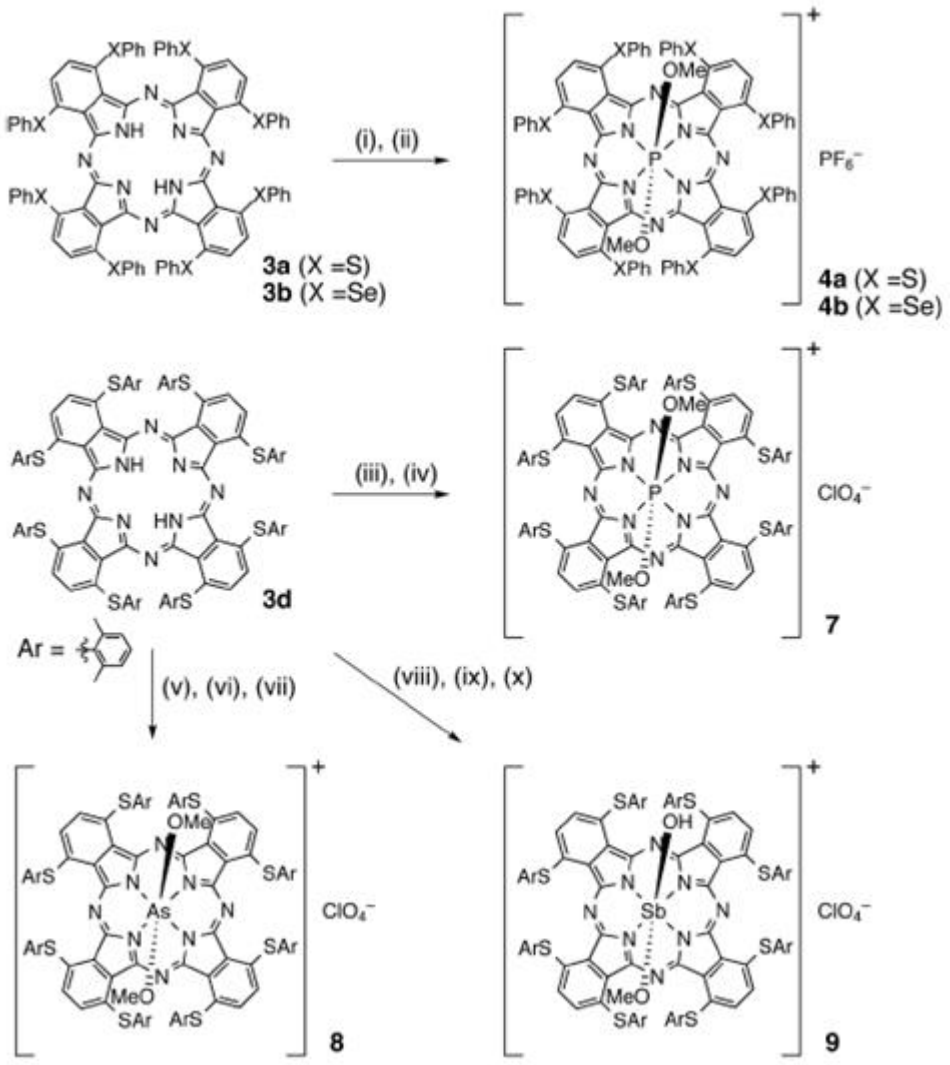

Figure 1.32 : Pcs containing group 15 elements.

As announced for the spectrum of phthalocyanine complexes absorbing in the near infrared area and Q bands of 3a–c Pcs were observed at 809, 811, and 835 nm in chloroform, respectively. It has been determined that the condition of the Q bands is connected with electronegativity of the chalcogenic elements. The π-conjugation structure of phthalocyanines was not be affected by group 16 elements. However, Q bands shifted to the red because of the electron-donating affect of the group 16 elements.

The absorption and MCD spectrum of Pc **7 - 9** are shown in Figure 1.33. The effect of P, As, and Sb atoms on the electronic features will be similar, because their

electronegativity is identical. Q bands of **7-9** Pcs were observed at 1032, 1018, and 1056 nm in CH_2Cl_2, respectively.

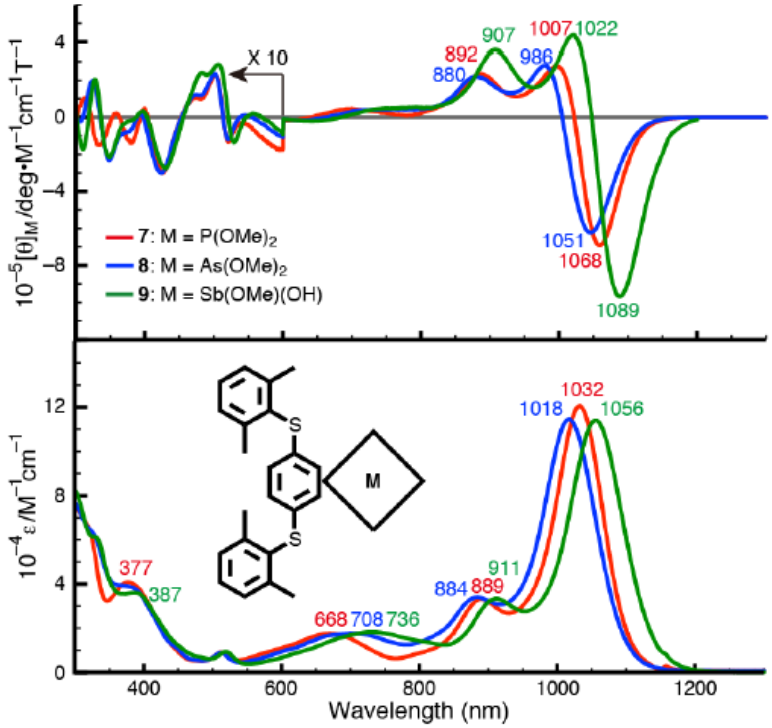

Figure 1.33 : UV-vis-NIR absorption (bottom) and MCD (top) spectra of **7** (red), **8** (blue), and **9** (green) in CH_2Cl_2.

Achieving emission beyond 1000 nm is only possible if the chromophore groups have strong absorption bands close to 1000 nm. In this context, 7-9 phthalocyanine derivatives which show absorption bands beyond 1000 nm were prepared. Synergistic effect of central group 15 atoms, peripheral group 16 atoms, and their positions was used to shift the Q band beyond 1000 nm.

Recently, the effect of substituents and density of the Q bands has been analyzed. It is observed that electron-donating groups at peripheral position transfers the Q band to longer wavelength as regards non-peripheral position analogues (Kobayashi et al., 1995-2003).

S. Yamamoto et al. synthesized two asymmetrical phthalocyanines substituted with thiophene groups and investigated their optical properties (Figure 1.34) (Yamamoto et al., 2016). The insertion of thiophene units at both peripheral and non-peripheral positions of metallo-Pc ring influences the electronic structure of π conjugation. Figure

1.34b shows absorption spectrum of peripheral substituted phthalocyanine **1** and non-peripheral substituted phthalocyanine **2** in tetrahyrofuran.

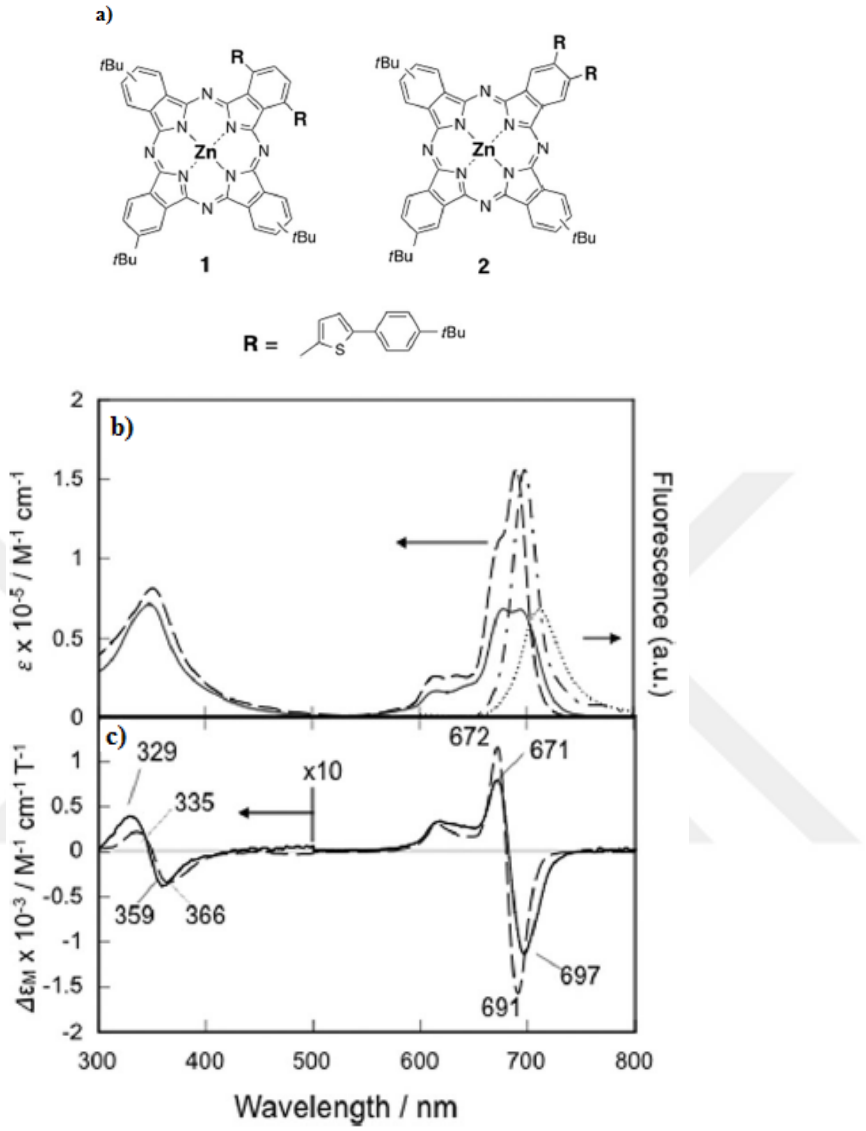

Figure 1.34 : a) $ZnPc(tBu)_4$; **b)** Absorption spectra of 1 (solid-dotted lines) and 2 (dashed-dashed dotted line); **c)** MCD spectra of 1 (solid line) and 2 (dashed line).

According to received information from Supporting Information, absorption spectra of $ZnPc(tBu)_4$ without thiophene groups gived intense Q band at around 670 nm. On the other side, Q bands of low-symmetry **1** and **2** shifted about 20 nm to red region compared to $ZnPc(tBu)_4$. Additionally, the molar extinction ε of **1** was significantly lower than that of **2** and differently from the previously reported literature, splitting of the Q band was observed.

1.2.4 Electrochemical properties of phthalocyanines

Electrochemistry is closely related with molecular orbital energy levels of the molecules and their capacity to accept or give electrons. Sulfonated phthalocyanines due to their solubility were the first phthalocyanine macrocycles studied by electrochemistry. In recent years, more soluble phthalocyanines were obtained by the development of synthesis of macrocyclic compounds.

Generally, redox state of the phthalocyanine has been represented as Pc^{2-}, for the common macrocyclic ligand; $Pc^{\bullet-}$ and Pc^{0} for the oxidized phthalocyanines and Pc^{3-}, Pc^{4-} for the reduced forms.

On the basis of the reported literature, electrochemical data on phthalocyanines have been classified in three groups. In the first group, metallophthalocyanines have redox inert metal centers and all redox processes originated from phthalocyanine rings. This group contains metal atoms as Aluminium, Barium, Bismuth, Cadmium, Copper, Gallium, Germanium, Hydrogen, Mercury, Indium, Lithium, Magnesium, Nickel, Phosphorus, Lead , Palladium, Platinum, Ruthenium, Antimony, Silicon, Tin, Titanium, Vanadium, and Zinc . The second group consists of sandwich complexes composed of lanthanides and actinides, Yttrium, Hafnium, Zirconium. In that group, macrocyclic ligands exchange electrons. In the last group, both the metal center and the macrocycle show redox properties and Silver, Cobalt, Chromium, Iridium , Iron, Manganese, Molybdenum, Osmium, Rhenium, Rhodium, Ruthenium, and Thallium complexes can be shown as example.

More recently, a series of new metal-free (**2**), Zinc(II) (**3**), Cobalt(II) (**4**), Copper(II) (**5**) and Manganese(III) (**6**) Pcs containing 2,6-dimethyl-4-(4-tert butyl-phenyazo)phenoxy units have been prepared. Also, their electrochemical properties were researched by CV and SWV by our research group (Garip et al., 2018). For this phthalocyanines, redox potentials are summarized in Table 1.1.

Table 1.1 : The electrochemical half wave potentials (E1/2, V vs. SCE) of **2**-**6**.

Comp.	R_3	R_2	R_1	Ox_1	Ox_2	Ox_3	R_3	R_2
2	-1.34	-1.04	-0.58	0.64	1.12		-1.34	-1.04
3	-1.30	-0.76	-0.44	0.59	0.90		-1.30	-0.76
4	-	-1.35	-0.76	0.64	1.02	1.16	-	-1.35
5	-1.42	-1.18	-0.70	0.61	1.07		-1.42	-1.18
6	-1.32	-0.89	-0.03	0.63			-1.32	-0.89

Figure 1.35 shows the CV and SWV voltammograms of Pc**2**, Pc**3**, Pc**4**, Pc**5** and Pc**6** in the mixture of tetrahydrofuran and tetrabutylammonium perchlorate. According to these voltammograms, one-electron oxidations and three reductions were obtained for phthalocyanine **2**, **3** and **5.** In contrast to phthalocyanine 2, reduction potentials of Pc**3** and Pc**5** were observed at negative area. It is a direct consequence of the effective nuclear charge differences between the with and without central metal of the Pc core.

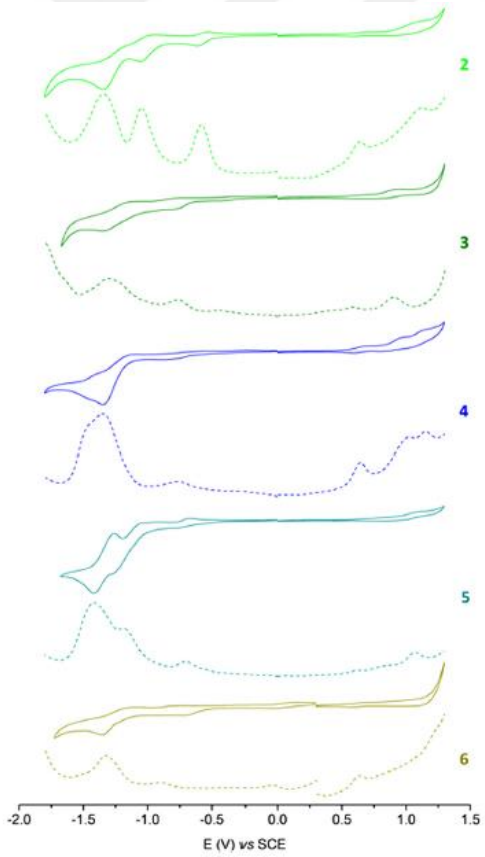

Figure 1.35 : CV and SWV of **2**-**6** in THF.

Cobalt Pc shows two reductions and three one electron oxidations. The first reduction peak derives from the reduction of the cobalt and the second peak derives from the reduction of the Pc ring. MnPc exhibits three reductions and one oxidation. The first and second reduction peaks are designated to be the reduction of the Mn and the third peak is designated to be the reduction of the Pc. In addition to them, the last reductions of Pc2, Pc3, Pc4, Pc5 and Pc6 are a multiple electron reduction of the Pc and four azobenzene units.

Koca A. and his co-workers reported electrochemical, spectroelectrochemical, and electrocolorimetric properties of double-decker Lu(III) Pc which conjugated with 3,4-ethylenedioxythiophene (EDOT) groups at β positions (Karadağ et al., 2014). In their study, five phthalocyanine ring reductions, three phthalocyanine ring oxidation, one EDOT group oxidation, and one electropolymerized EDOT-$LuPc_2$ based redox couple were observed (Figure 1.36).

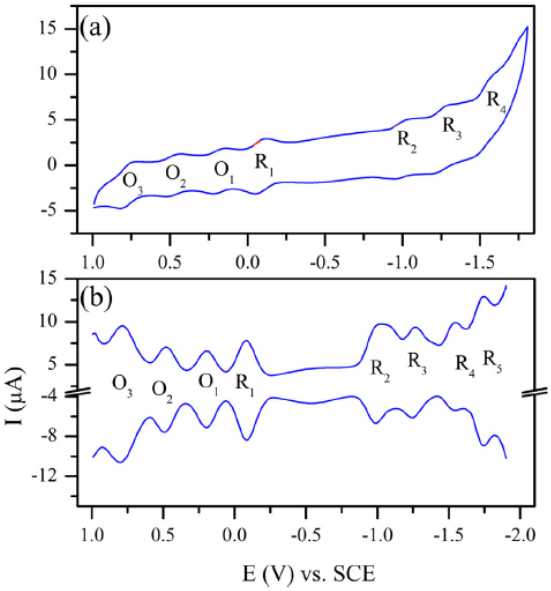

Figure 1.36 : a) CVs of EDOT-$LuPc_2$, **b**) SWV of EDOT-$LuPc_2$.

Electrochemical behavior and redox responses of EDOT-$LuPc_2$ was studied by CV and SWV in dicholoromethane/ tetrabutylammonium perchlorate electrolyte system with platinum working electrode. EDOT-$LuPc_2$ shows one redox couple R_1 at -0.08 V due to the reduction of the phthalocyanine structure and four reversible reduction processes, assignated to R_2 at -0.99 V, R_3 at -1.26 V, R_4 at -1.54 V, and R_5 at -1.75 V

respectively. Additionally, EDOT-$LuPc_2$ shows three reversible oxidations, O_1 at 0.20 V, O_2 at 0.49 V and O_3 at 0.79 V. The electrochemical results and ten redox couples indicate that EDOT-$LuPc_2$ enhance its potential usage in various areas of electrochemical applications.

1.3 Synthetic Approaches to Phthalocyanine Compounds

It is obvious that tetrapyrrolic macrocycles are very important in nature and they play vital roles in biological systems. The increased stability, enhanced spectroscopic properties, various coordination features and structural flexibility of phthalocyanines have made them one of the most studied compounds for various applications. Various utilizations, such as those recommended for phthalocyanines, require that these molecules have different physicochemical and electronic properties and that these properties are well defined. This requires synthetic methods with regioselectivity control and access to various types of substituents. This chapter will describe the various methods used for the preparation of substituted phthalocyanines, symmetrical and low-symmetric phthalocyanines and water soluble phthalocyanine derivatives.

1.3.1 Synthesis of substituted phthalocyanines

Almost all early phthalocyanine complexes do not contain any substituent in their peripheral and nonperipheral positions and the solubility of them is very low (less than 10^{-6}–10^{-7} M) (Moser et al., 1963). On the basis of the reported literature, the most suitable solvent for unsubstituted Pcs is H_2SO_4 and it can be used for purification of them. However, H_2SO_4 can not be used for lots of Pc derivatives, as it causes the demetalation and it protonates nitrogens at meso positions in the Pc ring.

Generally, the Pcs can be diversified by altering the central and the meso-atom or modifying the peripheral positions of the Pc core (Sharman et al., 2003; Özçeşmeci et al., 2018-2020). Peripheral substituents can be added to Pc core by modifiying the existing Pc ring with electrophilic substitution reactions and tetramerizaton of already functionalized Pc starting molecules. Functionalized ortho-phthalic molecules such as anhydrides, imides, amides, and nitriles are the most common precursors (Figure 1.37).

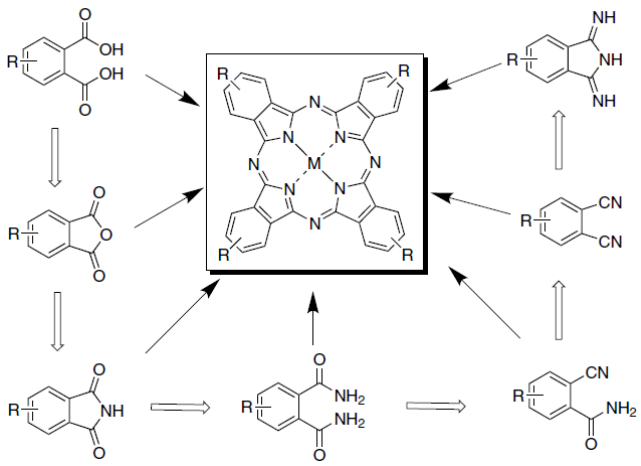

Figure 1.37 : Typical precursors for preparation of substituted phthalocyanines.

A fluorescent compound can absorb photon energy at one wavelength and then emit energy at another wavelength. More specifically, fluorescent probes absorbs the energy in the blue-green area and emitting in the green/red. In the literature, the synthesis of fluorescent probes which contain well-known classes of fluorophores were reported and they were suggested for cell imaging for the first time (Figure 1.38) (Bizet et al., 2018).

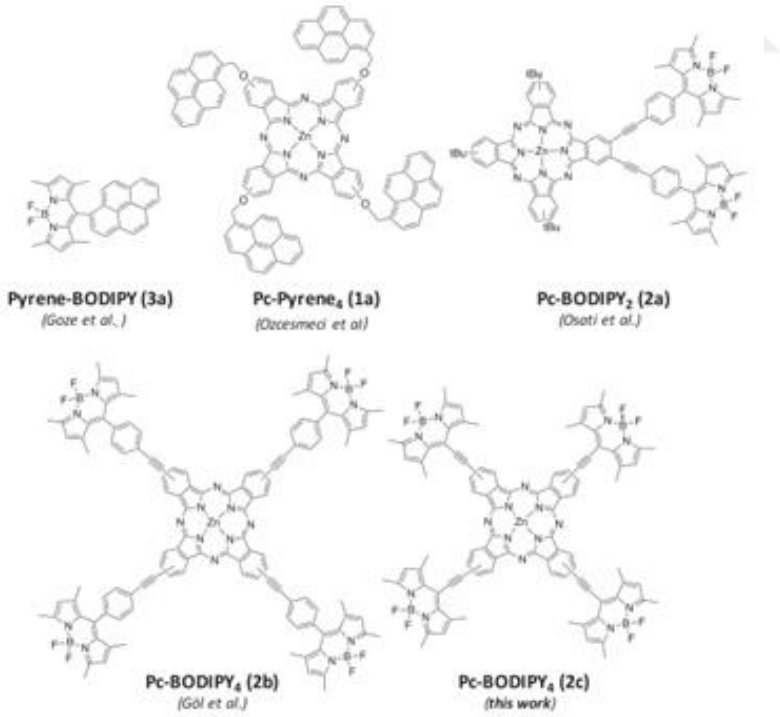

Figure 1.38 : Synthetic dyads/triads/pentads.

The preperation of Pc-pyrene (1) was carried out by cyclotetramerisation of pyrenyldicyanobenzene, though Pc-BODIPY (2c) was prepared by Sonogashira coupling reaction. Synthesis of pyrene including probes 1 and 3 are very easy to accomplish. In the synthesis of Pyrene-Pc 1, firstly pyrene carboxaldehyde are reduced with $NaBH_4$. In the second step, pyrenyl carbinol, which is achieved in the fisrt step, reacts with nitrodicyanobenzene to afford pyrenyloxydicyanonobenzene by S_NAr nucleophilic aromatic substitution mechanism. Target prob is synthesized with cyclotetramerized with zinc salt and 1,8-diazabicyclo[5.4.0]undec-7-ene. BODIPY substituted pyrene (3) was obtained in three stages. In this method, firstly pyrenyl-carbinol and dimethylpyrrole condensated by catalyzed of trifluoroacetic acid, then, p-chloranil was oxidated, deprotonated with triethylamine and lastly, borylated with boron trifluoride etherate.

Pc-BODIPY was prepared from BODIPY and tetraiodophthalocyanine $ZnPcI_4$ (Scheme 3.1). Dipyrromethane formed by condensation of dimethylpyrrole and trimethylsilyl propyl and then is oxidized, deprotonated and borylated to form compound 8. The tetrametilsilan (-TMS) protection was disassembled to obtain alkynyl-BODIPY 6 (Figure 1.39A).

In the synthesis of tetraiodophthalocyanine **7** was occured as follows: aminodicyanobenzene was reacted with $NaNO_2$ to form diazonium salt and then the salt reacted with iodide to prepare iododicyanobenzene **9**. In the next step, 1,8-Diazabicyclo(5.4.0)undec-7-ene catalyzed cyclotetramerization in refluxing $C_5H_{11}OH$ obtained $ZnPcI_4$ 7 (Figure 1.39B).

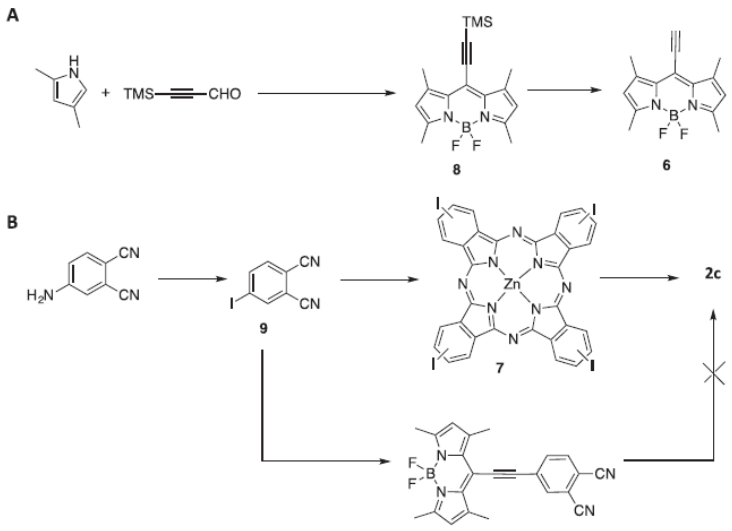

Figure 1.39 : Synthesis of BODIPY **6** and $ZnPcI_4$ **7**.

BODIPY-Pc conjugate 2c was synthesized by Copper(I)-Palladium(0) catalyzed Sonogashira coupling reactions with Pc 7 and alkynyl-BODIPY 6.

The Li/ $SOCl_2$ battery, which has attracted great interest of late years, is seen as a new energy source. Li / $SOCl_2$ battery has many advantages over other energy sources like high significant energy and power, high voltage, and low temperature performance. The Li/ $SOCl_2$ cell is comprise of carbon anode, lithium cathode and electrolyte solution of $SOCl_2$/ $LiAlCl_4$ (Szpak et al., 1984). At the present, in order to solve the voltage problems of battery, a lot of researches have been done. Jun Li et al. found that metalloporphyrins have potential application in Lithium/thionyl chloride battery and they used Li/ $SOCl_2$ battery as the catalyst to enhance the performance of battery (Zhang et al., 2014). In the other research, Y. Gao et al. synthesized a series of metalloPcs, conjugated with macrocylic aromatic systems by using microwave method and researched the effect of Pcs to Li/$SOCl_2$ battery (Figure 1.40).

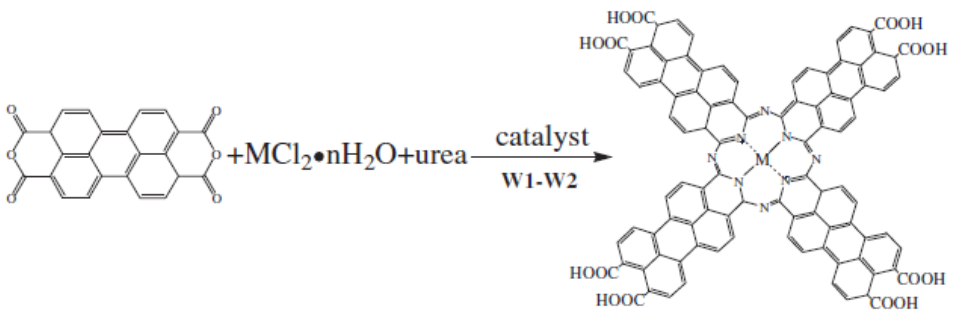

Figure 1.40 : Synthesis of MPcOc.

In order to prepare MPcOc, perylene-3,4,9,10-tetracarboxylic dianhydride, CH_4N_2O, $(NH_4)_2Mo_2O_7$, NH_4Cl, M $(OAc)_2 \cdot nH_2O$ were mixed. The mixture was exposed to microwave radiation with 400 watt for 3 minutes (w_1) and 640 watt for 5 minutes (w_2). The octacarboxyphthalocyanines with different central metals (manganese, iron, cobalt, nickel, copper, zinc) were achieved with same procedure with several metal derivatives. This paper proved that all of the catalysts improved the capacity by 19.34–55.64%, with the FePcOc increased the capacity by 55.64%.

In recent years, organic photovoltaics have attracted great interest as alternative energy sources. In particular, Bulk Heterojunction (BHJ) devices, which are seen as an alternative to silicon-based photovoltaics, show an increasing trend (Duan et al., 2016). BHJ solar cell consists of poly(3-hexylthiophen-2,5-diyl) as electron donor and fullerene derivatives as acceptor. Although significant advances of BHJ cells, limited absorption wavelenght of P3HT is a drawback for these high performance devices. Therefore, it is of paramount importance to develop new donors with broad absorption in the longer wavelength region.

1.3.2 Synthesis of low-symmetry phthalocyanines

Although the use of unsubstituted phthalocyanines is limited as a result of the excessive insolubility of them, phthalocyanines substituted with various functions have been prepared to increase solubility and enhance their capability in most of these potential applications. Asymmetrically substituted phthalocyanines display more sophisticated properties compared to unsubstituted or symmetrically substituted derivatives.

Recently, the development of low symmetrical phthalocyanines has attracted particular attention. Up to now, four types of unsymmetrical phthalocyanines have been identified such as A3B, ABAC, ABAB and AABB (Figure 1.41) (Wang et al., 2012).

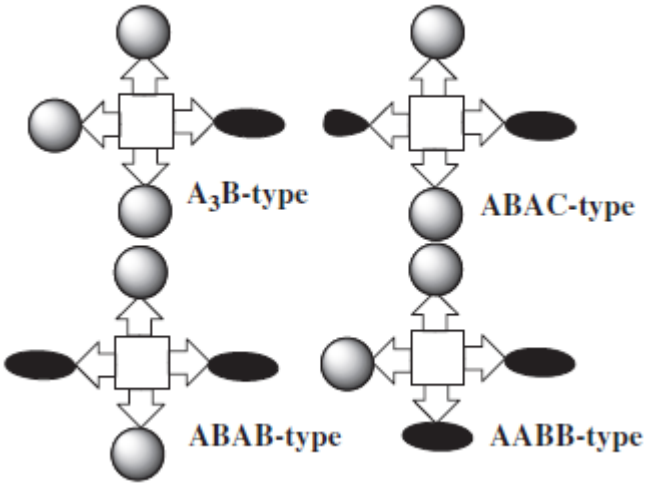

Figure 1.41 : Types of unsymmetrical phthalocyanines.

A_3B-type Pcs are mostly prepared by using the statistical condensation method. In that method, a mixture is obtained which every phthalocyanine molecule has three identical and one different isoindole units. In order to prepare A_3B type phthalocyanine, A and B subunits are employed from 3:1 to 9:1 ratio, rarely can this ratio be raised to 10:1 and even higher by reason of substituents. Difficulty in separating similar chemical structures in that mixture is the most common disadvantage.

Phthalocyanines and their analogs are seen as potential nonlinear optical materials, therefore especially unsymmetrical phthalocyanines are subject to many researches. Semiconductor quantum dots have been drawn interest in the field of photonics and optoelectronics. However, covalently bonded QDs and phthalocyanines that could tender developed nonlinear optical response are new reseach area. N. Nwaji et al. reported the synthesis of asymmetric benzothiazole substituted phthalocyanines and their binding to glutathione (GSH) substituted QDs (Figure 1.42) (Nwaji et al., 2018).

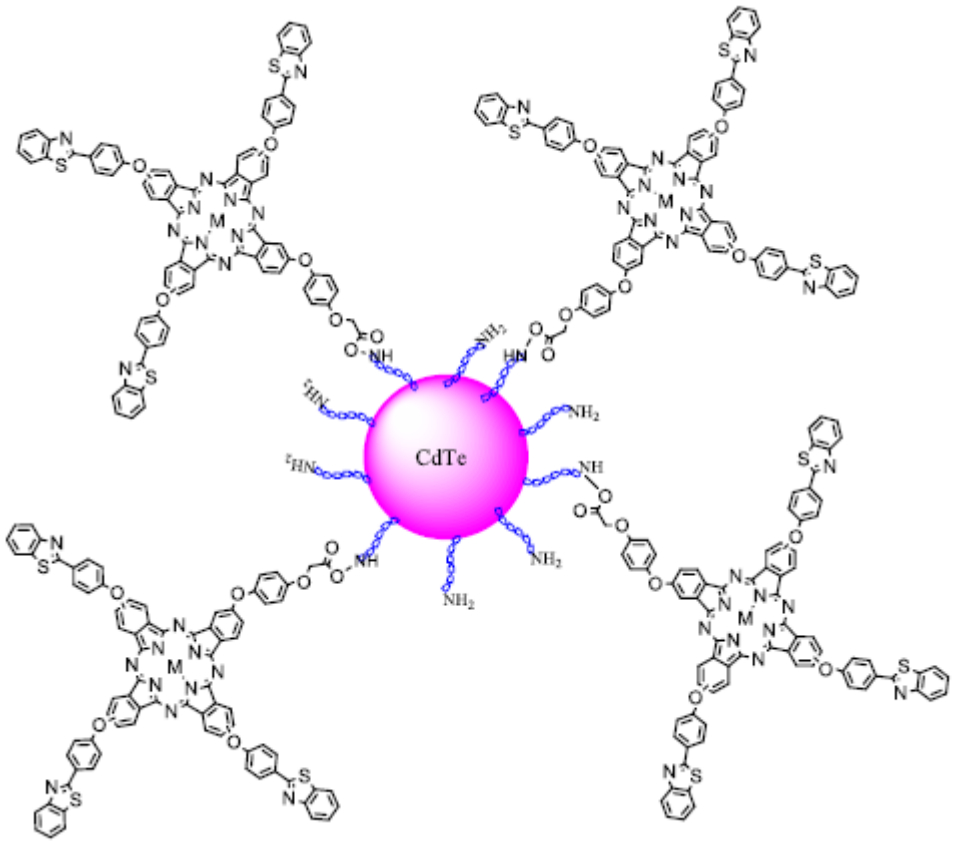

Figure 1.42 : Illustration of the Pc complexes to CdTe quantum dots.

In this work, primarily metal Pc complexes were obtained by using a trace amount of 1,8-diazabicyclo(5.4.0)undec-7-ene and $C_5H_{12}O$ as solvent. Later, carboxylic acid functional group of phthalocyanines were activated with DCC and CdTe nanoparticles were added covalently at room temperature. NLO features of Pc derivatives were searched by using open apeture Z-scan method at around 530 nm and 10 ns pulse duration. Z-scan experiments has showed that QDs contributed the NLO behavior of Pcs.

Due to the increasing need for advanced technological applications, multifunctional organic materials have attracted great concern. Organic field-effect transistors (OFETs) are promising constituents for organic electronic appliances which containing an organic semiconductor layer. An organic semiconductor used in the active layer of an organic field-effect transistor requires high capacitance and field-effect mobility. Recently, numerous studies showed that the expansion and extension of π-conjugation improved the charge carrier mobility and phthalocyanine derivatives

having π conjugated macro rings. In 2018, a ferrocenyl carborane containing unsymmetrical Zn phthalocyanine was synthesized for OFET (Nar et al., 2018). In that paper, OFET properties of a novel Pc−carborane derivative, which contain an low-symmetrical ZnPc attached to a ferrocenylcarborane cluster were investigated. The synthetic route to the target phthalocyanine-carborane-ferrocene triad system were shown in Figure 1.43.

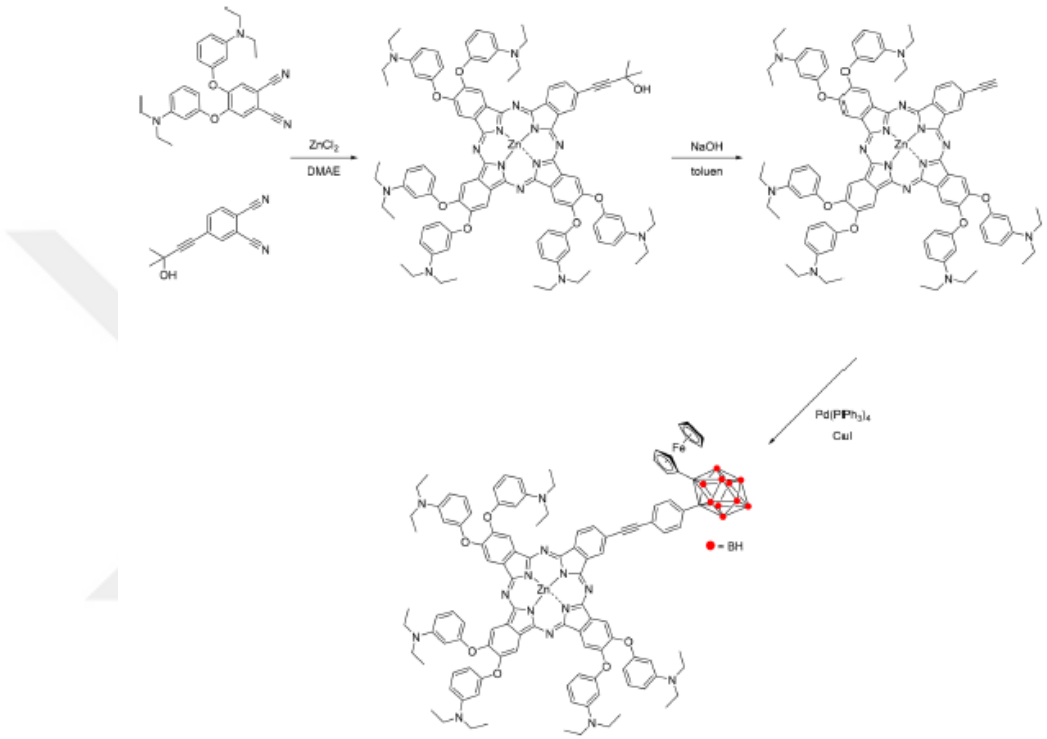

Figure 1.43 : Synthesis of phthalocyanine-carborane-ferrocene triad system.

Target phthalocyanine derivative was synthesized in three steps via ferrocenylcarborane subunit and unsymmetrical substituted zinc phthalocyanine intermediate. Ferrocenylcarborane was prepared by the reaction of ethynyl ferrocene with 1,4-diiodobenzene with bis(triphenylphosphine)palladium(II) dichloride as the actual and CuI as the cocatalyst and then reacted with decaborane in the presence of C_2H_3N and C_7H_8. Unsymmetrical substituted zinc phthalocyanine was synthesized from 4- (3-hydroxy-3-methyl-1-butynyl) phthalonitrile and 4,5-bis (3-dietylaminophenoxy) phthalonitrile with $ZnCl_2$. Then, ethynyl function was removed by reaction with NaOH. In the last step, the targeted triad system was prepared by the reaction between ethynyl-functionalized unsymmetrical phthalocyanine and

ferrocenylcarborane. Also, semiconductor properties of these phthalocyanine derivatives for use as an active side in the devices.

Electronic delocalization of phthalocyanines gives them a great number of exclusive properties and makes them beneficial in different applied fields. The ability to synthesize unsymmetrical phthalocyanines with the substituents in the predetermined positions allows for the fine-tuning of various physical features, thereby increasing the implementations of phthalocyanine compunds.

1.4 Medical Applications of Phthalocyanines and PDT

Besides all these individual electronic, optical and structural behaviors of phthalocyanine derivatives that have become increasingly important; antifungal, antibacterial and antioxidant properties were also researched. In recent years, by the reason of widespread usage of antimicrobial medications which is indicated to infectious diseases, multiresistance has been developed in human microorganisms. Therefore, researchers have been interested in researching new antimicrobial agents. Especially cationic phthalocyanines are distinguished by their antimicrobial properties.

In 2018, the synthesis and characterization of tetra-substituted phthalocyaninatochlorogallium (III) tetraiodide and phthalocyaninatochloroindium (III) tetraiodide were described and their antioxidant and antimicrobial efficiencies were compared with priorly prepared metallo and metal-free Pcs by Makbule Burkut Kocak's research group (Figure 1.44) (Saki et al., 2018).

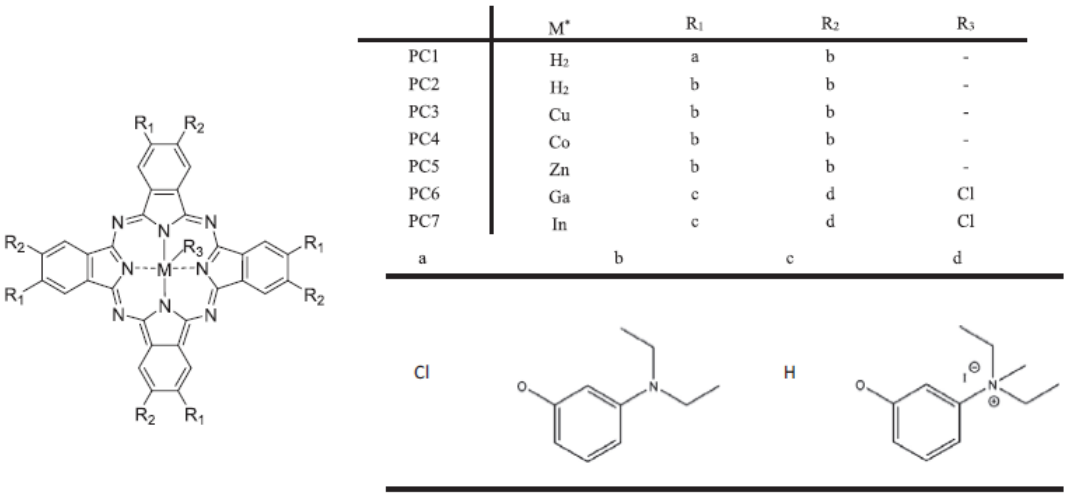

Figure 1.44 : Metallo and metal-free phthalocyanine derivatives.

In that research, different test methods were used in order to determine the antioxidant efficiencies and antimicrobial properties of phthalocyanines.

In the 1,1-diphenyl-2-picrylhydrazyl -free radical scavenging activity method, Pc4 has the highest scavenging activity (58.37 ± 0.14%) and Pc6 has the lowest scavenging activity (38.02 ± 1.07%) at 600 mg/mL concentration. Redox activity of the central atoms influences positively antioxidant property of Pcs, so Pc4 showed highest DPHH activity as 50.32 ± 0.17% at 400 mg/mL concentration. The interaction of carotenoids with free linoleic acid radicals determines the antioxidant activity of carotenoids. The highest antioxidant activity was demonstrated by Pc5 phthalocyanine as 71.83 ± 1.62% at 500 mg/mL. Also, Pc5 showed the highest reducing power as 0.391 nm. Among all the tested phthalocyanine derivatives, only quaternized Pc derivatives, Ga (Gallium) metal containing Pc complex Pc6 and In (Indium) metal containing phthalocyanine complex Pc7 displayed antimicrobial activity on all tests.

Phthalocyanines are highly suitable molecules for cellular imaging and phototherapies due to their high extinction coefficients and absorption characteristics in the near-IR area. Biomedical imaging methods provide considerable datas for early detection and therapy of diseases. In addition to them, phthalocyanine derivatives have been used in imaging methods involving photoacoustic imaging, PET, MRI, and fluorescence imaging. Also, Pcs have been seen potential theranostic molecules for fluorescence guided drug targeting systems and curation of tumors by PDT. Theranostic agents

comprise both the imaging agent and the therapeutic agent in the same structure, and both agents participate to treatment at the same time and with the same biodistribution. Despite the unique photophysical properties of phthalocyanine and its derivatives, their low solubility in water and limited selectivity for tumor tissues limit the use of phthalocyanines in clinical applications. In 2013, to solve these problems Taratula et al. synthesized a new theranostic for tumor-targeted delivery of dendrimer Pcs (Taratula et al., 2013). The synthesis of Pc−LHRH involves a two-step process as shown in Figure 1.45. In the first step, substituted Pc was encapsulated in PPI dendrimer. In the second step, the dendrimer surface was modified with PEG and LH-RH peptide.

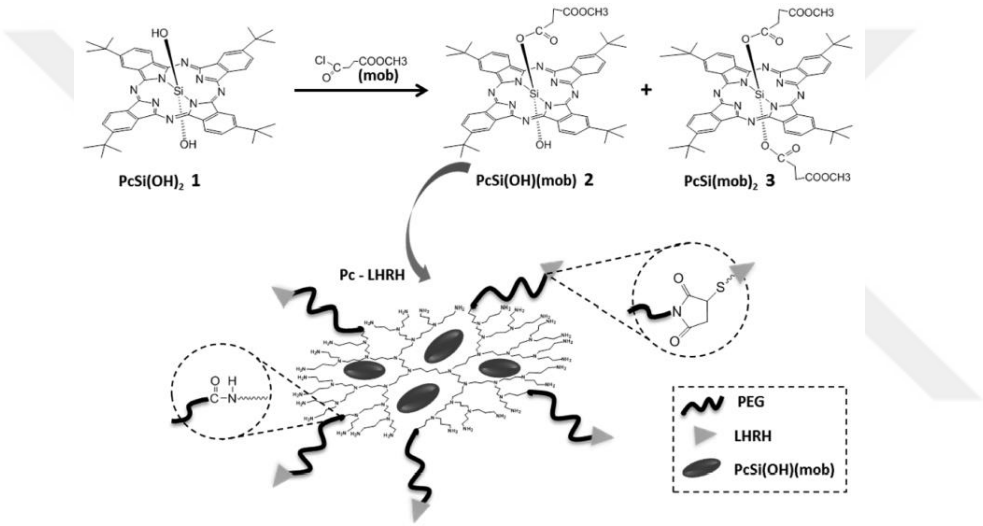

Figure 1.45 : Schematic representation of two-step process of Pc-loaded dendrimer.

The major challenge in developing an effective therapeutic agent for photodynamic therapy and fluorescent imaging is the transport of tumor-targeted carrier to cancer cells. To indicate the efficacy of the improved theranostic agent with in vivo study, theranostic agent was injected to mice carrying ovarian cancer and NIR fluorescence studies were noted at regular intervals (Figure 1.46). In the figure organs; 1, liver; 2, spleen; 3, kidneys; 4, heart; 5, lungs; 6, tumor. Blue color is expressing the lowest intensity of fluorescence, and red color is expressing the highest intensity of fluorescence.

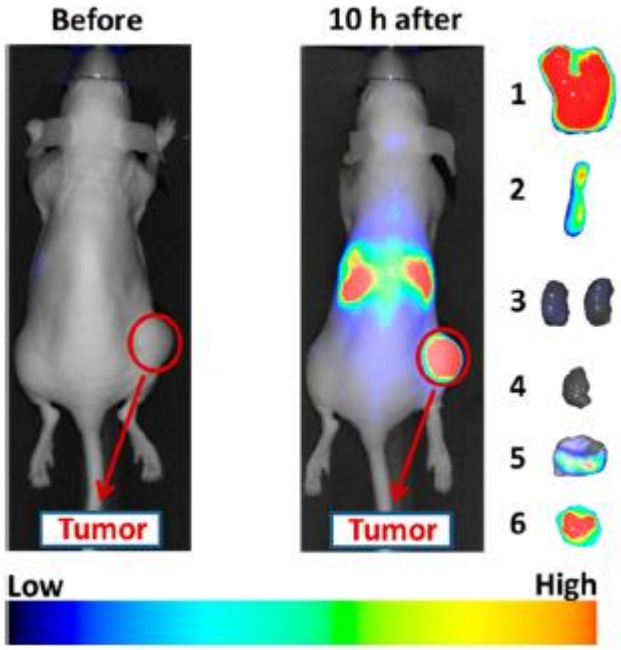

Figure 1.46 : In vivo images of mouse carrying ovarian cancer.

Tendency of accumulation of Pc−LHRH theranostic agent mostly in the cancer cell and liver shows that effective targated-transfer of Pc was improved. Consequently, Pc−LHRH complex is a promising NIR theranostic agent owning to outstanding phototherapeutic effect and effective subcellular accumulation.

Photodynamic Therapy is a new therapeutic procedure that combines a molecule used as a light-sensitive drug and visible light at appropriate wavelength. This treatment method, which has a long history dating back to 1985, is still used in cancer treatment. Traditional cancer treatments such as surgery, radiotherapy and chemotherapy can cause serious advers reactions, such as damage to healthy tissues as well as tumor tissues. Therefore, more selectivity for diseased tissues has been the priority in the development of new treatment methods. However, PDT allows selective treatment by restriction of the radiation to specific regions by selective photosensitizer.

PDT usually consists of three stages; first, administration of the photosensitizer, second, waiting for drug biodistribution, and at last, administration of red or near infrared radiation to the target area. The photochemical and photophysical rules of PDT have been comprehensively investigated. At the first stage, the PS is excited from the ground state to the first excited single state by absorbing light of a specific

wavelength. In the second stage, S1 is converted to the triple state (T1), and this triple state enables the excited PS to interact with the neighboring particles. It is agreed that cytotoxic species which are the key agents of cellular damage are produced in this stage. The T1 state then relaxes to ground state with two mechanisms, defined as Type I or Type II. In the Type I mechanism, T1 state molecule transfers to a surrounding substrate to produce radicals. In the Type II mechanism, energy from T1 state molecule transfers to ground state oxygen (Figure 1.47) (Liu, 2010).

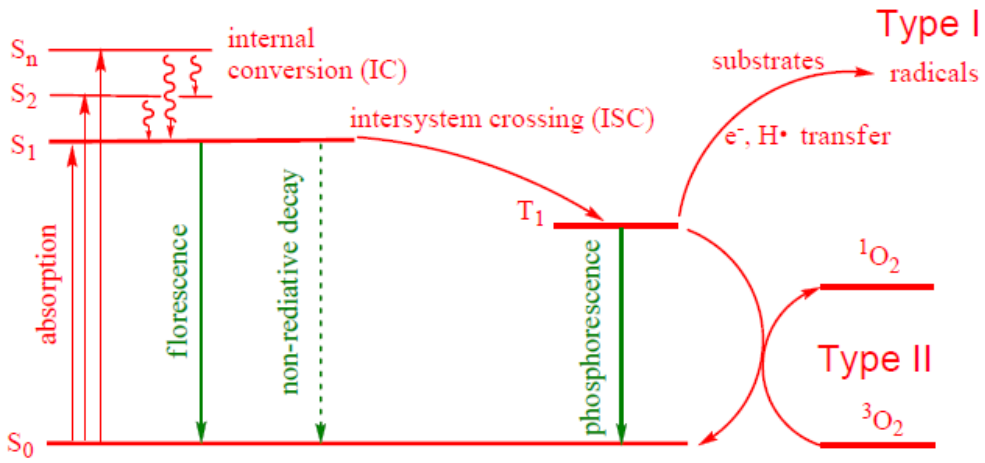

Figure 1.47 : Type I and II mechanisms of Photodynamic Teraphy.

Singlet oxygen which is a more active form of oxygen reacts with biomolecules and kill cancer cells directly.

An ideal photosensitizer for photodynamic therapy should satisfy requirements described below; chemically pure drug, selective tumor accumulation and excellent targeting, possession of low dark toxicity and high photocytotoxicity, strong absorption capability in the 680–800 nm of the visible spectrum.

Hematoporphyrin derivatives (HpD) such as Photofrin were used as first generation photosensitizers in early clinical trials of PDT (Allison et al., 2010). Excellent results have been achieved for the medication of lung cancer, oesophageal cancer, bladder cancer, gastric cancers, cervical cancer and cervical dysplasia with Photofrin photodynamic therapy (Figure 1.48) (Sharman et al., 1999).

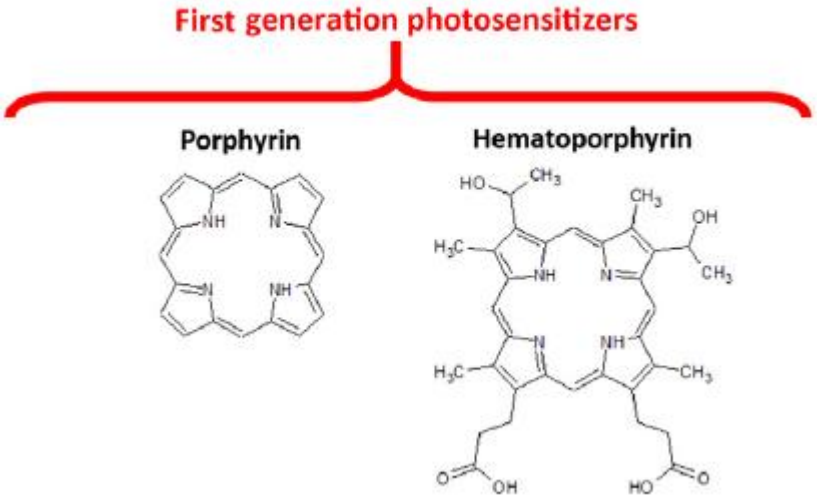

Figure 1.48 : First-generation photosensitizers.

Although the success of hematoporphyrin derivatives is proven, they have two major disadvantages. First one is about the accumulation of hematoporphyrin derivatives on tumor tissues and it takes ten weeks. This situation causes the skin photosensitivity and requires protection from bright sunlight. Secondly, Photofrin has a weak absorption band at aorund 600 nm is used mostly to excite the photosensitizer. These disadvantages have necessistated to the development of second-generation photosensitizers. The composition and structure of the second-generation photosensitizer are clear, and they are more photosensitive, absorbs more strongly, and more selective for tissue than first generation photosensitizers. Most of the second-generation photosensitizers are porphyrin derivatives such as benzoporphyrins, purpurines, texaphyrins, phthalocyanines, naphthalocyanines and protoporphyrin IX (PpIX) (Figure 1.49).

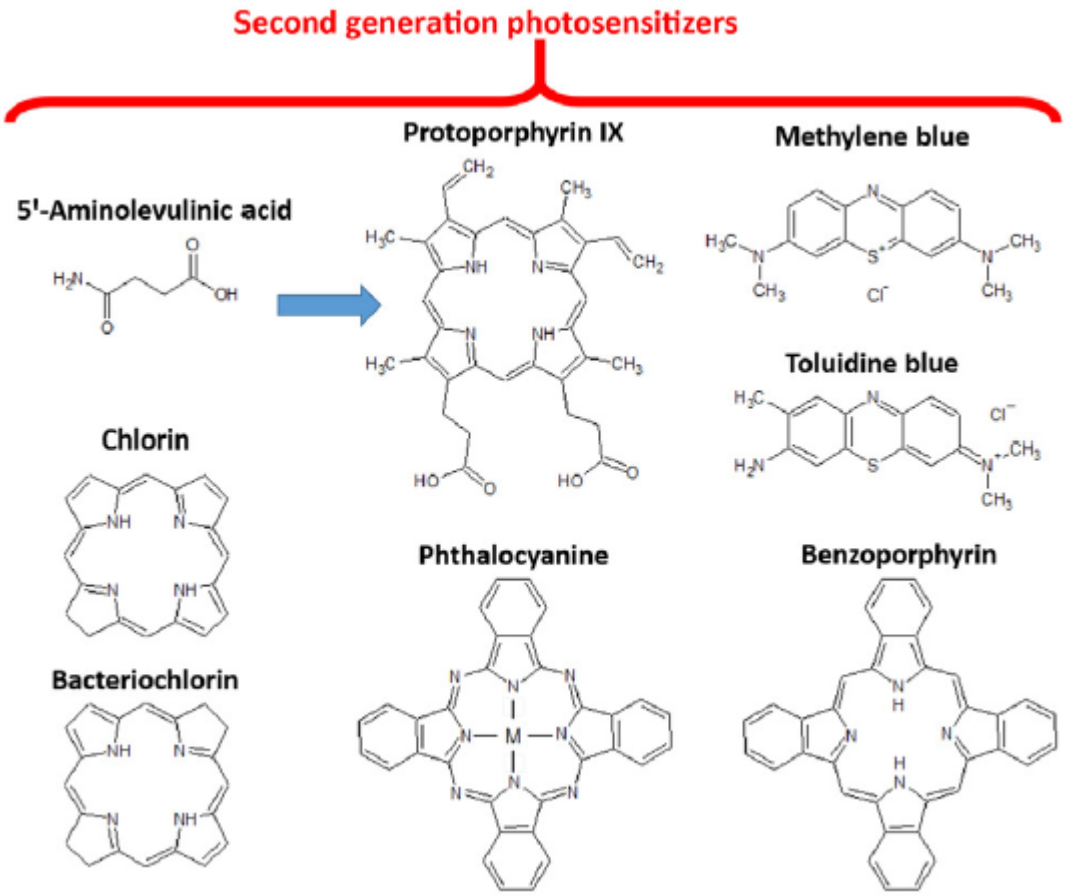

Figure 1.49 : Second-generation photosensitizers.

One of the promising groups of photosensitizers is Pc derivatives showing very good chemical homogenity, strong absorption at 675-700 nm of spectrum, high extinction coefficient, and high quantum yield of singlet oxygen. Lately, a lot of anionic and cationic Pcs, such as Photosens, Holosens, and Phthalosens, were proposed as PDT sensitizer. Photosens is a sulfated AlPc which has higher degree of hydrophilicity and the lowest photodynamic activity. Holosens is a cationic ZnPc which efficiently enters the cells. Phthalosens is a metal-free analog of Photosens which has highest photodynamic activity. One study performed a comperative tests of Photosens, Holosens, and Phthalosens for their cellular uptake dynamics, intracellular distribution, and dark and photo-induced toxicities (Brilkina et al., 2019).

All the compounds under study displayed intense absorption at 650-700 nm and maximum absorption of Photosens, Holosens and Phthalosens are recorded at 678, 685 and 675 nm, respectively (Figure 1.50).

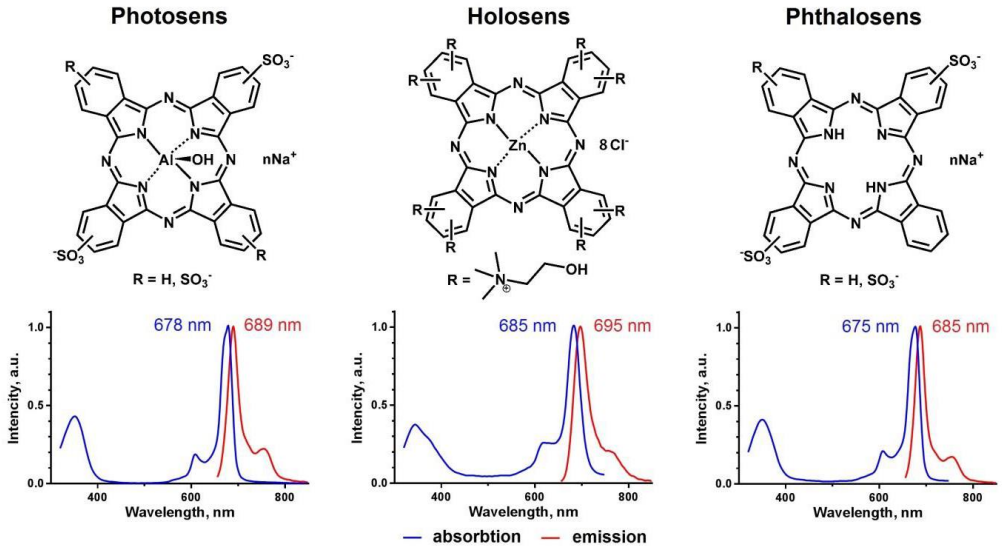

Figure 1.50 : Absorption and emission spectra of Photosens, Holosens and Phthalosens.

The cellular uptake of them into urinary bladder and human hepatic adenocarcinoma cells was examined and it was observed that they reached saturation after 4-8 hours. While the ratio of intake to the cells is maximum in Phthalosens, it is minimum in Photosens. Fluorescent LSM images show that the Photosens and Holosens are dispersed into the cell, and the Phthalosens accumulate in the plasma membrane of cell.

The phthalocyanine based photosensitizers were found to have different dark toxicity according to their localisation. Accordingly, Phthalosens and Holosens deposited in the Golgi complex and plasma membrane and Photosens accumulating only in lysosomes. Phthalosens and Holosens are more toxic than Photosens. As a result, Photosens has the most slowly cellular uptake, accumulates in lysosomes and has a less photodynamic effect. Cationic Holosens localize in the Golgi complex and has a remarkable photodynamic impact. Amphiphilic phthalocenes penetrate cells the fastest wherethrough the outer cell membrane into the cell plasma and bring about the maximum decrease in cell viability.

Despite PDT provides an effective and safe treatment on cancerous cells and tissues, its clinical applications are limited. Most of the photosensitizer (PS) drugs have low solubility in water due to their hydrophobic character, so their quantum yield is low and they are easily aggregated. In some cases, although PS drugs are modified to

increase their solubility in water, selective accumulation in target cells / tissues remains insufficient for clinical practice. In this context, targeting of PS drugs improves both specificity and effectivity of PDT and surpasses some of the present challenges of untargeted photodynamic therapy. It is thought that the combination of hydrophilic nanoparticles with PS drugs will help increase the solubility of PS drugs in water and thereby facilitate their uptake into the cell. Furthermore, the nanoparticles provide surface area for the binding of targeting moieties which will confer cell specificity to PS drugs. This also increases the bioavailability of PS drugs and prevents damage to healthy tissues.

Until today, various organic and inorganic nanomaterials have been researched for effective and targeted photosensitizer delivery. For example, liposomes and polymeric nanoparticles, have enabled PS drugs to be used as biocompatible and biodegradable materials and also delivered in a safe and controlled manner. Inorganic nanomaterials can provide additional functions such as diagnosis and imaging to PS drugs for PDT because of the adjustable optoelectronic properties. Both types of materials provide an effective solution to eliminate the drawbacks of existing PS drugs and to selectively deliver to target areas with greater surface functionality. Eun Ji Hong et al. have summarized PS drug formulations combined with various organic and inorganic nanomaterials that exhibit effective PDT in both in vitro and preclinical animal studies (Hong et al., 2016). To enhance the water solubility and selective accumulation in target tissues/cells of PS drugs need polymeric or lipid-based nanocarriers. In this context, the use of liposomes, polymeric micelles and polymeric nanoparticles as PS carriers in PDT was investigated. In a study, magnetoliposomes (MLs) containing ZnPc with cucurbituril were synthesized and the *in-vitro* cytotoxicity of photodynamic therapy was analyzed on B16-F10 cells incubated with CB: ZnPc-ML (Bolfarini et al., 2012). A remarkable reduction in cell viability was observed after irradiation and AC magnetic field application of melanoma cells incubated with CB: ZnPc-MLs. Accordingly, it has been shown that although both treatments are administered separately, co-administration may be more effective. Furthermore, the liposomal preparations prepared have enabled the use of synergistically combined PDT and Magnetohyperthermia (MHT) treatment.

The work on zinc monocarboxyphenoxy phthalocyanine conjugated with spermine as a targeting complex shows that improved the photodynamic therapy (PDT) effect on MCF-7 breast cancer cells (Figure 1.51) (Ogbodu et al., 2015).

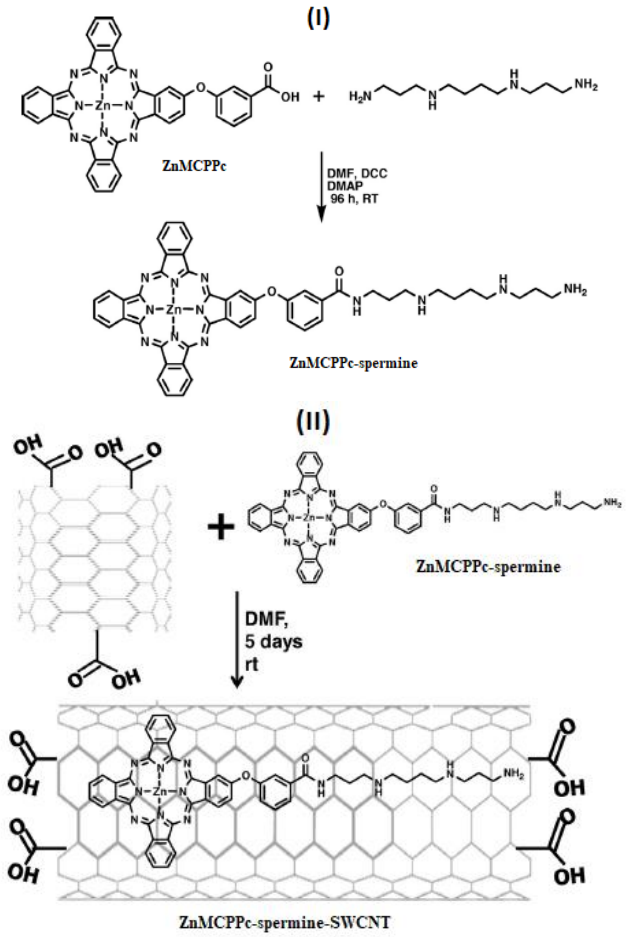

Figure 1.51 : Synthesis of ZnMCPPc-spermine (**I**) and ZnMCPPc-spermine-SWCNT (**II**).

R. O. Ogbodu et al. investigated the photophysical specialities of SWCNTs on ZnMCPPc-spermine complex and their efficiency on MCF-7 for the first time. PDT tests of ZnMCPPc, ZnMCPPc-spermine, and ZnMCPPc-spermine-SWCNT were carried out by treating the phthalocyanine derivatives with MCF-7 cancer cells. Then they were irradiated with photons. As a result of photodynamic therapy, only 64% reduction in cell viability was observed in ZnMCPPc complex, while the presence of sperm in ZnMCPPc-spermine improved the photodynamic therapy efficiency of ZnMCPPc molucule, leading to a 97% reduction in cell viability. In the presence of

SWCNT in ZnMCPPc-spermine-SWCNT complex decreased the PDT activity and resulted in 95% cell viability.

Since their discovery, numerous phthalocyanine derivatives which have types of photophysical and photochemical properties have been developed for medicinal applications. Solubility, therapeutic efficacy, targeting ability, and side effects are the main topics examined in phthalocyanine research, and these remain the main challenges for the future design of new medical phthalocyanines.

1.5 Boron Neutron Capture Theraphy (BNCT)

BNCT is a kind of radiotherapy bearing non-radioactive boron compounds which is administered by intravenous injection into the patient, and then irradiated with a suitable neutron beam. 10B isotope absorbs a neutron and converting excited 11B nucleus, and this nucleus produces highly cyototoxic $^{4}_{2}He^{+}$ and $^{7}_{3}Li^{+}$ particles and 2.4 meV of kinetic energy (Figure 1.52). When the reaction happens in a cell, two ionic molecules can cross the nucleus and induce irreversible damage to DNA.

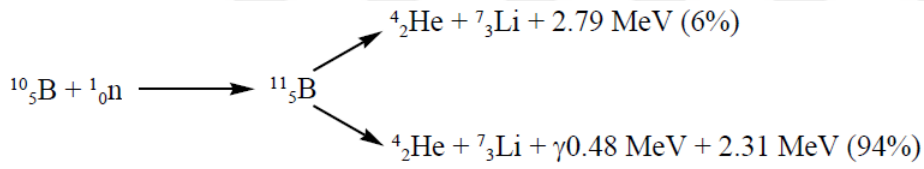

Figure 1.52 : Nuclear reaction of ^{10}B isotope with a neutron.

The potential effectiveness of BNCT is based on its selectivity, in fact, tumor tissues can be filled with a higher concentration of boron as regards healthy tissues using appropriate borate compounds.

The destructive effects of high energy $^{4}He^{+2}$ and $^{7}Li^{+3}$ particles are limited to tissues having boron. Theoretically, BNCT cannot selectively destroy malignant cells and adjacent healthy tissues, since these particles (5-9 μm) have very short path lengths.

Clinical trials for BNCT were primarily conducted for patients with gliomas and head and neck tumors, in which traditional treatment failed.

About 50 years ago, the development of boron-conjugated molucules for BNCT was started by evaluating small boron compounds as first-generation agents.

A BNCT delivery agent must have the following characteristics: 1) low toxicity and normal tissue uptake, with a tumor: normal tissue and tumor: blood (T: B1) boron concentration rates of ~3; 2) tumor boron concentration of ~20 μg 10B/ g tumor; 3) relatively fast clearance from blood and normal tissues and persistence in the tumor during neutron irradiation.

1.5.1 History and current status of BNCT

After the discovery of the neutron, first, in 1936 the idea of using boron neutron capture emerged for therapeutic application. The first clinical practice of BNCT, which is defendeed as a modernist therapy with the potential to be the suitable cure for various types of cancer, was carried out in the USA in the early 1950s (Farr et al., 1954).

Boron containing delivery agents are grouped into three generations. The first one comprises water-soluble inorganic borates, the second agents are the polyhedral boranes, and the third agents are biomolecular analogs that may be located in subcellular structures.

Sodium borates are named as first-generation BNCT agents. fact that the method was not selective, the persistence of tumor cells was short, and the boron: tumor concentration ratio was low.

Then, in 1961, about 40 patients received 3 series of treatments using simple inorganic boron compounds. During these treatments, untreated radio dermatoses were observed in some patients (Archambeau, 1970). In 1961, after having disappointing results in the United States, in 1968, H. Hatanaka started to implement BNCT into clinics in Japan by using disodium mercaptoundecahydro-closo-dodecaborate (Hatanaka, 1991). The exciting results which was reported by Hatanaka on patients have grade III and grade IV malignant glioma, have been led to the attention of clinical applications of BNCT in both the US and Europe. Also, in 1987, p-borophenylalanine (BPA) was introduced to treat superficial malignant melanoma (Mishima et al., 1989).

In 1994, epithermal neutrons were used for irradiation for the first time at the BNL, USA. This innovation improved the penetration, and provided to reach higher boron concentration in the tumour owing to neutron thermalization (Coderre, et al., 1997).

In 1997, a research programme was started for the cure of cerebral tumors in Netherland and Germany in university hospitals and then in 1999 and 2000 in Sweden and Finland (Moss, 1990; Capala et al., 2003; Joensuu et al., 2003).

In 2001, a patient has liver with multiple metastasis influenced by primary colon carcinoma was cured by using a new treatment (Pinelli et al., 2002).

The BNCT method using thermal neutron beams can be used to treat other tumors outside the central nervous system, such as skin melanoma. Currently, sodium borocaptate and p-borophenylalanine are the only two medications used in clinics (Figure 1.53). Despite more than 60 years, BNCT is still hindered by some technical problems. The lack of suitable clinical studies, the necessity of clinical irradiation in nuclear reactors, and the use of the same ^{10}B complexes for 60 years are the most important of these barriers. Contrary to the aforementioned statements, there have been some developments in recent years that have led to optimism about the future of the BNCT.

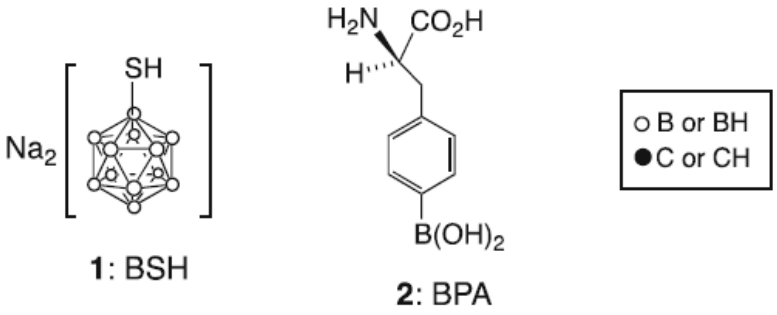

Figure 1.53 : BSH and BPA boron delivery agents.

Thanks to the importance attached to the synthesis of boronated derivatives of biological molecules, the design of therapeutic complexes that have the ability to accumulate in subcellular structures have accelerated.

1.5.2 Phthalocynines as BNCT agents

Carboranes are very good sources of boron atoms that electron-delocalized clusters composed of boron, carbon, and hydrogen atoms that have wide variety of potential applications in medicinal chemistry. Carboranes and other polyhedral boranes are considered as a suitable boron sources for BNCT. Compared to most anti-cancer drugs, carboranes are not classified as chemotherapeutic agents due to some disadvantages such as low water solubility, rapid blood purification, and low tumor selectivity. Accomplished medication of cancer cells with BNCT requires selective accumulation of the ^{10}B fragment in cancer cells. One way to overcome this challenge is to bind the ^{10}B complex to different biomolecules, i.e. tumor-specific molecules. The challenge for chemists is the synthesis of boron containing molecules that overcomes all these problems described above.

Polyhedral closo- and nido-carboranes and closo-dodecaborate anions are used as boron containing fragments for boron neutron capture teraphy (Figure 1.54).

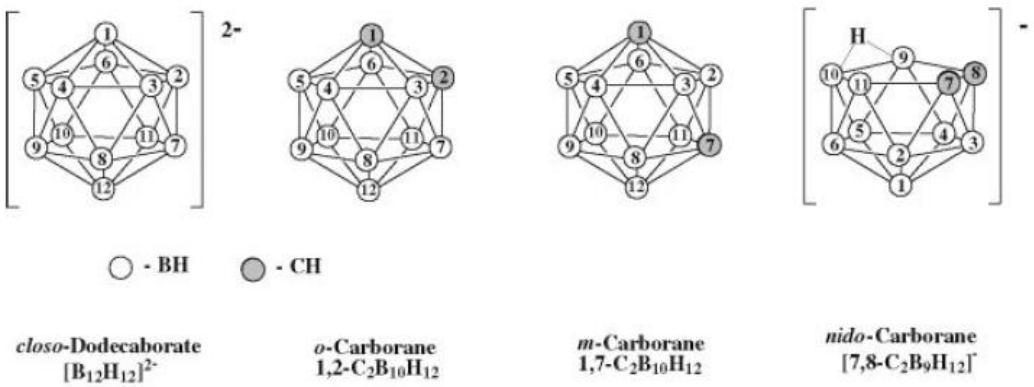

Figure 1.54 : Structure of dodecaborate and carboranes.

The boron groups mentioned have different solubility character in water. Closo-carboranes are hydrophobic, nido-carboranes and closo-dodecaborate are very soluble in water owing to their anionic structure.

Some phthalocyanines (Pcs) have been proved to be localized and persisted in various solid tumors. Thereby, using a phthalocyanine to deliver boron atoms to cancer cells may be a suitable strategy to solve the accumulation problem. The low solubility of phthalocyanines is an obstacle in the purification and characterization stages.

Therefore, the main problem is the synthesis of a boron containing Pc with both lipophilic and hydrophilic units in therapeutic solutions.As the first sample of carborane-containing phthalocyanine was synthesized in 1989 (Figure 1.55) (Alam et al., 1989).

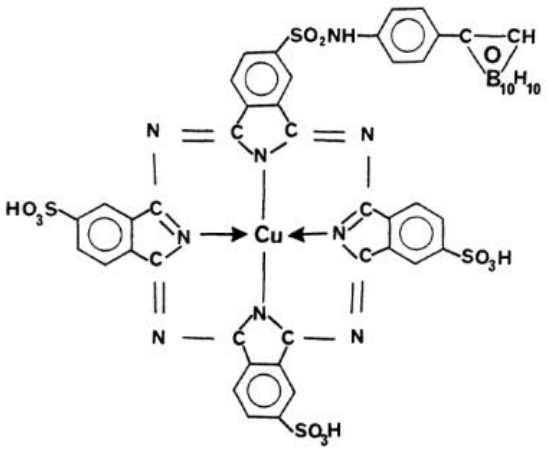

Figure 1.55 : First sample of carborane-containing phthalocyanine.

BNCT is arise from the interaction of two innocuous particles, the ^{10}B and the thermal neutron. The ^{10}B nucleus has the ability to effectively capture low-energy thermal neutrons. The excited ^{11}B nucleus that formed by the ^{10}B nucleus capturing the thermal neutron forms the highly energetic ^{4}He and ^{7}Li particles. The effective range of each of these highly energetic particles in the tissue is approximately 10 μm. The area of influence of cellular damage is approximately the diameter of the cell.

The molecule with the highest boron content is a supramolecular cuboctahedron containing 240 boron atoms. The cuboctahedron was synthesized from Cu2+ paddle-wheel nodes and carborane–isophthalic acids with easily with high yield (Clingerman et al., 2013). Its nanostructure was characterized in the solid state via X-ray diffraction method. Its structure is illustrated in Figure 1.56. **(a)** crystallographic c axis and this axis correspond to a molecular C_3 symmetry axis. **(b)** molecular C_4 symmetry axis. Color key for **(a)** and **(b)**: pink icosahedra = carborane cages; blue squares = biscopper paddlewheel nodes; grey hexagons = benzene rings. **(c)** part is the space-filling illustration of cuboctahedron. Color key: pink = B; red = O; blue = Cu; grey = carbon; white = hydrogen.

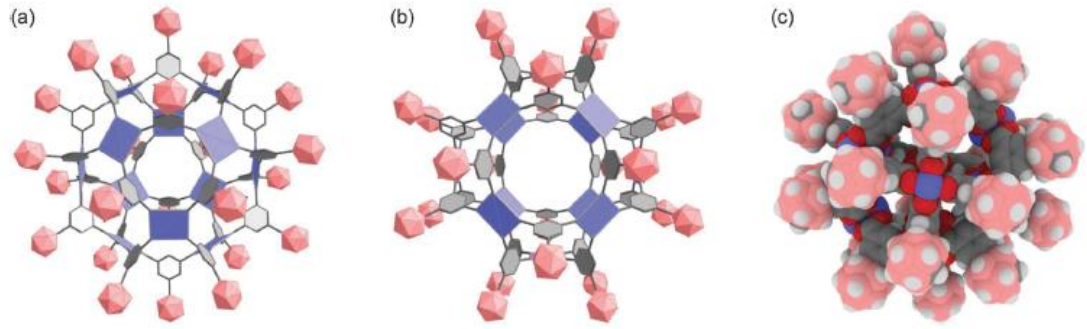

Figure 1.56 : Molecular structure of cuboctahedron.

In this article, it is stated that the preparation of ^{10}B-rich supramolecular structures that may be useful for BNCT is continued.

In 2013, B. Birsöz et al. reported a paper that described a ZnPc comprising 96 boron atoms per molecule (Birsöz et al., 2013). In this study, the synthesis of metallophthalocyanine substituted with eight hydroxy units at peripheral positions was explained, and by in vitro studies, it was proven that high boron concentrations in the cell can be maintained with this molecule. The synthetic route of novel phthalocyanines containing eight dodecaborate groups with diethyleneoxyphenoxy fragments at α-positions was shown in Figure 1.57 and Figure 1.58.

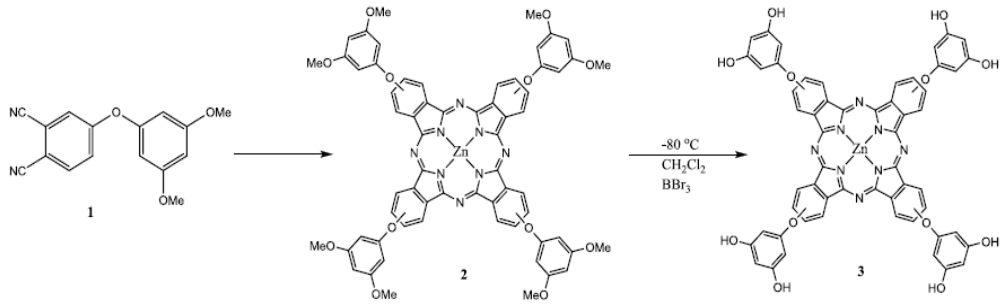

Figure 1.57 : Synthetic route for phthalocyanine **3**.

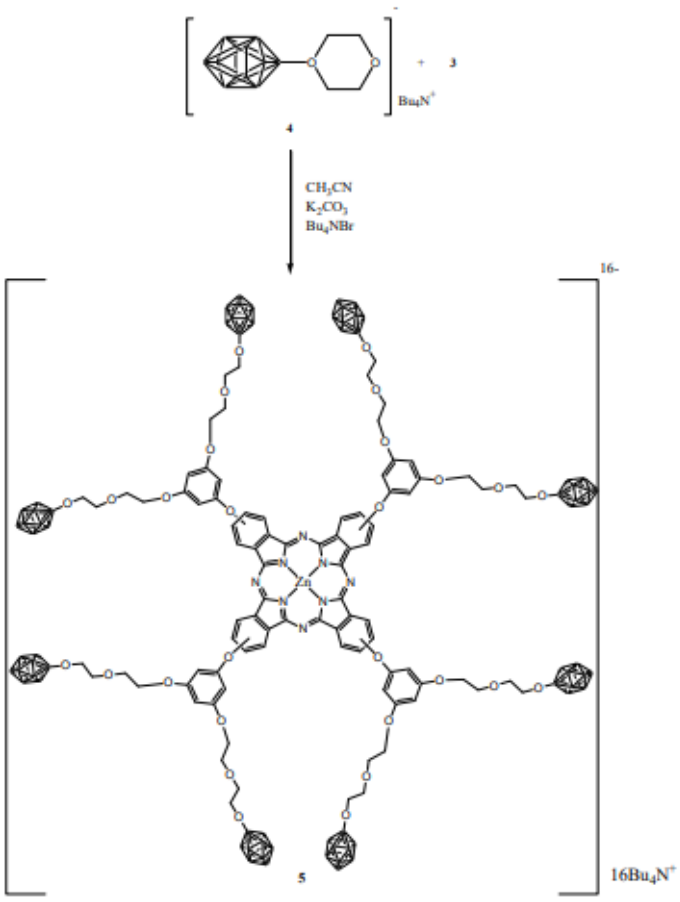

Figure 1.58 : Synthetic route for phthalocyanine **5**.

All the new compounds have been analyzed by spectroscopic methods like elemental analysis, NMR, FT-IR, UV-Vis and confirmed the targated structures.

As part of in vitro studies, the interactions of new phthalocyanine derivative (phthalocyanine **5**) with some nucleic acids, some proteins have been studied and fluorescence spectra of phthalocyanine **5** in aqueous and membrane mimetic environment was recorded. The results showed that phthalocyanine **5** forms conjugates with human globulins and attach to CrEL droplets easily.

It has been demonstrated by using laser scanning confocal microscopy that during the interaction of phthalocyanine **5** with A549 human lung adenocarcinoma cells, phthalocyanine **5** penetrates A549 cells and distributed in the cytoplasm. The average cytoplasmic concentration (ACC) of phthalocyanine **5** increased nearly with extracellular conjugate concentration (Fig. 1.57a). Complex has a fast uptake (50%

uptake of phthalocyanine **5** in cells is 41±5 min) and relatively long retention (50% efflux of phthalocyanine **5** from cells is 9.1±0.4 h) in A549 cells (Fig. 1.57b).

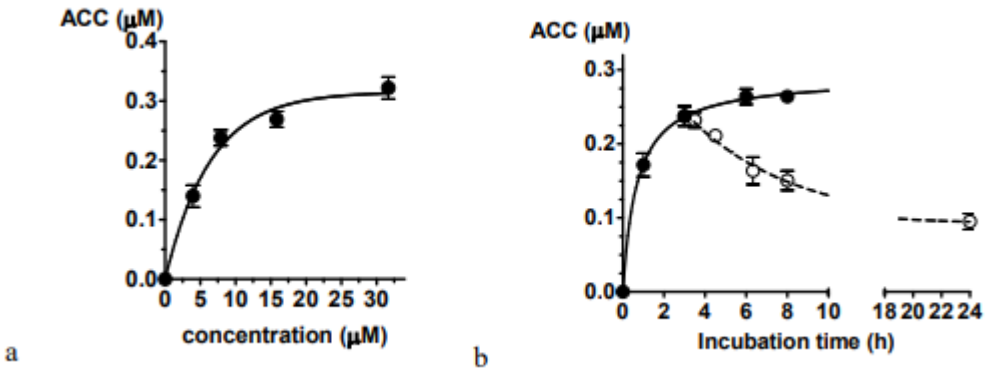

Figure 1.59 : Accumulation and retention of compound **5** in A529 cells.

Generally, phthalocyanines with extremely high negative charge and a relatively low intracelular molar concentration are not considered suitable agents for BNCT. However, the high accumulation of phthalocyanine **5** in tumor tissues can be described as a auspicious procedure for the preparation of novel Pcs involving ^{10}B atoms.

Polyhedral boron hydrides have three-centered two-electron bonds or multicentered bonds. William Lipscomb was awarded the Nobel Prize in 1976 for his work on the structure of boranes that illuminate chemical bonding problems (Lipscomb, 1993).

Until recently, these moieties have not been used in the synthesis of boron-containing biomolecules because there was not a suitable way for functionalizing them. The nucleophilic ring-opening reaction of the cyclic oxonium derivatives of the *closo*-dodecaborate anion $[B_{12}H_{12}]^{2-}$ can be seen as a new synhesis method for the functionalization of polyhedral boron hydrides. Monosubstituted derivatives of cobalt bis (dicarbollide) [3,3'-Co(1,2-$C_2B_9H_{11})_2]^-$ were synthesized by nucleophilic opening of 1,4-dioxane oxonium group with the same methodology.

Since the cobalt bis (dicarbollide) anion [3,3'-Co(1,2-$C_2B_9H_{11})_2]^-$ shows remarkable chemical-, thermal- and photo-stability, it has attracted great attention among other boron clusters and it has been used in the functionalization of phthalocyanine compounds. I Nar et al. reported new Pc–cobaltacarborane derivatives (Figure 1.60) (Nar et al., 2015).

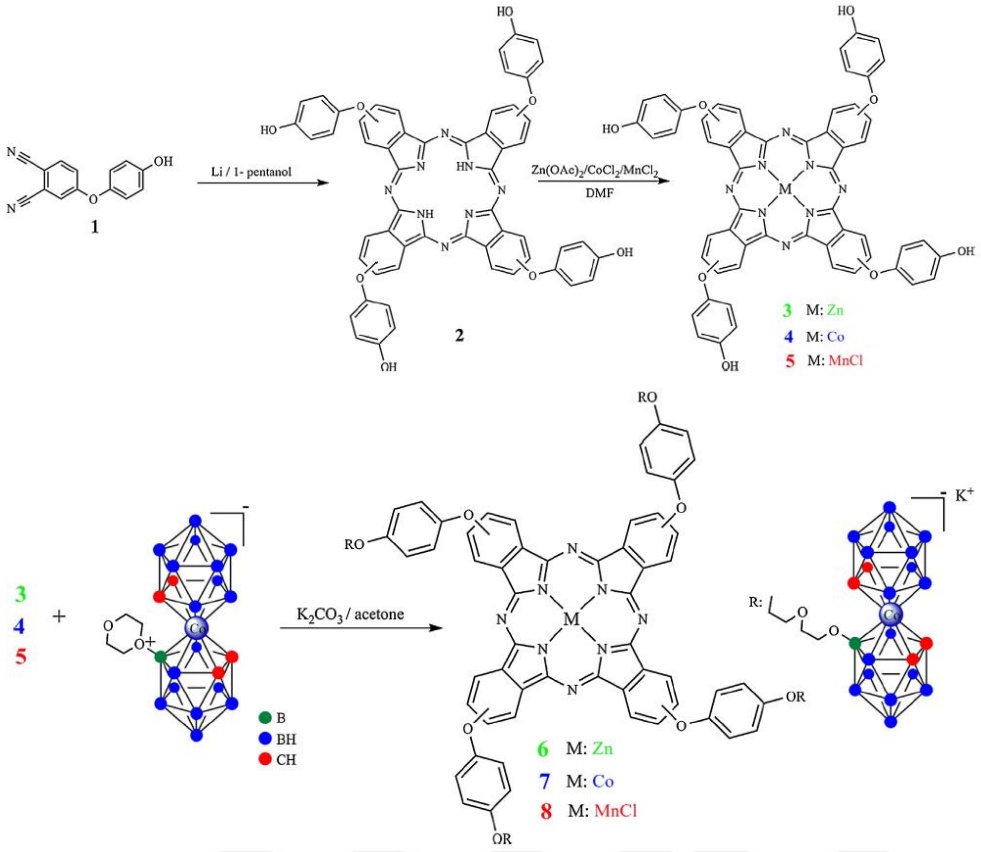

Figure 1.60 : Synthesis of novel phthalocyanine–cobaltacarborane conjugates.

In this study, firstly 4-hydroxyphenoxyphthalonitrile was synthesized by nucleophilic substitution of 4-nitrophthalonitrile and hydroquinone. Later, dilithium phthalocyanine intermediate was synthesized by cyclotetramerisation of phthalonitrile 1 with lithium in 1-pentanol. In the next stage, $PcLi_2$ was converted to metal-free Pc derivative by treating with CH_3COOH. Metal-free phthalocyanine was reacted with metal salts in C_3H_7NO under reflux to synthesize metallophthalocyanines. The highly boronated new Pc derivatives were obtained by the nucleophilic attack of hydroxyl group to the oxonium unit of cobalt bis(dicarbollide).

This paper also includes the study about how redox properties of phthalocyanines are changing with substituents and metal core and affecting the spectral and electrochemical properties of the molecule. Studies have proven that cobaltacarborane units increase the redox properties of metallophthalocyanines. In Co-and Mn- metals containing phthalocyanines which conjugated with cobaltacarborane units, ring-based

reduction and metal-based reductions were observed in both Pc ring and cobaltacarborane groups.

To contribute to developing boronated molecular systems for BNCT application, hexa-cationic, low-symmetry Pc complexes, were prepared by Prof. Dr. Esin Hamuryudan's research group (Nar et al., 2019). Also, the cytotoxicity of phthalocyanine **6** was investigated and the boron uptake by the MR-106 (UMR) cells of rat osteosarcoma was analyzed by quantitative neutron autoradiography methods.

The fact that the o-carborane units are hydrophobic causes the Pcs containing o-carborane to be insoluble in water. Two strategies can be followed to solve this problem: adding water-soluble substituents or converting the o-carborane clusters to the anionic nido-carborane units. In this paper, positively charged quaternary ammonium groups were used to enhance the solubility of novel carboranylphthalocyanine (Figure 1.61).

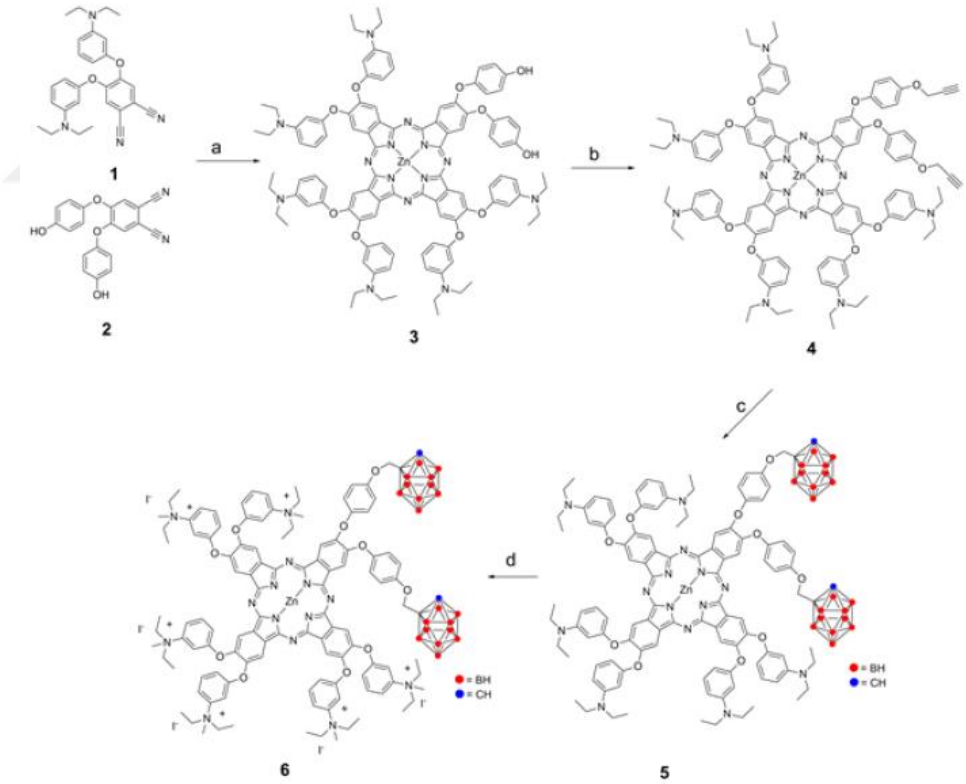

Figure 1.61 : Synthetic pathway of low-symmetrical phthalocyanine derivative.

In the study conducted to understand whether phthalocyanine **6** is a suitable agent for BNCT, UMR-106 rat osteosarcoma cells were subjected to phthalocyanine **6** for 4 hours with different concentration. Cytotoxicity was controlled with the standard clonogenic assay. Results showed that cell survival is depending on the 10-B concentration.

Boron concentration measurements were carried out by quantitative neuton autoradiography of UMR cells (Table 1.1).

Table 1.2 : ^{10}B concentration in the cell samples.

Protocol	Boron concentration in ppm (μg of 10-B per g of cells)
UMR CTR	0 ± 1
UMR 1 ppm (4 h)	17 ± 4
UMR 5 ppm (4 h)	34 ± 9

Consequently, when the UMR cells are loaded with phthalocyanine 6 at an exceptionally low polycationic complex, cell survival is reasonable, and the boron uptake is high in these cells. Considering this data, phthalociyanine **6** can be considered as an interesting example for the boron neutron capture teraphy/ photodynamic teraphy agents.

Research on targeting deposition into tumor cells has led to increased interest in BNCT nowadays. All work done to date seeks to explore different methodolgies to prepare Pc-based agents. Some promising results have been obtained and indicated that these molecules are potentially useful for BNCT.

2. PURPOSE OF THESIS

Boron neutron capture therapy contributed greatly to radiotherapy research in the 20th century, with its effectiveness proven in many X-ray resistant cancers. BNCT is the most widely used type of therapy to cure for malignant brain tumor and head and neck cancer, and its effectiveness has been proven in both types of cancer. The selectivity of accumulation of ^{10}B compounds in tumors is a cricial factor in the effectiveness of BNCT. Currently, only BPA (p-borophenylalanine) is used clinically in BNCT and BSH (undecahydrodode-caborate disodium) can find limited use. Although the usefulness of some newly developed compounds has been experimentally confirmed, whether they can be used clinically is still being investigated. In all studies, the aim is to prepare a new boron compound that shows a higher tumor: normal tissue rate than existing boron based compounds and accumulates in a high concentration in the tumor. Additionally, the homogeneous distribution of boron based drugs in the tumor is one of the most important requirements. Non uniform distribution causes excessive inhomogeneities in the dose and treatment failure.

Phthalocyanines are among the interesting subjects of coordination chemistry with their applications increasing every day in parallel with the developing technology. Pcs have superior photophysical and photochemical features and these features could be changed with different substituents at peripheral and non-peripheral positions attached to the macrocycle or around the metal center. Phthalocyanines generally exhibit low solubility which impedes sufficient purification and characterization. In most of potential applications, phthalocyanines have been substituted with various functional groups to improve their solubility and increase their effectiveness.

Studies have shown that compounds containing both polyhedral boron derivatives and phthalocyanine macrocycles can be considered potential drugs for BNCT. The aim of the studies carried out in this thesis is to synthesise new water-soluble phthalocyanine

derivatives with high boron contents that can give therapeutic boron dose to cancer cells specifically for application in BNCT.

In the first part of this study, the synthesis of the starting materials is emphasized. For this purpose, firstly, the synthesis of phthalonitrile derivative and carborane derivative starting materials was achieved and then they were characterized by spectroscopic methods and elemental analysis.

In the second part, unsymmetrical novel metal free and metallo Pc complexes were synthesized in multistep reaction sequences. Column chromatography was used for the isolation of the targeted A_3B type products.

In the third part, A_3B type phthalocyanines and decaborane ($B_{10}H_{14}$) and oxonium derivative of cobalt bis(dicarbollide) were reacted to give the *o*-carborane and cobaltacarborane functionalized phthalocyanines. Also, carbonyl phthalocyanine derivative that is soluble in aqueous media was prepared by quaternized amino groups on peripheral positions. Characterization of the newly synthesized phthalocyanine derivatives was achieved by elemental analysis and spectral methods. These data prove the successful syntheses of the proposed structures.

In the last part, we reported spectroscopic characterization, aggregation tendency and electrochemical features of these novel unsymmetrical phthalocyanine derivatives.

3. EXPERIMENTAL PART

3.1 Materials

4,5-Dichloro-1,2-dicyanobenzene (Wöhrle et al., 2013) and 4-nitrophthalonitrile (J.G. Young et al., 1990), were synthesized as reported by literature. All reagents and solvents were purchased from commercial manufacturers as reagent grade quality. Anhydrous K_2CO_3 and Na_2CO_3 were ground very thin and dried at 100 °C.

3.2 Instruments

FT-IR spectra were recorded on a Bruker Optics ALPHA-E spectrophotometer in the 650-4000 cm^{-1} area. Absorption spectra in the UV-Vis region were taken on a Scinco S-3100 spectrophotometer. ^{1}H NMR and ^{11}B NMR spectra were recorded using Agilent VNMRS 500 MHz at 25 °C. Mass spectra were measured on a Bruker Microflex MALDI-TOF/MS mass spectrometers. The elemental analysis was performed on a Costech ECS 4010 CHNS elemental analyzer.

3.3 Synthesis of Phthalonitrile Derivatives

3.3.1 4,5 Di(hexylthio) phthalonitrile (1)

1-Hexanethiol (7.0 g, 60.0 mmol) was dissolved in 35 mL of DMF under nitrogen. 4,5-dichloro-1,2-dicyanobenzene (6.0 g, 30.0 mmol) was added and reaction was stirred for 15 minutes. Dry potassium carbonate (15.0 g, 110.0 mmol) was added portionwise within 2 hours. The mixture was stirred at room temperature for 12 hours. Then the mixture was poured into 300 mL of ice-water, and precipitate was filtered off. The residue was crystallized from C_2H_5OH (Gürek et al., 1994). Yield: 8 g (74%); m.p. 70 °C. IR υ (cm^{-1}): 3073 (Ar-H), 2955-2858 (alkyl-CH), 2228 (-C≡N); ^{1}H NMR ($CDCl_3$): 7.40 (s, 2H, Ar-H), 2.99 (t, 4H, SCH_2), 1.73 (q, 4H, $SCCH_2$), 1.49 (m, 4H,

CCH_2C), 1.33 (m, 8H, CCH_2C), 0.89 (t, 6H, CH_3); anal. calcd. for $C_{20}H_{28}N_2S_2$; C, 66.62; H, 7.83; N, 7.77; found: C, 66.51; H, 7.99; N, 7.56%;

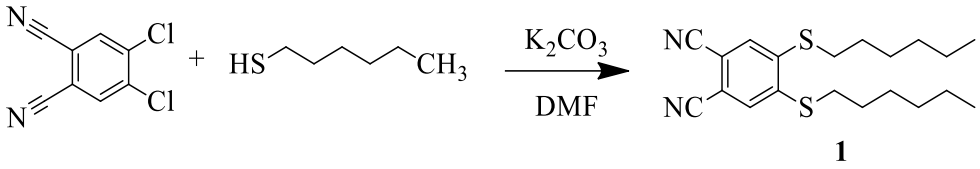

1

Figure 3.1 : 4,5-Di(hexylthio) phthalonitrile (**1**).

Table 3.1 : Elemental analysis of **1**.

	C	H	N
Calculated	66.62	7.83	7.77
Found	66.51	7.99	7.56

3.3.2 4-[(2-Hydroxyethyl)thio] phthalonitrile (2)

1.0 g of 4-nitrophthalonitrile (0.6 mmol) and 1 mL of 2-hydroxyethylmercaptan (1.0 g, 1.2 mmol) were stirred in 20 mL of dry dimethyl sulfoxide. After 10 min, anhydrous 3.0 g of Na_2CO_3 (2.8 mmol) was added portionwise over 2 hours and stirred at room temperature for a further 6 hours. The mass was then poured into 200 mL of iced-water and the precipitate was filtered off, washed with H_2O and crystallized from C_7H_8. It was washed first with cold C_6H_{14} and then with $(C_2H_5)_2O$ (Özçeşmeci et al., 2007). Yield: 1.49 g (76%); m.p. 92 °C. IR υ (cm^{-1}): 3332 (-OH), 3094 (Ar-H), 2932, 2881 (alkyl-CH), 2226 (-C≡N); ^1H NMR ($CDCl_3$): 7.59 (d, 1H, Ar-H), 7.52 (d, 1H, Ar-H), 7.49 (d, 1H, Ar-H), 3.83 (t, 2H, OCH_2), 3.16 (t, 2H, SCH_2), 2.04 (s, 1H, OH); anal. calcd. for $C_{10}H_8N_2OS$; C, 58.80; H, 3.95; N, 13.72; found: C, 58.92; H, 3.86; N, 13.55%; MS: m/z 205 $[M+1]^+$, 206 $[M+2]^+$.

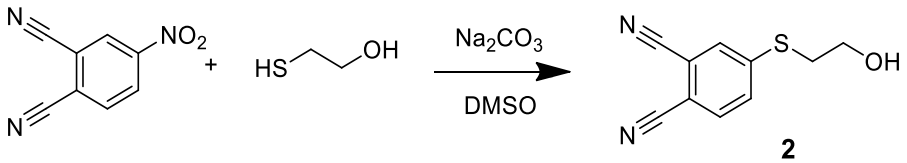

2

Figure 3.2 : 4-(2-Hydroxyethylthio) phthalonitrile (**2**).

Table 3.2 : Elemental analysis of **2**.

	C	H	N
Calculated	58.80	3.95	13.72
Found	58.92	3.86	13.55

3.3.3 4-[3-(Diethylamino)phenoxy] phthalonitrile (3)

Dry sodium carbonate (1.3 g, 11.56 mmol) was added to a solution of 3-(diethylamino)phenol (1.15 g, 6.94 mmol) and 4-nitrophthalonitrile (1.0 g, 5.78 mmol) in dry dimethylformamide (20 mL) within 2 h. The solution was stirred for 48 hours under nitrogen. Then it was poured into 200 mL of distilled water. The product was extracted with ethylacetate from the water phase and dried from Na_2SO_4. Ethylacetate was evaporated and the sticky brownish product was crystallized from n-hexane (Dei et al., 2006). Yield: 1.64 g (98%); IR υ (cm^{-1}): 3083 (Ar-H), 2966-2924 (alkyl-CH), 2234 (-C≡N); ^1H NMR ($CDCl_3$): 7.69 (1H, d), 7.30 (1H, d), 7.22 (2H, dd), 6.57 (1H, t), 6.32 (1H, dd), 6.26 (1H, m), 3.35 (4H, q), 1.18 (6H, t); anal. calcd. for $C_{18}H_{17}N_3O$; C, 74.20; H, 5.88; N, 14.42; found: C, 74.39; H, 5.54; N, 14.55%.

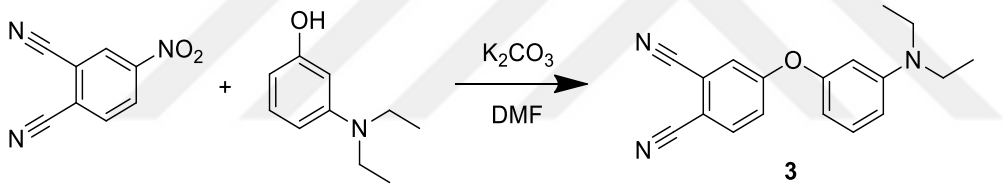

Figure 3.3 : 4-[3-(Diethylamino) phenoxy] phthalonitrile (**3**).

Table 3.3 : Elemental analysis of **3**.

	C	H	N
Calculated	74.20	5.88	14.42
Found	74.39	5.54	14.55

3.4 Synthesis of Carborane Derivatives

3.4.1 7,8-Dicarba-*nido*-undecarborate (4)

O-carborane (10.0 g, 69.0 mmol) and KOH (7.74 g, 138.0 mmol) were refluxed in ethanol for 48 hours. Ethanolic phase was filtered off and then C_2H_5OH was evaporated. Distilled water was put into to the product and $C_3H_9N.HCl$ was dropped into water phase in order to precipitate the trimethylammonium salt. Pure white

compound was filtered off and dried under vacum (Wiesboeck et al., 1964). Yield: 13 g (98%); ^{1}H NMR (d6-acetone) ***δ***, ppm: -0.5-2.0 (b, 10H, BH), 3.12 (s, 9H, -NH(CH_3)$_3$); ^{11}B NMR (d6-acetone) ***δ***, ppm: -10.9 (s, 2B), -16.8- (-17.6) (d, 4B), -22.3 (s, 2B), -33.2 (s, 1B), -37.8 (s, 1B).

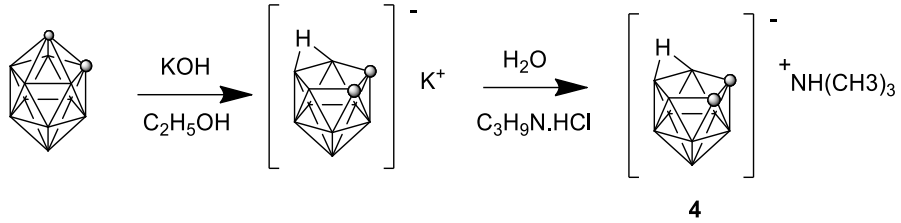

4

Figure 3.4 : 7,8-Dicarba-*nido*-undecarborate (**4**).

3.4.2 [3,3'-Co(1,2-$C_2B_9H_{11}$)$_2$]$^-$ (5)

9.415 g of 7,8-dicarba-*nido*-undecaborate (**4**) (65.0 mmol) was put into a solution of 10.0 g NaOH in water. After dissociation of salt, 15.415 g of $CoCl_2.6H_2O$ (65.0 mmol) was added and it was stirred for a further 30 minutes. The orange product that formed was extracted with ether. Sodium salt of cobaltocarborane was dissolved in H_2O, CsCl solution was slowly added into solution. Light orange precipate was filtered off and dried in vacuo (Sivaev et al., 1999). Yield: 20.3 g (72%); ^{11}B NMR (DMSO) δ, ppm: 5.19 (s, 2B), 0.27 (s, 2B), -7.0 (s, 8B), -18.1 (s, 4B), -23.7 (s, 2B).

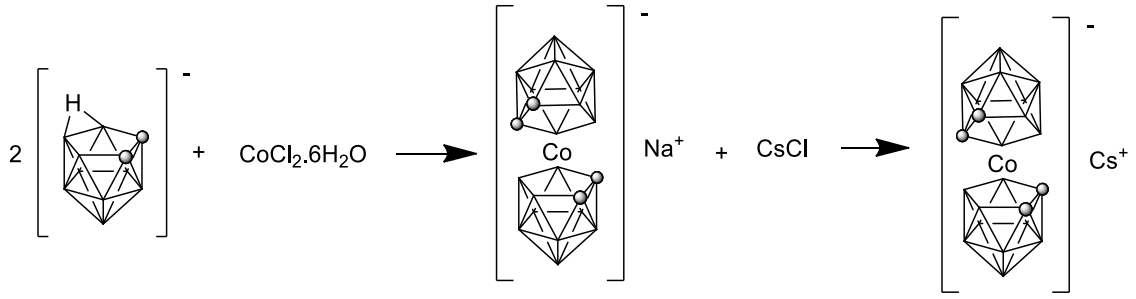

5

Figure 3.5 : [3,3'-Co(1,2-$C_2B_9H_{11}$)$_2$]$^-$ (**5**).

3.4.3 [3,3'-Co(8-$C_4H_8O_2$-1,2-$C_2B_9H_{10}$)(1',2'-$C_2B_9H_{11}$)] (6)

2 mL (16.0 mmol) of boron trifluoride etherate was added into a solution of 0.90 g (2.0 mmol) Cs[3,3′-Co(1,2-$C_2B_9H_{11}$)$_2$] (**5**) in 100 mL of 1,4-dioxane under nitrogen and

reaction mixture was refluxed for 5h. After product was cooled to ambient temperature, it was filtered off and dried. The rest was purified by column chromatography on silica gel with DCM (Teixidor et al., 2003). Yield: 0.76 g (94%); ^{1}H NMR (d6-acetone) δ, ppm: 4.72 (t, 4H, -OCH_2CH_2). ^{11}B NMR (d6-acetone): 24.7 (1B, s), 8.6 (1B, s), 5.8 (1B,s), -2.31 (1B, d), -3.8 (4B, d), -8.06 (2B, d), -9.78 (2B, d), -14.83 (2B, d), -18.57 (2B, d), -21.04 (1B, d), -27.05 (1B, d).

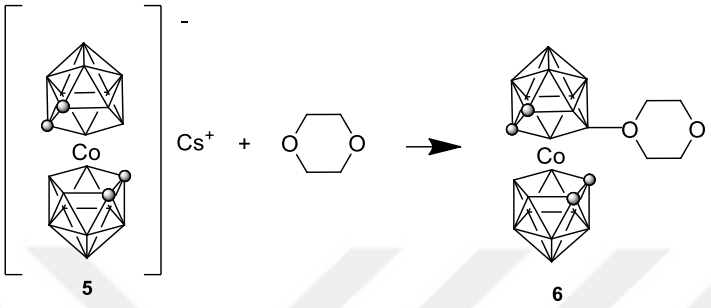

Figure 3.6 : [3,3'-Co(8-$C_4H_8O_2$-1,2-$C_2B_9H_{10}$) (1',2'-$C_2B_9H_{11}$)] (**6**).

3.5 Synthesis of Unsymmetrical Phthalocyanine Derivatives

3.5.1 2,3,9,10,16,17-Hexakis(hexylthio)-23-hydroxyethylthiophthalocyanine (7)

A mixture containing 0.432 g (1.2 mmol) of 4,5-di(hexylthio) phthalonitrile (**1**) and 0.08 g (0.4 mmol) of 4- (2-hydroxyethylthio) phthalonitrile (**2**) in 3 mL $C_5H_{12}O$ was heated and stirred at 140 °C under nitrogen in a sealed tube. After 15 min, 0.015 g (2.0 mmol) lithium metal was added to the mixture and refluxed for 4 hours. The reaction mixture was cooled to ambient temperature and then poured into 25 mL methanol and acidified with CH_3COOH until the crude product precipitated. Therefore, Li_2Pc derivatives were converted into metal free phthalocyanines. The precipitate was centrifuged and washed several times with hot CH_3OH. Finally, the green residue was chromatographed on silica gel using dichloromethane: methanol as the eluent, changing from 150:1 to 75:1 (v/v), to afford in Pc **7** as a green solid on the second fraction. Yield: 0.13 g (26%); m.p. > 200 °C; IR υ (cm^{-1}): 3300 (-OH), 3290 (-NH), 2950-2850 (alkyl -CH); ^{1}H NMR ($CDCl_3$) δ ppm: 8.42-7.57 (m, 9H, Ar-H), 4.71 (s, H, OH), 4.19 (m, 2H, OCH_2), 3.68 (m, 2H, SCH_2), 3.56-3.24 (m, 12H, SCH_2), 2.03-1.26 (m, 48H, -CH_2), 1.05 (m, 18H, CH_3), -4.3 (br, 2H, N-H); UV-Vis λmax (nm) in

THF: 342, 694, 725; MALDI-TOF MS (matrix DHB) m/z: 1287.85 $[M]^+$; anal. calcd. for $C_{70}H_{94}N_8OS_7$; C, 65.28; H, 7.36; N, 8.70; found: C, 65.17; H, 7.45; N, 8.78%.

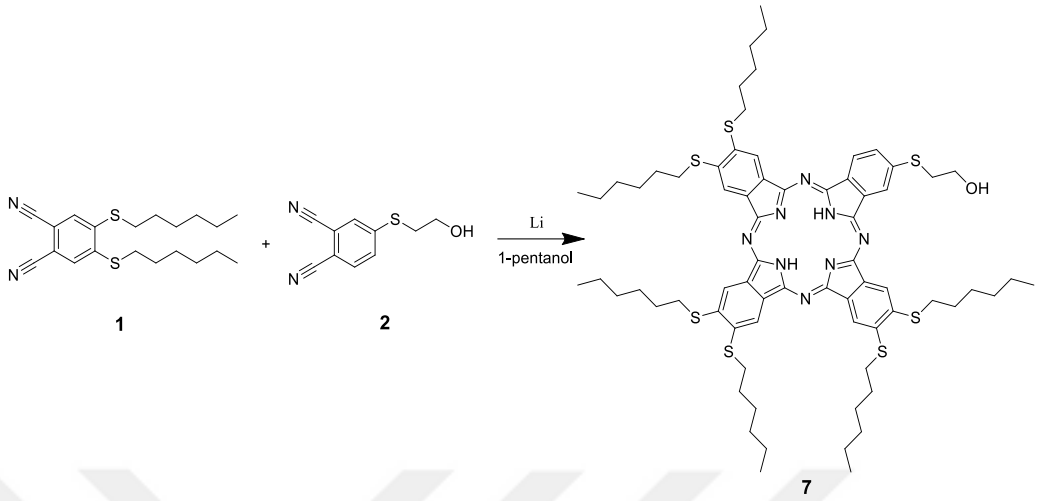

Figure 3.7 : 2,3,9,10,16,17-Hexakis(hexylthio)-23-hydroxyethylthiophthalocyanine (**7**).

Table 3.4 : Elemental analysis of **7**.

	C	H	N
Calculated	65.28	7.36	8.70
Found	65.17	7.45	8.78

3.5.2 [2,3,9,10,16,17-Hexakis(hexylthio)-23-hydroxyethylthiophthalocyaninato] zinc(II) (8)

A solution of 0.1 g (0.08 mmol) of Pc **7** and 0.044 g (0.24 mmol) of $Zn(CH_3COO)_2$ was refluxed in 2 mL of 1-pentanol with stirring for 4 hours under N_2. The resulting suspension was cooled to ambient temperature and then poured into 20 mL of methanol. The precipitate was filtered off, washed successively with water, hot methanol, hot acetone and hot n-hexane. The purification was carried out by column chromatography on silica gel using dichloromethane: methanol (50:1) as the eluent to result in Pc **8** as a green solid. Yield: 0.10 g (94.4%); m.p.> 200 °C; IR υ (cm^{-1}): 3360 (-OH), 2950-2850 (alkyl -CH); ^1H NMR ($CDCl_3$ + 1 drop of pyridine *d5*) δ ppm: 9.10-8.82 (br, 5H, Ar-H), 8.55 (s, 1H, Ar-H), 8.03 (m, 2H, Ar-H), 7.62 (s, 1H, Ar-H), 4.64 (s, H, OH), 4.15 (m, 2H, OCH_2), 3.84 (m, 2H, SCH_2), 3.44-2.86 (m, 12H, SCH_2), 2.02-

1.72 (m, 24H, CH_2),1.44-1.22 (m, 24H, CH_2), 0.96 (m, 18H, CH_3); UV-Vis λmax (nm) in THF: 361, 629, 699; MALDI-TOF MS (matrix DHB) m/z: 1352.52 $[M+H]^+$; anal. calcd. for $C_{70}H_{92}ZnN_8OS_7$; C, 62.21; H, 6.86; N, 8.29; found: C, 62.25; H, 6.77; N, 8.35%.

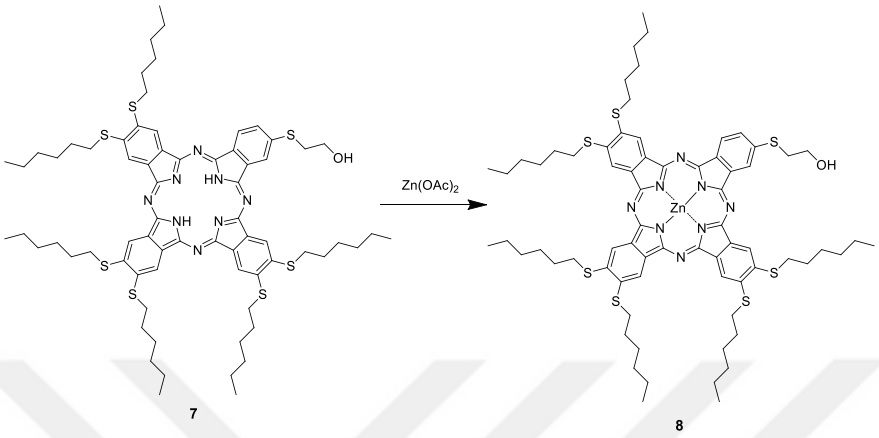

Figure 3.8 : [2,3,9,10, 16,17-Hexakis(hexylthio)-23-hydroxyethylthiophthalocyaninato] zinc(II) (**8**).

Table 3.5 : Elemental analysis of **8**.

	C	H	N
Calculated	62.21	6.86	8.29
Found	62.25	6.77	8.35

3.5.3 [2,3,9,10,16,17-Hexakis(hexylthio)-23-1-pentynyloxyethylthio phthalocyaninato] zinc(II) (9)

0.01 g of 4-pentynoic acid (0.12 mmol) and 20 mL of anhydrous dichloromethane were added to a three-necked 50 mL flask. After the 4-pentynoic acid was dissolved, 0.15 g (0.11 mmol) of Pc **8** and 0.024 g (0.12 mmol) of dicyclohexylcarbodiimide (DCC) were added. Then 0.007 g (0.055 mmol) of N,N-dimethylaminopyridine (DMAP), dissolved in 1.5 mL of anhydrous dichloromethane, was added. The mixture was stirred for 48 hours at room temperature under N_2 atmosphere. The solution was filtered and the filtrate was placed in the freezer for 30 min and then filtered again. Following the evaporation of the solvent, purification of the solid crude product **9** was accomplished by column chromatography with CH_2Cl_2:CH_3OH (50:1) as eluents to give a dark green solid. Yield: 95 mg (59.8%); m.p.> 200 °C; IR υ (cm^{-1}): 3310

(alkynyl -CH), 2950-2850 (alkyl -CH), 2202 (-C≡CH), 1720 (-C=O); UV-Vis λmax (nm) in THF: 360, 630, 698; MALDI-TOF MS (matrix: DHB) m/z: 1432.47 $[M + H]^+$; anal. calcd. for $C_{75}H_{96}ZnN_8O_2S_7$; C, 62.93; H, 6.76; N, 7.83; found: C, 63.01; H, 6.71; N, 7.88%.

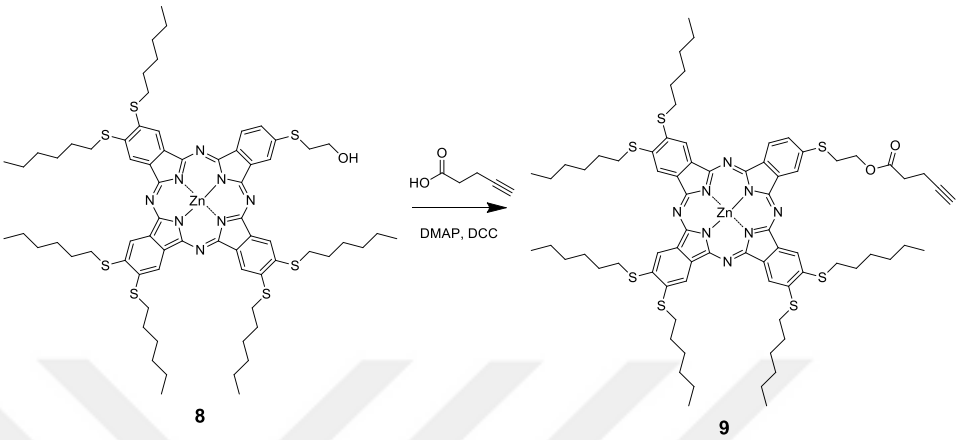

Figure 3.9 : [2,3,9,10, 16,17-Hexakis(hexylthio)-23-1-pentynyloxyethylthiophthalocyaninato] zinc(II) (**9**).

Table 3.6 : Elemental analysis of **9**.

	C	H	N
Calculated	62.93	6.76	7.83
Found	63.01	6.71	7.88

3.5.4 Tris-9(10),16(17),23(24)[3-(diethylamino)phenoxy]-2-hydroxyethylthio phthalocyanine (10)

0.14 g (0.68 mmol) of 4-(2-hydroxyethylthio) phthalonitrile (**2**) and 0.6 g (2.04 mmol) of 4-[3-(diethylamino) phenoxy] phthalonitrile (**3**) were dissolved in 3 mL of $C_5H_{12}O$ at 80°C. After stirring 15 min, 0.007 g (1.03 mmol) of lithium was added and heated at 140°C. The reaction mixture was stirred for 4 h more under nitrogen. The green suspension which was prepared via cyclotetramerization by using 3:1 of **3** and **2** was diluted in methanol and 0.5 mL of acetic acid was added in order to convert Li_2Pc to metal free Pc. The precipitate form was filtered off and washed with CH_3OH until the washing CH_3OH was clear. The resultant solid was subjected to alumina column chromatography with CH_2Cl_2: MeOH as eluent system changing from 75:1 to 50:1

(v/v). The second band contained the desired A_3B type Pc **10** was collected. Yield: 150 mg (21%); IR υ (cm^{-1}): 3285 (N-H), 3040(O-H), 2966 (alkyl-CH), 1272 (C-O-C); ^1H NMR (pyridine *d5*) δ, ppm: 9.60– 9.27 (m, Har), 8.25–8.07 (m, Har), 7.41(m, Har), 6.99–6.66 (m, Har), 4.37 (m, CH–O), 3.87–3.76 (m, CH–O), 1.26–1.21 (CH_3); UV-Vis λmax (nm) in DCM: 343, 672, 702; MALDI MS m/z: 1080 $[M]^+$; anal. calcd. for $C_{64}H_{61}N_{11}O_4S$; C, 71.15; H, 5.69; N, 14.26; found: C, 71.55; H, 5.63; N, 14.56%.

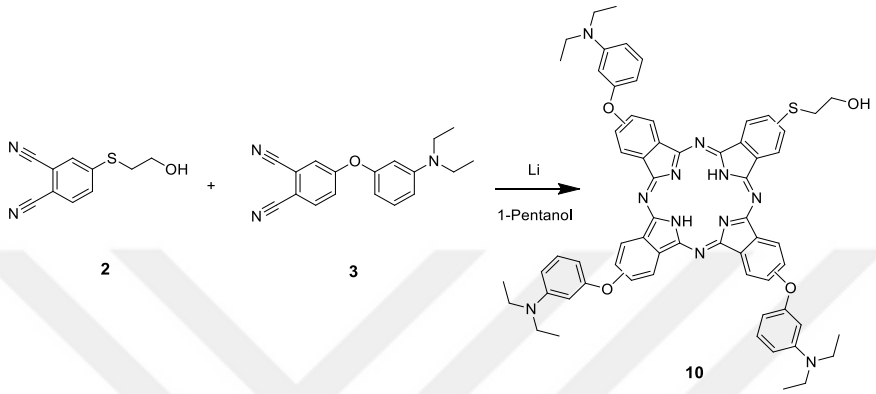

Figure 3.10 : Tris-9(10), 16(17), 23(24)[3-(diethylamino)phenoxy]-2-hydroxyethylthio phthalocyanine (**10**).

Table 3.7 : Elemental analysis of **10**.

	C	H	N
Calculated	71.15	5.69	14.26
Found	71.55	5.63	14.56

3.5.5 {Tris-9(10), 16(17), 23(24)[3-(diethylamino)phenoxy]-2-hydroxyethylthio phthalocyaninato} zinc(II) (11)

0.68 g (0.63 mmol) of Pc **10** was reacted with 0.12 g (0.63 mmol) of anhydrous zinc acetate in 3 mL of dry $C_5H_{12}O$ at 140 °C under nitrogen for 4 h. After cooling to room temperature, the reaction was quenched with distilled water and green precipitate was filtered off. Solid product was washed with hot C_2H_5OH, acetone and hexane and then dried in vacuo. Yield: 0.68 g (89 %); IR υ (cm^{-1}): 3040(O-H), 2925 (alkyl-CH), 1272 (C-O-C). UV-Vis λmax (nm) in DCM: 358, 617, 683; anal. calcd. for $C_{64}H_{59}N_{11}O_4SZn$; C, 67.21; H, 5.20; N, 13.47; found: C, 66.98; H, 5.23; N, 13.65.

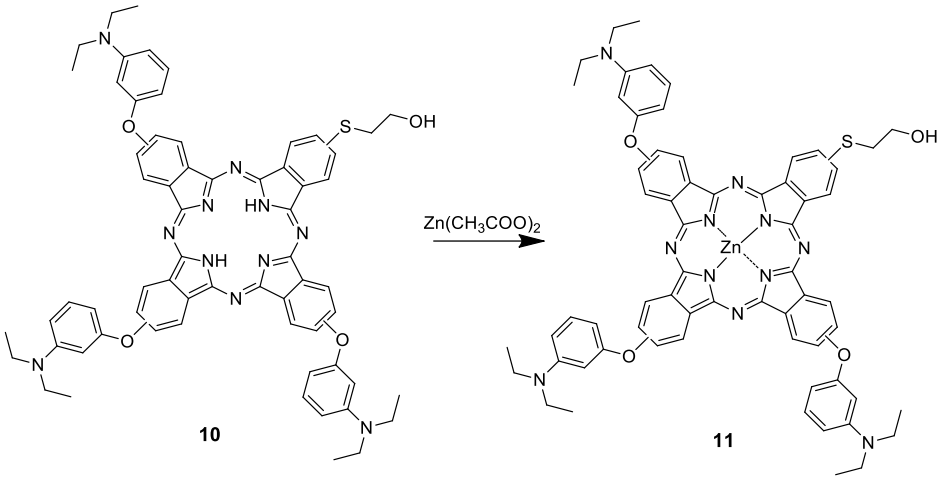

Figure 3.11 : {Tris-9(10), 16(17), 23(24)[3-(diethylamino)phenoxy]-2-hydroxyethylthio phthalocyaninato} zinc(II) (**11**).

Table 3.8 : Elemental analysis of **11**.

	C	H	N
Calculated	67.21	5.20	13.47
Found	66.98	5.23	13.65

3.5.6 {Tris-9(10), 16(17), 23(24)[3-(diethylamino)phenoxy]-2-1-propynloxyethylthio phthalocyaninato} zinc(II) (12)

0.50 g (0.43 mmol) of Pc **11** was dissolved in 20 mL of toluene and cooled to 0° C. 0.021 g (0.86 mmol) of sodium hydride was added to the solution under N_2 atmosphere. The obtained solution was stirred for 1 h, followed by the addition of the solution of 0.102 g (0.86 mmol) propargyl bromide in toluene via a syringe. After addition, mixture was stirred for another 4 h, and then the suspension was filtered off and extracted with distilled water repeatedly. After removal of the solvent under reduced pressure, the product was dried in vacuo. Yield: 0.46 g (80%); IR υ (cm^{-1}): 3289 (alkynyl -CH), 2925 (alkyl-CH), 2160 (C≡C), 1272 (C-O-C); ^{1}H NMR (*d*DMSO) δ, ppm: 8.94 (b, Har), 8.54 (b, Har), 7.67 (b, Har), 7.37 (b, Har), 6.69 (b, Har), 4.45 (b, CH–O), 3.44 (m, CH–O), 1.26–1.19 (CH_3), UV-Vis λmax (nm) in DCM: 353, 619, 684; anal. calcd. for $C_{67}H_{61}N_{11}O_4SZn$; C, 68.10; H, 5.20; N, 13.04; found: C, 68.45; H, 5.13; N, 13.27.

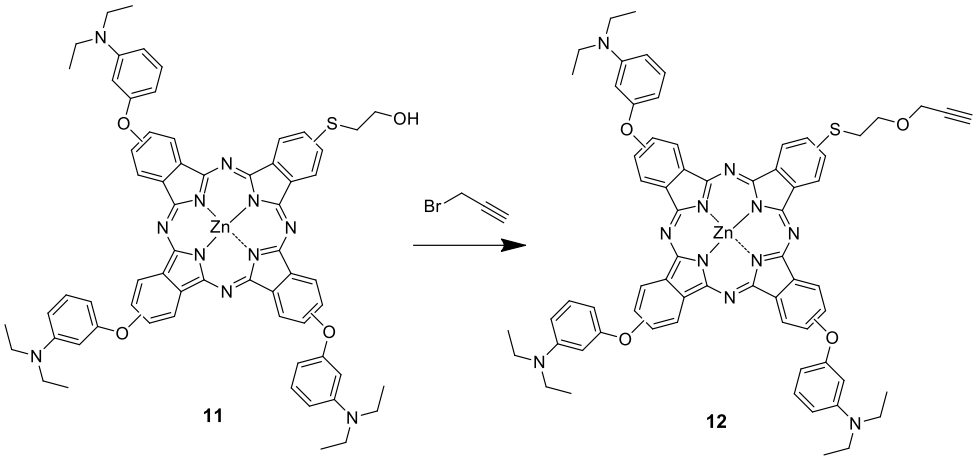

Figure 3.12 : {Tris-9(10), 16(17), 23(24)[3-(diethylamino)phenoxy]-2-1-propynloxyethylthio phthalocyaninato} zinc(II) (**12**).

Table 3.9 : Elemental analysis of **12**.

	C	H	N
Calculated	68.10	5.20	13.04
Found	68.45	5.13	13.27

3.5.7 {Tris-9(10), 16(17), 23(24)[3-(diethylamino)phenoxy]-2-1-pentynyloxyethylthio phthalocyaninato} zinc(II) (13)

To an ice bath cooled a solution of compound **11** (0.12 g, 0.11 mmol) and 4-pentynoic acid (0.01 g, 0.12 mmol) in DCM (20 mL) was added DMAP (0.007 g, 0.055 mmol) and the mixture was stirred for 30 minutes under nitrogen. A solution of DCC (0.024 g, 0.12 mmol) in DCM (2 mL) was added to the reaction mixture at 0°C. After the addition, the mixture was left at room temperature for 24 hours. The solvent was removed under reduced pressure. The crude product was dissolved in CH_2Cl_2 and placed in cold for 30 minutes, then filtered through a crucible in order to remove 1,3-dicyclohexyl urea (DCU). The solvent was evaporated in vacuum and product was washed with hot ethanol. Yield: 86 mg (67 %); IR υ (cm^{-1}): 3285 (alkynyl -CH), 2926 (alkyl -CH), 2273 (-C≡CH), 1737 (-C=O); UV-Vis λmax (nm) in DCM: 358, 617, 683; anal calcd. for $C_{69}H_{63}N_{11}O_5SZn$; C, 67.72; H, 5.19; N, 12.59; found: C, 67.64; H, 5.33; N, 12.62.

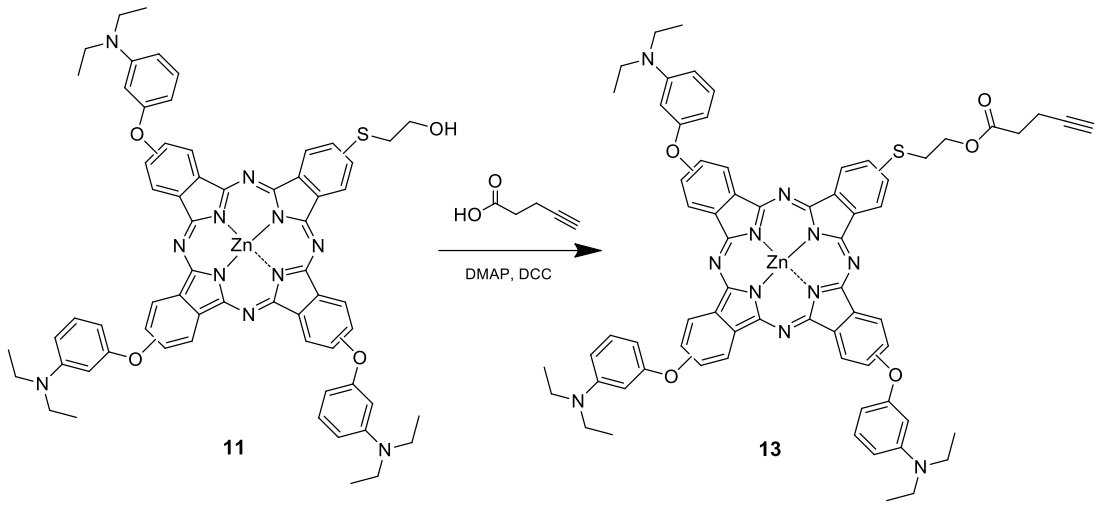

Figure 3.13 : {Tris-9(10), 16(17), 23(24)[3-(diethylamino)phenoxy]-2-1-pentynyloxyethylthio phthalocyaninato} zinc(II) (**13**).

Table 3.10 : Elemental analysis of **13**.

	C	H	N
Calculated	67.72	5.19	12.59
Found	67.64	5.33	12.62

3.6 Synthesis of Carborane Containing Phthalocyanines

3.6.1 [2,3,9,10,16,17-Hexakis(hexylthio)-23-1-(o-carboranyl) propanoxyethylthio phthalocyaninato] zinc(II) (14)

0.019 g (0.154 mmol) of decaborane ($B_{10}H_{14}$) was dissolved in a mixture of 10 mL dry toluene and 6 mL dry acetonitrile. The reaction mixture was heated to 90 °C. After 2 h, 0.20 g (0.140 mmol) Pc **9** was added. This mixture was heated to reflux for 48 h. After the reaction mixture was cooled to room temperature, it was filtered, and all solvents were evaporated. Purification of the solid crude product **14** was carried out by column chromatography with THF as eluent to give a green solid. Yield: 0.086 g (40.0%); m.p. > 200 °C. IR υ (cm^{-1}): 2950-2850 (alkyl -CH), 2571 (-BH); ^{1}H NMR (pyridine *d5*): 9.73-9.45 (m, 6H, Ar-H), 8.97-8.38 (m, 3H, Ar-H), 4.74 (m, 2H, CH_2), 4.41 (s, H, CH), 3.92 (m, 2H, OCH_2), 3.80 (m, 2H, SCH_2), 3.56 (m, 12H, SCH_2), 3.22-1.10 (b, 10H, BH), 2.84 (m, 2H, $CH_2OC{=}O$), 2.13 (m, 2H, CCH_2), 2.03 (m, 12H, $SCCCH_2$), 1.70-1.30 (m, 24H, CCH_2), 0.93 (m, 18H, CH_3); ^{11}B NMR (pyridine *d5*):

δ, ppm -2.34 (b, 1B); -5.34 (b, 1B), -9.18 (b, 3B), -11.21 (b, 5B).; UV-Vis λmax (nm) in THF: 361, 632, 700; MALDI-TOF MS (matrix DHB) m/z: 1551.72 $[M]^+$, 1352.090 $[M\text{-}C_5H_{17}B_{10}O]^+$; anal. calcd. for $C_{75}H_{108}B_{10}ZnN_8O_2S_7$; C, 58.05; H, 7.02; N, 7.22; found: C, 57.96; H, 6.93; N, 7.28%.

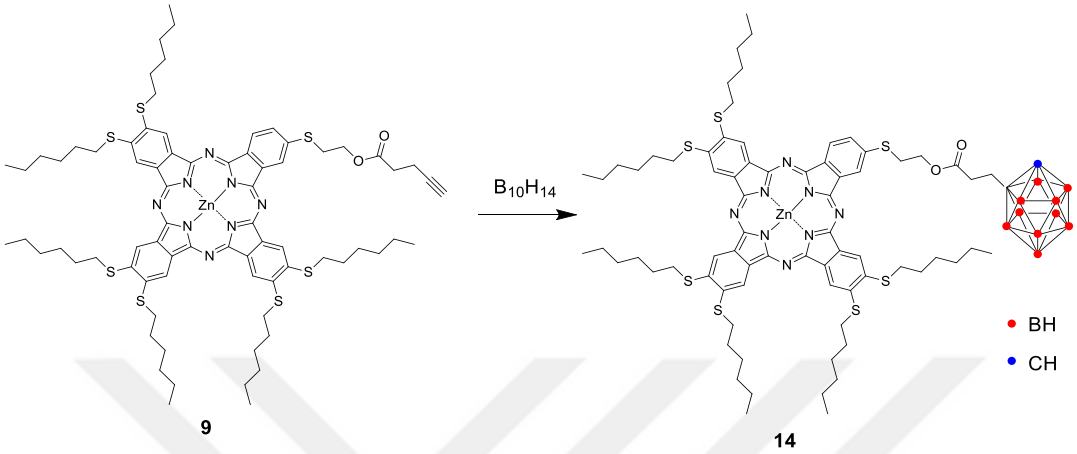

Figure 3.14 : [2, 3, 9, 10, 16, 17-Hexakis(hexylthio)-23-1-(o-carboranyl)propanoxyethylthiophthalocyaninato] zinc(II) (**14**).

Table 3.11 : Elemental analysis of **14**.

	C	H	N
Calculated	58.05	7.02	7.22
Found	57.96	6.93	7.28

3.6.2 {Tris-9(10),16(17),23(24)[3-(diethylamino)phenoxy]-2-1-(o-carboranyl) propanoxyethylthio phthalocyaninato} zinc(II) (15)

0.01 g (0.085 mmol) of $B_{10}H_{14}$ was heated in the mixture of dry acetonitrile (15 mL) and toluene (15 mL) under reflux. After 1 h the solution turned to yellow. After cooling to room temperature, 0.08 g (0.07 mmol) of Pc **13** was added and refluxing continued for 48 hours under nitrogen atmosphere. Acetonitrile and toluene were evaporated and the solid was washed with hot C_2H_5OH and C_6H_{14}. The crude product was purified by column chromatography with THF to give compound **15**. Yield: 62.5 mg (68%); IR υ (cm^{-1}): 2968-2928 (alkyl-CH), 2511 (B-H), 1732 (C=O); UV-Vis λmax (nm) in THF:

349, 620, 679; anal. calcd. for $C_{69}H_{75}B_{10}N_{11}O_5SZn$; C, 70.76; H, 4.82; N, 11.35; found: C, 70.53; H, 4.48; N, 11.53.

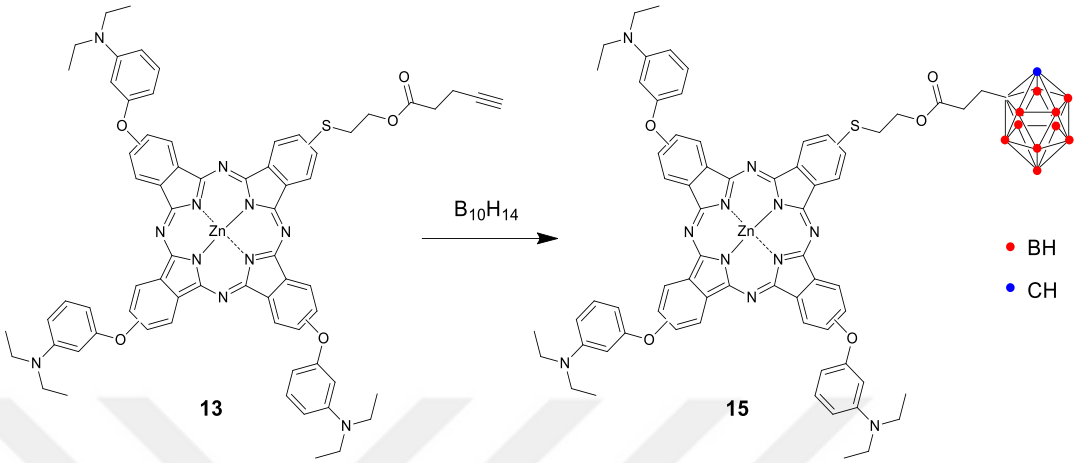

Figure 3.15 : {Tris-9(10),16(17),23(24)[3-(diethylamino)phenoxy]-2-1-(o-carboranyl)propanoxyethylthio phthalocyaninato} zinc(II) (**15**).

Table 3.12 : Elemental analysis of **15**.

	C	H	N
Calculated	70.76	4.82	11.35
Found	70.53	4.48	11.53

3.6.3 {Tris-9(10),16(17),23(24)[3-(N, N, N diethylmethylammonium)phenoxy]-2-1-(o-carboranyl) propanoxyethylthio phthalocyaninato} zinc(II) triiodide (16)

A mixture of Pc **15** (0.027 g, 0.02 mmol) and CH_3I (0.014 g, 100.0 mmol) in 5 mL $CHCl_3$ was heated and stirred at 50° C for 2 days in the dark. After cooling to ambient temperature, the resultant suspension was filtered off and washed with hot $CHCl_3$. Then, water soluble ionic Pc **16** was dried in vacuo. Yield: 30 mg (84%); ^{1}H NMR (*d*$_6$-DMSO) δ, ppm: 9.46-9.34 (m, 4H, Ar-H), 8.93-8.87 (m, 4H, Ar-H), 8.07-7.60 (m, 16H, Ar-H), 4.15 (m, 6H, N-CH_2), 4.02 (m, 2H, OCH_2), 3.93 (m, 6H, N-CH_2), 3.81 (m, 2H, SCH_2), 3.60 (m, 9H, N-CH_3), 2.63 (b, 2H, CH_2OC=O), 1.90 (m, 2H, CCH_2), 1.22 (m, 18H, CH_3); ^{11}B NMR (*d*DMSO): δ, ppm -3.29 (b); -9.25-(-13.94) (b), -9.49 (b); UV-Vis λ_{max} (nm) in (H_2O+triton X): 352, 615, 681.

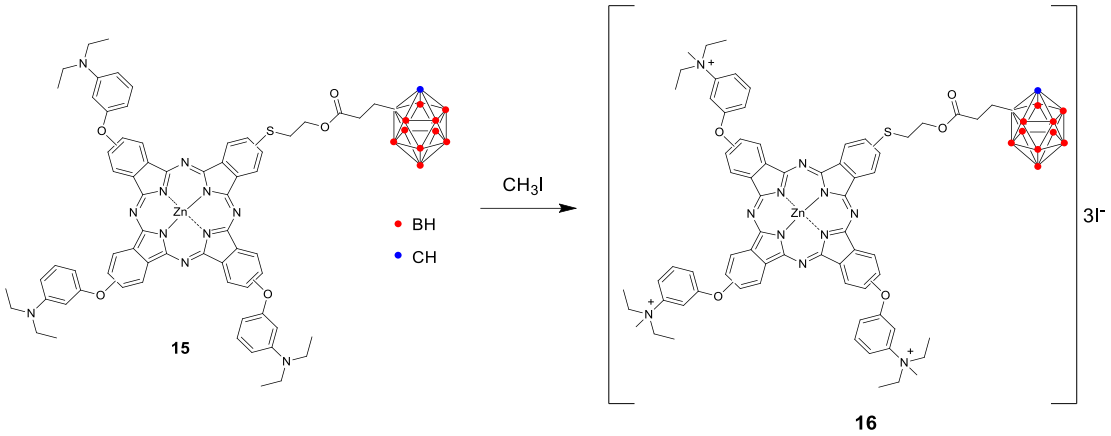

Figure 3.16 : {Tris-9(10),16(17),23(24) [3-(N, N, N diethylmethylammonium) phenoxy]-2-1-(o-carboranyl)propanoxyethylthiophthalocyaninato}zinc(II) triiodide (**16**).

3.7 Synthesis of Cobalt Bis(dicarbollide) Substituted Phthalocyanine Derivatives

3.7.1 Synthesis of phthalocyanine 17

0.08 g (0.06 mmol) of Pc **8**, 0.06 mg (0.07 mmol) of 3,3′-Co(8-$C_4H_8O_2$-1, 2-$C_2B_9H_{10}$)(1′,2′-$C_2B_9H_{10}$) **6** and 0.007 g (177.6 mmol, %60) of NaH were refluxed in 5 mL of toluene for 12 h. After the reaction mixture was cooled to room temperature, it was filtered, and solvent was evaporated. Purification of the solid crude product **17** was accomplished by column chromatography with DCM. Yield: 0.072 g (52%); FT-IR υ (cm^{-1}): 2956-2855 (alkyl-CH), 2558 (-BH); ^{11}B NMR ($CDCl_3$): 24.17 (1B, s), 6.0 (1B, d), 1.26 (1B, d), -1.79 (1B, d), -2.6 (1B, d), -6.8 (8B,b), -16.85 (5B, b), -28.3 (1B, d); UV-Vis λmax (nm) in DMSO: 312, 369, 635, 704.

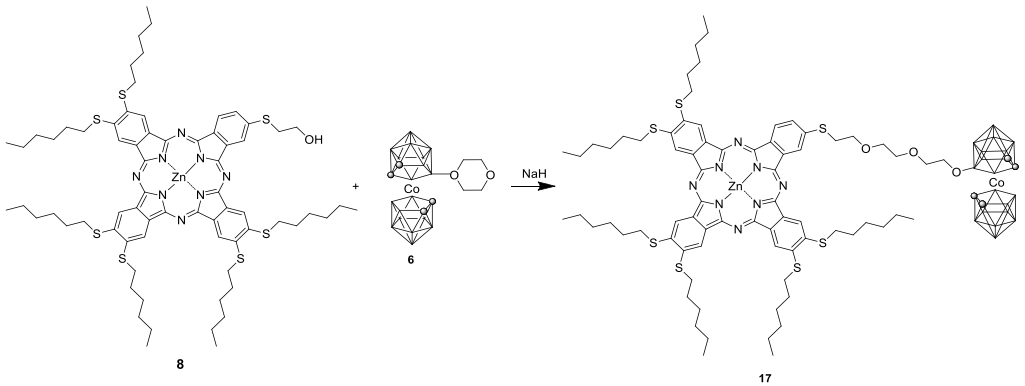

Figure 3.17 : Synthesis of Phthalocyanine **17**.

3.7.2 Synthesis of phthalocyanine 18

0.1 g (0.09 mmol) of Pc **11**, 0.043 g (0.105 mmol) of 3,3′-Co(8-$C_4H_8O_2$-1, 2-$C_2B_9H_{10}$)(1′,2′-$C_2B_9H_{10}$) (**6**) and 0.01 g (0.262 mmol, %60) of NaH were refluxed in 5 mL of C_7H_8 for 12 hours. After the reaction mixture was cooled to room temperature, it was filtered, and solvent was evaporated. Purification of the solid crude product **18** was accomplished by column chromatography with DCM. Yield: 0.095 g (73%); ^{1}H NMR (acetone-*d6*, ppm): δ, ppm: 9.01-8.79 (b, Har), 8.58-8.40 (b, Har), 7.73-7.61(b, Har), 7.37(b, Har), 6.78–6.68 (b, Har), 4.45 (m, CH–O), 3.95-3.33 (m, CH_2) 3.43 (m, CH–O), 1.25–1.19 (CH_3), ^{11}B NMR (acetone-d6, ppm): 24.33 (1B, s), 6.01 (1B, d), 0.37 (1B, d), -2.59 (1B, d), -4.29 (2B, d), -7.35 (2B, d), -8.2 (4B, d), -17.23 (2B, d), -20.42 (2B, d), -21.9 (1B, d), -28.31 (1B, d)., UV-Vis λmax (nm) in DMSO: 313, 358, 617, 685.

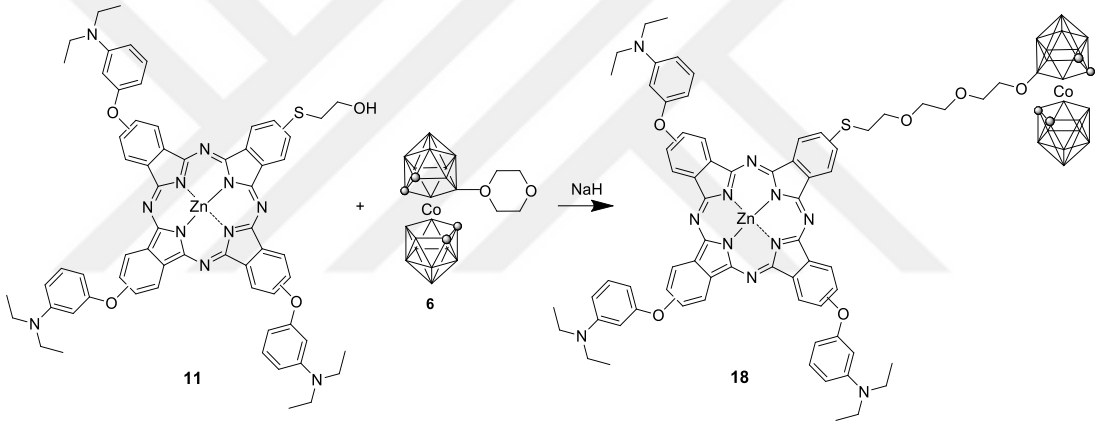

Figure 3.18 : Synthesis of Phthalocyanine **18**.

4. CONCLUSION

This thesis study consists of four sections. In section 4.1, synthesis and characterization of starting materials consisting of phthalonitrile and carborane were described. In section 4.2, the synthesis steps of novel unsymmetrical phthalocyanine derivatives were explained and the methods used to elucidate their structures were mentioned. In section 4.3 shows synthesis methods for the preparation of carborane and metallocarborane-substituted phthalocyanines that can be used for BNCT. It also includes the characterization of complexes using different spectroscopic techniques. In Section 4.2 and 4.3, special emphasis has been placed on increasing the solubility of phthalocyanine derivatives for BNCT. In the last section, electrochemical properties of newly synthesized unsymmetrical phthalocyanine derivatives were investigated.

4.1 Synthesis and Characterization of Phthalonitrile and Carborane Derivatives

The structures of phthalonitrile derivatives and boron-containing units, which are the phthalocyanine starting materials required for the synthesis of the new phthalocyanine complexes targeted in this work, are shown in Figure 4.1.

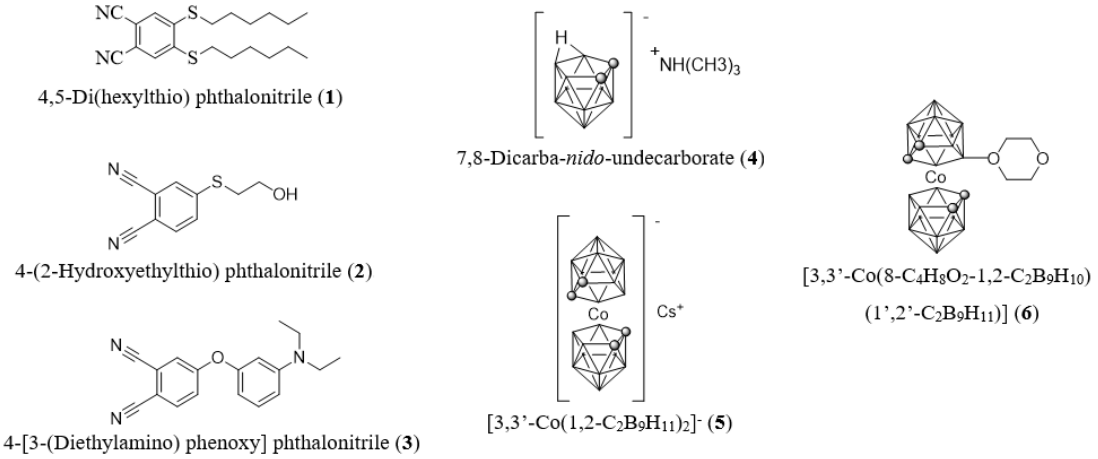

Figure 4.1 : Phthalonitrile and carborane precursors.

The advantageous phthalocyanine precursors are phthalonitriles, which give good yields of phthalocyanine complexes with most metals. Phthalocyanine synthesis is generally easily accomplished by reacting the phthalonitrile with a metal atom in a suitable solvent. However, the syntheses which using precursors such as phthalic anhydrides or phthalimides require a nitrogen supplier like CH_4N_2O and a catalyst like $(NH_4)_6Mo_7O_{24}$ or H_3BO_3.

Our primary aim has been the synthesis of phthalonitrile derivatives bearing long-chain alkylthioether (**1**), thioether (**2**) and dialkylaminophenoxy (**3**) substituents.

4,5 Di(hexylthio) phthalonitrile (**1**) was obtained from 4,5-dichloro-1,2-dicyanobenzene through base-catalyzed nucleophilic aromatic displacement by using the method already described with some changes (Gürek et al., 1994). The reaction was done at ambient temperature with 74% yields. Spectroscopic data (FT-IR and ^{1}H NMR) and elemental analysis confirmed the assigned structure for phthalonitrile **1**.

4-[(2-Hydroxyethyl) thio] phthalonitrile (**2**) was synthesized by the aromatic nitro-displacement between 4-nitrophthalonitrile and 2- hydroxyethylmercaptan with Na_2CO_3 in DMSO (Özçeşmeci et al., 2007). In this reaction, Na_2CO_3 was used as the base and dry DMSO as the solvent. FT-IR, ^{1}H NMR and MALDI-TOFF spectral data and elemental analysis were consequent with the targeted structures of phthalonitrile **2**.

4-[3-(Diethylamino) phenoxy] phthalonitrile (**3**) was accomplished in 98% yield from 4-nitrophthalonitrile and 3- (diethylamino)phenol in dry DMF and Na_2CO_3 was used as base (Dei et al., 2006). This reaction is commonly used in the synthesis of various ether or thioether containing phthalonitrile. Characterization of the phthalonitrile **3** was carried out with elemental analysis and spectroscopic data (FT-IR and ^{1}H NMR). Spectral studies for the phthalonitrile **3** proved the determined structure.

In the FT-IR spectra of phthalonitrile **1**, **2**, and **3** indicated CN group with intense bands at 2228 cm^{-1}, 2226 cm^{-1} and 2234 cm^{-1}, respectively.

In the ^{1}H NMR spectrum of phthalonitrile **1**, the aromatic protons were appeared at 7.40 ppm (s, 2H) and aliphatic protons were appeared at 2.99 (t, 4H), 1.73 (q, 4H), 1.49 (m, 4H), 1.33 (m, 8H) and 0.89 (t, 6H) ppm.

In the ^{1}H NMR spectrum of phthalonitrile **2**, the aromatic protons were appeared at 7.59 (d, 1H), 7.52 (d, 1H) and 7.49 (d, 1H) ppm; -OCH_2, -SCH_2 and -OH protons were appeared at 3.83 (t, 2H), 3.16 (t, 2H) and 2.04 (s, 1H) ppm, respectively.

In the ^{1}H NMR spectrum of phthalonitrile **3**, the aromatic protons were present around 7.69 – 7.22, 6.57 – 6.26 ppm.

Carborane derivatives attract attention with their extraordinary properties such as high boron content and low toxicity as ^{10}B carrier agents for boron neutron capture teraphy. The polyhedral closo- and nido-carboranes and closo-dodecaborate unit are the primary ^{10}B compounds suggested for boron neutron capture therapy. Cyclic oxonium derivatives of polyhedral boron hydrides are compounds with great potential for cancer treatment. Also, cobaltacarborane containing Pc derivatives show the strongest near-IR absorptions, which can use light with deeper penetrating power into most human tissues (Kennedy et al., 1996). The cobalt bis (dicarbollide) anion has three different rotamers with the gradual conformation of the two dicarbollide fragments separated by three retained transition states (Figure 4.2). With the transoid arrangement of the two dicarbollide groups, the minimum energy is preferred for cobalt bis (dicarbollide) over the cisoid conformation (Sivaev et al., 1999; Dash et al., 2017).

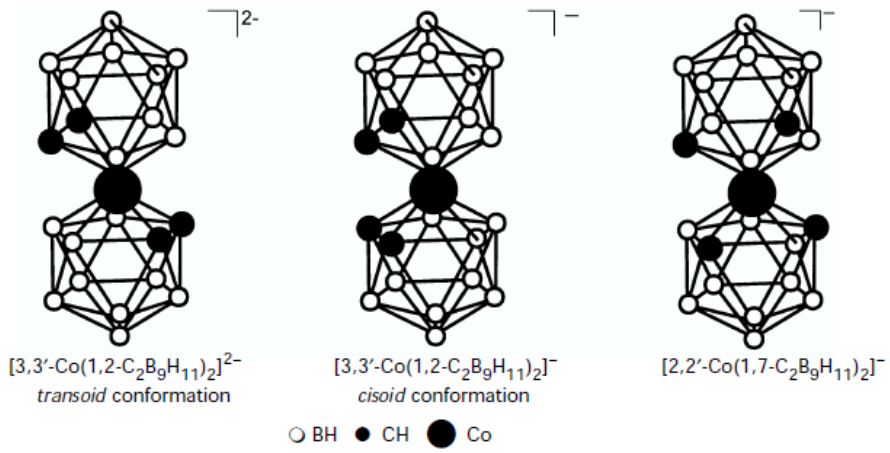

Figure 4.2 : Structure of cobalt bis (dicarbollide) anions.

The preparation of oxonium derivative of cobalt bis(dicarbollide) **6** was carried out in three steps. First, *o*-carborane was degraded by potassium hydroxide and 7,8-dicarba-*nido*-undecarborate anion (**4**) was obtained with 98% yields (Wiesboeck et al., 1964). In the second step, 7,8-dicarba-*nido*-undecaborate is deprotonated to the dianion and followed by reacted with $CoCl_2$. In this reaction is 7,8-dicarba-*nido*-undecaborate was

treated with NaOH in aquous solution to obtain the cesium salt of cobaltocarborane anion **5** (Sivaev et al., 1999). In the last step, the reaction of cobaltocarborane cesium salt with $BF_3.OEt_2$ in 1,4-dioxane results in the corresponding oxonium functionalized cobalt bis(dicarbollide) **6**. This synthesis procedure was carried out as represented in the paper with high yield (Teixidor et al., 2003).

In the ^1H NMR spectrum of cobalt bis(dicarbollide) **6**, CH protons of cobalt bis(dicarbollide) unit was appeared at 4.72 ppm.

The ^{11}B NMR spectra of cobalt bis(dicarbollide) **6** show typical eleven signals in the range of 24.7 to -27.05 ppm.

4.2 Synthesis and Characterization of Unsymmetrical Phthalocyanine Derivatives

More recently, the focus is on the the development of non-symmetrical Pcs which have superior properties in various fields such as second order NLO, PDT of cancer, liquid crystals, and Langmuir–Blodgett film formation. In the present work, novel Pcs involving one different (B) and three identical (A) isoindole subunits (A_3B type) have been synthesized. Statistical condenzation is the most common method to synthesis A_3B-type phthalocyanines. This is a nonselective synthesis procedure and generally provides a mixture of six derivatives with similar physicochemical characteristics. In this method, unit A and unit B are generally used in ratios varying between 3: 1 and 9: 1. However, this ratio increases up to 10: 1 or even 40: 1 due to the different effects of the substituents (Nemykin et al., 2014; Tolbin et al., 2007; Kudrik et al., 2000; de la Torre et al., 2000).

After the synthesis of starting materials, A_3B type metal free and metallo Pc derivatives were synthesized and they were characterized by elemental analysis, NMR, FT-IR, UV-Vis and mass spectral data. Aggregation behavior and electrochemical features of some of them were also reported.

A_3B type metal free phthalocyanine derivative **7** was synthesized in two steps. In the first step, dilithium phthalocyanine was prepared with the lithium templated cyclotetramerization of long-chain alkylthioether (**1**) and thioether (**2**) substituted phthalonitriles in a solvent (1-pentanol). In the second step, dilithium phthalocyanine was converted to metal-free Pc **7** by acidification with CH_3COOH. Column

chromatography was used for the isolation of the A_3B type product with 26% yield. After that, Pc **7** was reacted with $Zn(CH_3COO)_2$ in $C_5H_{12}O$ to give the targated zinc (II) Pc **8** in 94.4% yield following purification by column chromatography using CH_2Cl_2:CH_3OH (50:1) as the eluent. Characterization of the newly synthesized phthalocyanine derivatives Pc **7** and Pc **8** was achieved by FT-IR, UV-vis, ^{1}H NMR, and MALDI-TOF spectral data and elemental analysis. The data were conform with the targeted structures.

The IR spectra of metal-free Pc **7** and metallated Pc **8** were very similar. The IR spectrum of Pc **8** confirmed the targeted structure by the disappearance of the -NH stretching vibrations of the inner phthalocyanine core in the metal-free complex, which are present in Pc **7** around 3290 cm^{-1}. Aliphatic C-H of hexylthio and ethylthio side chains induced intense stretching bands at around 2950 -2850 cm^{-1}.

The ^{1}H NMR spectrum of Pc **8** is similar to that of Pc **7** in deuterated chloroform and one drop of deuterated pyridine. The ordinary shielding of the inner core protons leading to a chemical shift in negative ppm region which was observed at the -4.3 ppm pertains to metal-free phthalocyanine. ^{1}H NMR spectrum of Pc **7** indicated the aromatic protons as multiplets at around 8.42-7.57 ppm; the SCH_2 protons as multiplets at 3.68 and 3.56-3.24 ppm; the aliphatic protons -CH_3 and -CH_2 protons adjacent to them appeared at around 1.05 and 2.03-1.26 ppm. ^{1}H NMR spectrum of Pc **8** exhibited the aromatic protons at around d 9.10–7.62 ppm as multiplets; the SCH_2 protons at 3.84 and 3.44-2.86 ppm as multiplets; the aliphatic protons -CH_3 and -CH_2 protons adjacent to them appeared at around 0.96 and 2.02-1.22 ppm as multiplets. Also, OH protons of Pc **7** and Pc **8** were observed at 4.71 and 4.64, respectively.

The successful formation of the desired molecules was further confirmed by MALDI/TOF MS measurements. In case, the molecular peak of Pc **7** was recorded at *m/z*= 1287.85 $[M]^+$, whereas for Pc **8,** the molecular peaks were observed at *m/z*= 1352.52 $[M+H]^+$.

The electronic absorption spectra of Pc **7** exhibit a Q bands absorptions at 694 and 725 nm bands in THF. Q band absorption for Pc **8** was observed at 699 nm as an intense sharp band with a weaker absorption peak at 629 nm in THF. Also, B bands of these Pcs appeared in the UV area at 342 and 361 nm, respectively.

Aggregation is a common problem for photosensitizing applications of Pc and Pc-like compounds. The aggregation decreases the solubility and excited state lifetime and complicates the characterization and purification of Pc complexes due to the dimers, trimers and higher oligomers formed (Maya et al., 2003; Kostka et al., 2006; Kobak et al., 2015). The formation of aggregation can be prevented by adding long alkyl chains or large substituents around the phthalocyanine macrocycle.

From this point of view, the aggregation behavior of Pc **7** and Pc **8** was observed at different concentrations in $CHCl_3$. No aggregation tendencies were discovered in the absorption spectra of Pc 7 and Pc 8, as the appearance of the Q-band absorption maxima remained unchanged as the concentration increased. Considering these results, Pc **7** and Pc **8** have monomeric structures and obeyed Beer-Lambert law in that concentration range (Figure 4.3).

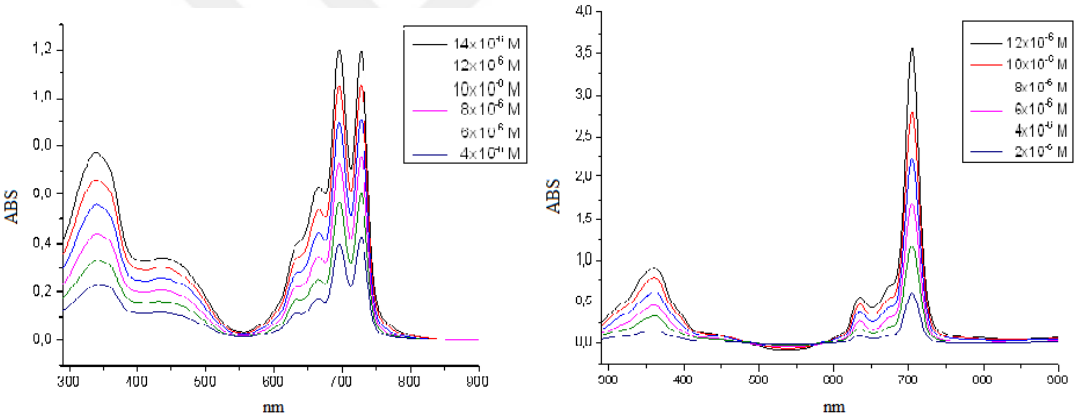

Figure 4.3 : UV-Vis Spectra of Pc **7** and Pc **8**.

By using the same method, conversion of phthalonitrile **2** and phthalonitrile **3** into metal free Pc derivative **10** was accomplished. In addition, Pc **10** was separated from other isomers by multiple column chromatography by using CH_2Cl_2 and CH_3OH as eluents. Metallation of Pc **10** was carried out by refluxing in pentanol with $Zn(CH_3COO)_2$ under N_2 atmosphere. This procedure provided the pure Pc **10** and Pc **11** in 21% and 89% yield, respectively. Pc **10** and Pc **11** were fully characterized with various spectroscopic methods like FT-IR, ^1H NMR, UV-vis, mass spectroscopy, and elemental analysis.

In the FT-IR spectrum of Pc **10**, sharp C≡N vibrations was seen at around 2200 cm^{-1}. The FT-IR spectrum of Pc **10** and Pc **11** are very similar, with the exception of the metal-free Pc **10** showing an NH stretching band at 3285 cm^{-1}.

^{1}H NMR investigations of Pc **10** have provided the characteristic chemical shifts for the expected structures.

The electronic absorption spectrum of the Pc **10** and Pc **11** recorded in DCM. The absorption bands of Pc **10** were recorded B band at 343 and Q bands at 672 and 702 nm. Zinc phthalocyanine derivative Pc **11** exhibits a strong Q band around 683 nm with a weaker absorption peak at 617 nm and B band at 358 nm.

Mass (MALDI-TOF) spectrum showed the molecular ion peak at *m/z*= 1080 $[M]^+$ for Pc **10**.

Steglich esterification is a general method of preparation of ester functional group under very mild conditions (Akkurt et al., 2008). Steglich esterification was achieved with dicyclohexylcarbodiimide (DCC)/ N, N dimethylaminopyridine (DMAP) by reacting the 4-pentynoic acid with Pc **8** and Pc **11** in the presence of anhydrous dichloromethane. Ester functionalized Pc **9** and Pc **13** were obtained in 59.8% and 67% respectively. During the reactions, only small amounts of urea derivatives were formed, and they were removed by routine techniques including precipitation and column chromatography.

In FT-IR spectrum of Pc **9**, stretching band of ≡C-H (3310 cm^{-1}), -C≡C-H group (2202 cm^{-1}), and -C=O (1720 cm^{-1}) appeared at expected frequencies.

Pc **9** exhibited typical electronic spectra with two strong absorption areas. The Q band of this complex was observed at 698 nm with no split and weaker absorption at 630 nm and the B band was observed at around 360 nm in THF.

In the mass spectrum of Pc **9**, the presence of molecular ion peaks at m/z = 1432.47 $[M + H]^+$ confirmed the targeted structure.

In the IR spectra of Pc **13,** absorption bands at 3285 cm^{-1} associated with ≡C-H. Characteristic signals around at 2273 cm^{-1} and 1737 cm^{-1}, due to the -C≡C-H and -C=O groups respectively, are present in the spectra of the Pc **13.**

The absorption bands of metallo Pc **13** were observed B band at 358 nm and Q bands at 617 and 683 nm.

In this thesis, monocarborane containing phthalocyanines were prepared from the reactions between alkynyl units of the Pcs and decaborane. Therefore, Pc **11** was

reacted with propargyl bromide to give Pc **12** including terminal alkynyl group in a yield of 80%.

In the FT-IR spectrum of phthalocyanine Pc **12** the disappearance of O-H band at around 3040 cm^{-1} and observation of –C≡CH unit absorption band at 2160 cm^{-1} are immedidiate indication of substitution.

In the ^{1}H NMR spectrum of Pc **12**, the aromatic protons appeared as broad peaks at 8.94, 8.54, 7.67, 7.37 and 6.69, CH-O protons as broad and multiplets at 4.45 and 3.44 ppm, CH_3 protons at 1.26 – 1.19 ppm. It is likely that broadness is due to both chemical changes caused by probable aggregation at the concentration for NMR measurements.

UV-Vis spectrum of Pc **12** in DCM shows absorption at 684 nm with a shoulder at 619 nm is due to the Q band. The band at 353 nm is attributed to the phthalocyanine Soret band.

4.3 Synthesis and Characterization of Carborane Containing Phthalocyanine Derivatives

The fact that phthalocyanines used for photodynamic therapy show a selective accumulation in cancer cells and their long-term retention there has increased interest in the synthesis of phthalocyanines containing ^{10}B complexes as BNCT agents. Two approaches have been used for the synthesis of boron-containing phthalocyanines; phthalonitrile route and phthalocyanine route. In the first one, carborane containing phthalonitriles are synthesized and then phthalocyanine derivative is prepared by cyclotetramerization and in the phthalocyanine route carborane unit were covalently bound to substituted phthalocyanine complex (Tsaryova et al., 2004; Wöhrle et al., 2013). In this thesis, phthalocyanine route was preferred to synthesis of carborane containing phthalocyanines. Highly hydrophobic character of the closo-carborane cages decreases the solubility of phthalocyanines in water (Renner et al., 2006). To give the carboranylphthalocyanines partial water solubility, either water solubilizing groups (such as amino, hydroxyl or carboxylate) are added to phthalocyanine derivatives or the o-carborane lattices are deboronized to anionic nidocarboranes (Kahl et al., 1996; Pietrangeli et al., 2015).

A monocarborane including Pc **14** was synthesized by reaction of Pc **9** and $B_{10}H_{14}$ in a mixture of dry C_2H_3N and dry C_7H_8. At this stage, boron was added by condensation of $B_{10}H_{14}$ with the alkynyl group of Pc **9**.

In the FT-IR spectra of phthalocyanine Pc **14**, -BH stretching vibration was detected at 2571 cm^{-1} with disappearance of the alkynyl -CH bands at 3310 cm^{-1} and -C≡CH bands at 2202 cm^{-1} was significant evidence of the formation of carborane cluster on Pc **14**.

The ^{1}H NMR spectrum of Pc **14** showed a singlet signal of the CCH proton on *o*-carborane at 4.41 ppm and broad signal of BH protons at 3.22-1.10 ppm.

The ^{11}B-NMR spectra of Pc **14** showed four broad signals. This pattern is typical of the expected o-carborane system.

The successful synthesis of the targeted complexes was confirmed by MALDI/TOF MS measurements. In the MALDI-TOF MS spectrum, molecular ion peak was observed the at 1551.72 as $[M]^+$ and at 1352.090 as $[M\text{-}C_5H_{17}B_{10}O]^+$ for *o*-carborane containing Pc **14**.

The UV–Vis spectra of Pc **9** and Pc **14** were recorded in THF. In case, Q band absorptions were observed at 698 and 700 nm without splitting with weaker absorptions at 630 and 632 nm respectively. Furthermore, B bands of Pc **9** and Pc **14** were observed at 360, 361 respectively.

Aggregation properties of Pc **14** was investigated by recording UV-Vis absorptions at different solvents and at different concentrations in THF (Figure 4.4).

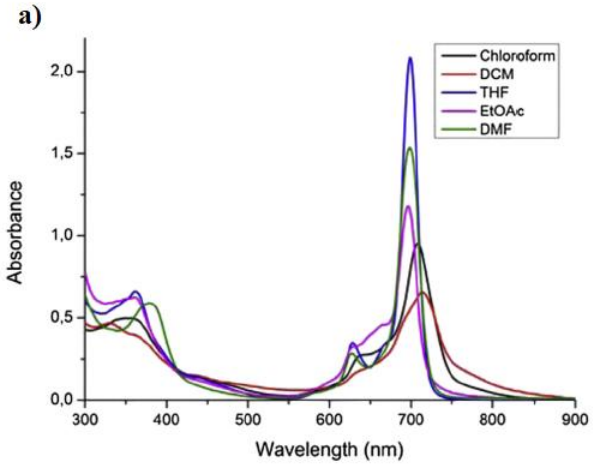

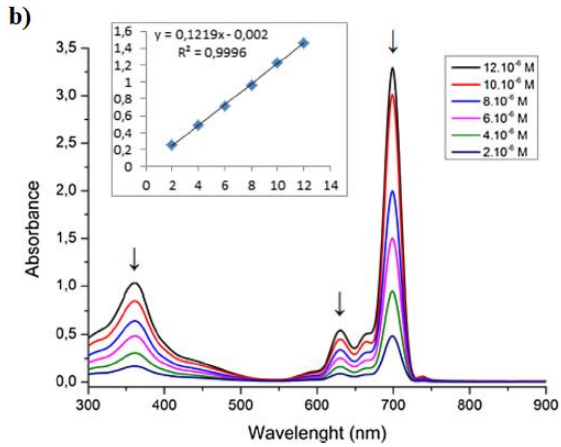

Figure 4.4 : UV-Vis Spectra of Pc **14** in different solvents (Concentration: 10^{-5} M) (a), at different concentrations in THF (b).

As shown in Fig. 4.4 a), The Q-band positions and intensities of Pc **14** were changed by the refractive index of the solvents. Intensity of absorption of the Q-band for Pc **14** was increased in parallel with increasing concentration without any new absorption band adjacent to Q band (Fig. 4.4 b)). Considering these results, Pc **14** has monomeric structure and obeyed Beer-Lambert law in that concentration range.

Using the same procedure described for Pc **14**, alkynyl-substituted Pc **13** and decaborane were reacted in a mixture of C_2H_3N and C_7H_8 to obtain the carborane containing Pc **15**. $B_{10}H_{14}$ insertion to Pc **15** gave the mono-*o*-carborane substituted Pc derivative in 68% yield. After that, Pc **16** which has positively charged quaternary ammonium groups was synthesized by quaternization of Pc **15** with CH_3I in chloroform at 50° C in 2 days by protecting from light. The purity of the newly synthesized phthalocyanine derivatives was verified by elemental analysis, infrared (FT-IR), UV-Vis and NMR spectroscopies.

The infrared spectra of Pc **15** exhibit strong B-H absorption band at 2511 and 2590 and a strong carbonyl absorption band at 1732 cm^{-1}.

The UV-Vis spectrum of Pc **15** displays the B band at 349 nm in the UV area and the Q band at 679 nm in the visible part.

The ^1H NMR spectra of compound Pc **16** in deuterated dimethyl sulfoxide show the Pc ring protons between 9.46 and 7.60 ppm area. The N–CH_2 group protons were observed at 4.15 and 3.93 ppm and N–CH_3 group protons were observed at 3.60 ppm.

The ^{11}B NMR chemical shifts of Pc **16** had broad signals at -3.25 ppm, -9.25 – (-13.94) and – 9.49 ppm, which indicate the carborane cluster.

Pc **16** showed appreciable solubility in water. In the electronic spectra of quaternized compound, the Q-band absorption presented as a shoulder around 615 nm is the main peak at 681 nm and the B band appeared at around 352 nm.

Effective tumor cell killing can only be achieved with a high concentration of ^{10}B nuclei (~ 20 μg of 10B / g tumor) in BNCT (Li et al., 2008). Several porphyrin and phthalocyanines substituted with cobaltacarboranes have been prepared and evaluated as ^{10}B containing agents for BNCT (Hao et al., 2008; Li et al., 2009; Shmal'ko et al., 2014).

Cobaltacarborane functionalized metallophthalocyanine complexes Pc **17** and Pc **18** were prepared from Pc **8** and Pc **11**, respectively. The synthetic way to these cobaltacarborane containing Pcs contains the nucleophilic attack of -OH unit in Pc to the oxonium derivative of cobalt bis(dicarbollide). Cobaltacarborane containing A_3B-type Pc **17** and Pc **18** were separated by column chromatography using DCM as eluent with 52% and 73% yields, respectively.

The ^{11}B NMR spectra of Pc **17** and Pc **18** characteristically show the cobalt bis(dicarbollide) structures boron signals (Nar et al, 2015-2018).

In the absorption spectrum of Pc **17** and Pc **18**, typical Pc strong Q-bands at 704 nm and 685 nm, with weak vibronic shoulders at 635 nm and 617 nm were observed, respectively. Besides, novel Pc derivatives showed Soret bands at 369 nm and 358 nm with additional bands for the cobalt bis(dicarbollide) unit at 312 nm and 313 nm.

4.4 Electrochemistry of Carborane Containing Phthalocyanine Derivatives

Electrochemical properties of newly synthesized unsymmetrical phthalocyanine derivatives were reported. To examine the reduction and oxidation potentials of unsymmetrical phthalocyanine complexes Pc **8**, Pc **9** and Pc **14**, electrochemical studies were carried out by means of CV and SWV in dichloromethane using TBAP as supporting electrolyte system on a platinum working electrode.

CV and SWV voltammograms of Pc **8** are shown in Fig. 4.5. It displayed two one electron reductions and an oxidation versus SCE. The $E_{1/2}$ (ΔE/mV) values were

determined as -0.97 V and -1.32 V for the first and the second reduction waves and 0.70 V for oxidation at 0.1 V s^{-1} scan rate. In Fig. 4.6 *o*-carborane containing phthalocyanine complex Pc **14** showed very similar responses with phthalocyanine complexes Pc **8** and Pc **9**. It displayed two one electron reduction process at -0.89 V and -1.21 V and one oxidation process at 0.68 V versus SCE at 0.1 V s^{-1}. The results we obtained are tabulated on Table 4.1 and the electrochemical behavior of phthalocyanines Pc **8**, Pc **9** and Pc **14** were compared with zinc phthalocyanine with similar substituents other than o-carborane.

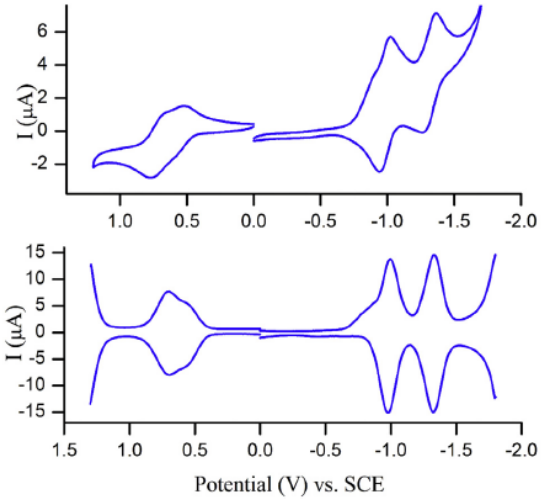

Figure 4.5 : Cyclic and square wave voltamograms of Pc **8** in DCM/TBAP .

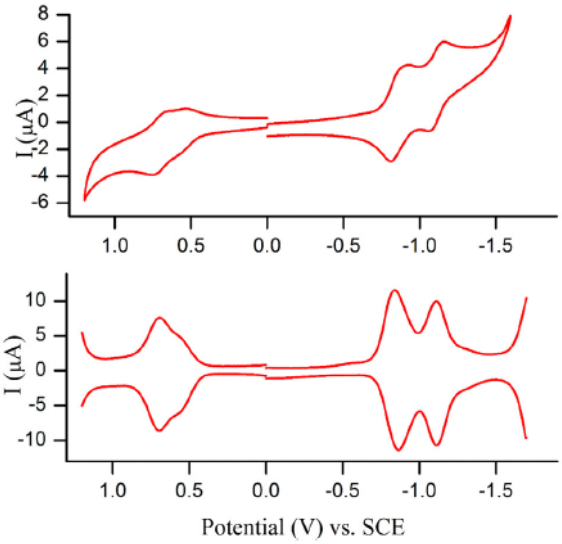

Figure 4.6 : Cyclic and square wave voltamograms of Pc **14** in DCM/TBAP .

Table 4.1 : The electrochemical potentials of Pc 8, Pc 9 and Pc 14.

Compound	Solvent	Ox_2	Ox_1	RR_1	RR_2	Ref.
Pc **8**	DCM		0.70	-0.97	-1.32	tw.
Pc **9**	DCM		0.71	-0.87	-1.22	tw.
Pc **14**	DCM		0.68	-0.89	-1.21	tw.
ZnPc	DCM	0.805	0.60	-0.79	-1.10	(Özkaya et al., 1997)
ZnPc	THF	0.36	0.14	-1.37	-1.76	(Topal et al., 2014)
ZnPc	DCM	0.814	0.633	-0.78	-1.027	(Kalkan et al., 2004)

tw.: This work, RR: Ring Reduction, Ox: Oxidation.

Spectroelectrochemical measurements were executed to enlighten the nature of the redox processes. It is known that the oxidation state of the central zinc ion with completely full d-orbitals does not change (Şen et al., 2014; Birsöz et al., 2014; Karaoğlu et al., 2013; Özçeşmeci et al., 2013; Özkaya et al., 1997; Topal et al., 2014). Thus, all reduction and oxidation processes of the complexes should be referred to phthalocyanine ring or to the connected group. Pc **14** indicated only phthalocyanine ring-based reduction or oxidation during spectroelectrochemical measurements. The spectral changes of Pc **14** are shown in Fig. 4.7. Fig. 4.7a shows the in situ UV-Vis spectral changes during controlled potential reduction of Pc **14** at -0.90 V. The intensity of the Q band at 705 nm increases with a shift to 699 nm while the intensity of B band at 359 nm increases with a shift to 375 nm during the reduction of Pc **14** at -0.9 V potential application. In the spectrum, there are clear isosbestic points at 360, 407, 668, and 712 nm. All of these data support that the reduction is a phthalocyanine ring reduction. Decrease in the Q band intensity at 698 nm without shift and decrease in the B band intensity with a shift to 382 nm indicate the second ring reduction process during the potential application at -1.3 V (Fig. 4.7b). During the oxidation process of Pc **14**, the decrease in the absorption of the Q band and B band in intensity without shift shows ring based oxidation.

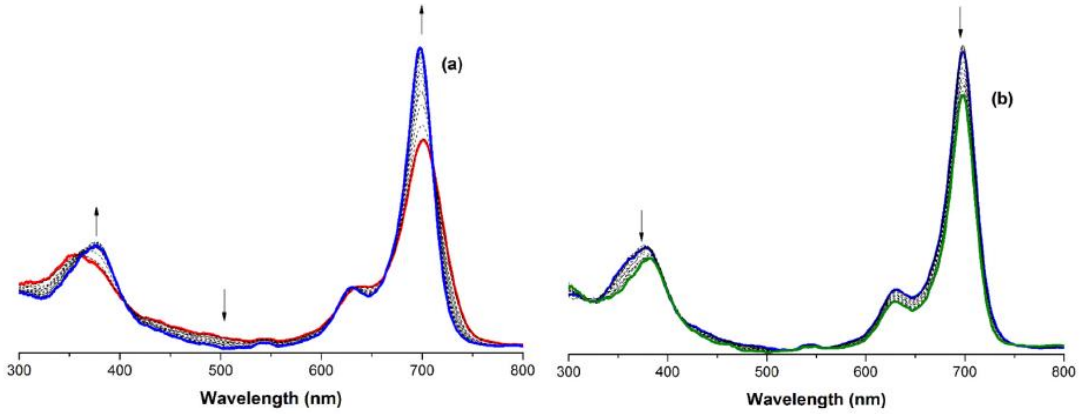

Figure 4.7 : Absorption spectral changes in the electrolysis at (a) -0.90 V and (b) -1.3 V vs. SCE for the first and second reduction of 6 in deaerated DCM containing TBAF. The arrows show the direction of the changes.

Also, in this thesis the electrochemical behavior of Pc **17** was accomplished. A redox inactive metal ion (Zn^{2+}) was preferred in the inner core to distinguish cobaltacarborane and ring-based oxidation-reduction reactions. To determine the reduction and oxidation potentials of low symmetrical Pc derivatives Pc **17**, we undertook electrochemical studies with CV and SWV in CH_2Cl_2 using $C_{16}H_{36}ClNO_4$ electrode.

CV and SWV voltammograms of Pc **17** are shown in Figure 4. 8 undergo three reduction couples, two of which are Pc based and one is characterized by reduction of cobalt ion versus SCE. The $E_{1/2}$ (ΔE/mV) values were determined as −0.88 V and −1.25 V for the first and the second reduction waves and -1.60 V for third reduction at 0.1 V s^{-1} scan rate. The reversible reduction potential at $E_{1/2}$ = –1.25 V is clearly assigned to the reduction processes of the cobalt bis(dicarbollide) unit. Upon scanning to positive potentials, two clear reversible waves are observed at 0.9 V and 1.3 versus SCE, which are associated with redox at the Pc sites.

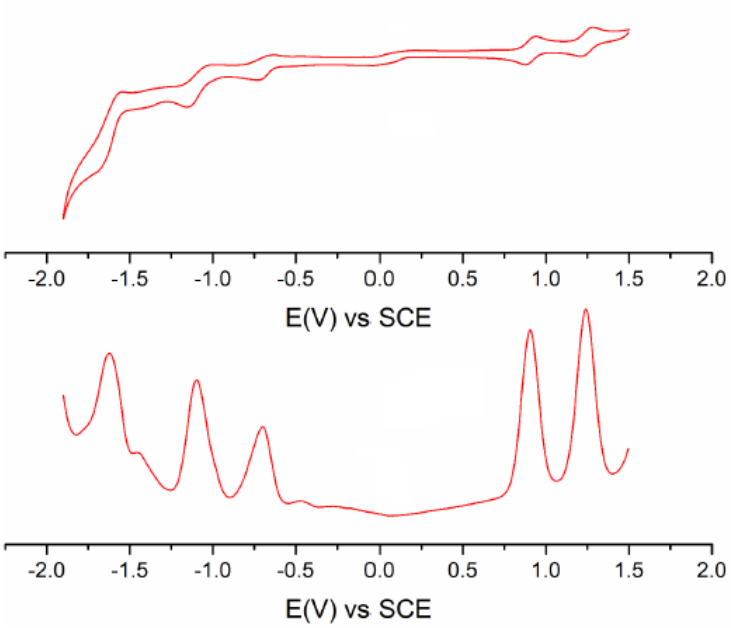

Figure 4.8 : Cyclic and square wave voltamograms of Pc **17** in DCM/TBAP .

REFERENCES

Akkurt, B. & Hamuryudan, E. (2008). Enhancement of Solubility via Esterification: Synthesis and Characterization of Octakis (Ester)-substituted Phthalocyanines, *Dyes and Pigments*, *79*, 153–158.

Alam, F., Soloway, **A. H., Bapat, B. V., Barth, R. E. & Adams, D. M.** (1989). Boron Compounds for Neutron Capture Therapy. Fairchild, R. G., Bond, V. P., Woodhead, A. D., Vivirito, K. (Eds.), *Clinical Aspects of Neutron Capture Therapy* (pp. 107-111). Springer, US: Basic Life Sciences.

Allison, R. R. & Sibata, C. H., (2010). Oncologic photodynamic therapy photosensitizers: a clinical review, *Photodiagnosis and Photodynamic Therapy*, *7*, 61-75.

Archambeau, J. O., (1970). The Effect of Increasing Exposures of the $^{10}B(n,alpha)^{7}Li$ Reaction on The Skin of Man, *Radiology, 94***,** 178–187.

Ayhan, M. M., Durmuş, M. & Gürek, A. G., (2009). Synthesis, Photophysical and Photochemical Studies of Novel Liquid Crystalline Phthalocyanines, *J. Porphyrins Phthalocyanines*, *13*, 722–738.

Birsöz, B., Efremenko, A. V., Ignatova, A. A., Gül, A., Feofanov, A. V., Sivaev, I. B. & Bregadze, V. I. (2013). New Highly-Boronated Zn(II)-Phthalocyanines: Synthesis and *in vitro* Study, *Biochem. Biophys. J. Neutron Ther. Cancer Treat., 1***,** 8-14.

Birsöz, B., Nar, I. & A., Gül (2014). Synthesis, characterization and electrochemical investigation of phthalocyanines carrying 96 boron atoms, *Journal of Organometallic Chemistry, 755***,** 64-71.

Bizet, F., Ipuy, M., Bernhard, Y., Lioret, V., Winckler, P., Goze, C., Perrier-Cornet, J. M. & Decréau, R. A., (2018). Cellular imaging using BODIPY-, pyrene- and phthalocyanine-based conjugates, *Bioorganic & Medicinal Chemistry, 26 (2),* 413-420.

Blochwitz, J., Pfeiffer, M., Fritz, T. & Leo, K., (1998). Low Voltage Organic Light Emitting Diodes Featuring Doped Phthalocyanines as Hole Transport Material, *Appl. Phys. Lett., 73*, 729–731.

Bolfarini, G. C., Siqueira-Moura, M. P., Demets, G. J. F., Morais, P. C. & Tedesco, A. C., (2012). *In vitro* Evaluation of Combined Hyperthermia and Photodynamic Effects Using Magnetoliposomes Loaded with Cucurbit[7]uril Zinc Phthalocyanine Complex on Melanoma, *Journal of Photochemistry and Photobiology B: Biology, 115*, 1–4.

Bonnett, R. (2000). *Chemical Aspects of Photodynamic Therapy*, (pp. 199-222) Amsteldijk, The Netherlands: Gordon and Breach Science.

Bottari, G., Torre, G., Guldi, D. M. & Torres, T., (2010). Covalent and Noncovalent Phthalocyanine-Carbon Nanostructure Systems: Synthesis, Photoinduced Electron Transfer, and Application to Molecular Photovoltaics, *Chem. Rev., 110*, 6768–6816.

Braun, A. & Tcherniac, J. (1907). Uber die producte der einwirkung von acetanhydrid auf phatalamid, *Ber, Deutsch. Chem. Ges., 40*, 2709–2714.

Brilkina, A. A., Dubasova, L. V., Sergeeva, E. A., Pospelov, A. J., Shilyagina, N. Y., Shakhova, N. M. & Balalaeva, I. V., (2019). Photobiological Properties of Phthalocyanine Photosensitizers Photosens, Holosens and Phthalosens: A Comparative *in vitro* Analysis, *Journal of Photochemistry and Photobiology B: Biology*, *191,* 128-134.

Buchler, J. W. (1975). Static Coordination Chemistry of Metalloporphyrins. *In:* Smith, K. M. (eds.), *Porphyrins and Metalloporphyrins*, Amsterdam: Elsevier.

Byrne, G. T., Linstead, R. P. & Lowe, A. R. (1934). Phthalocyanines Part II. The Preparation of Phthalocyanine and Some Metallic Derivatives from Ocyanobenzamide and Phthalimide, *J. Chem. Soc., 28*, 1017–1022.

Calavia, P. G., Chambrier, I., Cook, M. J., Haines, A. H., Field, R. A. & Russell, D. A., (2018). Targeted Photodynamic Therapy of Breast Cancer Cells Using Lactose-Phthalocyanine Functionalized Gold Nanoparticles. *Journal of Colloid and Interface Science*, *512*, 249-259.

Capala, J., Stenstam, B. H., Skold, K., Af Rosenschold, P. M., Giusti, V., ….. Henriksson, R. (2003). Boron Neutron Capture Therapy for Glioblastoma Multiforme: Clinical Studies in Sweden, *J. Neuro-Oncol., 62 (1-2),* 135–144.

Clingerman, D. J., Kennedy, R. D., Mondloch, J. E., Sarjeant, A. A., Hupp, J. T., Farhaa, O. K. & Mirkin, C. A. (2013). An Exceptionally High Boron Content Supramolecular Cuboctahedron, *Chem. Commun., 49 (98),* 11485-11487.

Coderre, J. A., Elowitz, E. H., Chadha, M., Bergland, R., Capala, J., Joel, D. D., Liu, H. B., Slatkin, D. N., & Chanana, A. D., (1997). Boron Neutron Capture Therapy for Glioblastoma Multiforme Using p-boronophenylalanine and Epithermal Neutrons: Trial Design and Early Clinical Results, *Journal of Neuro-Oncology, 33,* 141–152.

Cook, M. J., (1999). Phthalocyanine Thin Films. *Pure Appl. Chem., 71,* 2145–2151.

Dandridge, A. G., Dunworth, S. W., Drescher, H. A. E. & Thomas, A. L. (1929). *United Kingdom Patent No. GB322169.* London: U.K. Patent and Trademark Office.

Dash, B. P., Satapathy, R., Swain, B. R., Mahanta, C. S., Jena, B. B. & Hosmane, N. S. (2017). Cobalt bis(dicarbollide) Anion and its Derivatives, *Journal of Organometallic Chemistry, 849-850,* 170-194.

de la Torre, G., Claessens, C. G. & Torres, T. (2000). Phthalocyanines: The Need for Selective Synthetic Approaches, *Eur. J. Org. Chem*, 2821-2830.

Dei, D., Chiti, G., De Filippis, M. P., Fantetti, L., Giuliani, F., Giuntini, F., Soncin, M., Joric, G. & Roncucci, G. (2006). Phthalocyanines as Photodynamic Agents for the Inactivation of Microbial Pathogens, *J. Porphyrins Phthalocyanines, 10,* 147-159.

Dent, C. E. & Linstead, R. P. (1934). Phthalocyanines Part IV. Copper Phthalocyanines, *J. Chem. Soc., 28,* 1027–1031.

Dent, C. E. & Linstead, R. P. (1934). Phthalocyanines Part VI. The Structure of Phthalocyanines, *J. Chem. Soc., 28,* 1033–1039

Diesbach, D. & Von der Weid, E. (1927). Quelques Sels Complexes Des O-Nitriles Avec Le Cuivre Et La, *Helv. Chim. Acta, 10 (1),* 886–888.

Dini, D. & Hanack, M. (2003). Phthalocyanines: Properties and Materials *In:* Kadish, K. M., Smith, K. M. & Guilard,R. (eds.), *The Porphyrin Handbook.*, Amsterdam: Academic Press.

Duan, C., Zango, G., Iglesias, M. G., Colberts, F. J. M., Wienk, M. M., Martnez-Daz, M. V., Janssen, R. A. J. & Torres, T., (2016). The Role of the Axial Substituent in Subphthalocyanine Acceptors for Bulk-Heterojunction Solar Cells, *Angew. Chem. Int. Ed., 56 (1),* 148-152.

Erk, P. & Hengelsberg, H. (2003). Applications of Phthalocyanines *In:* Kadish, K. M., Smith, K. M. & Guilard,R. (eds.), *The Porphyrin Handbook.*, Amsterdam: Academic Press.

Farr, L. E., Sweet, W. H., Locksley, H. B. & Robertson, J. S., (1954). Neutron Capture Therapy of Gliomas Using Boron, *Trans Am Neurol Assoc., 79,* 110–113.

Fielding, P. E. & Stephenson, N. C., (1965). Crystallographic Constants for Some High-Density β-Phthalocyanines. *Australian Journal of Chemistry, 18 (10),* 1691–1693.

Fox, M. R. (1987). *Dye-makers of Great Britain, 1856-1976: a history of chemists, companies, products, and changes*. Manchester: Imperial Chemical Industries.

Fukuda, T., Hata, K. & Ishikawa, N., (2012). Observation of Exceptionally Low-Lying π–π* Excited States in Oxidized Forms of Quadruple-Decker Phthalocyanine Complexes. *J. Am. Chem. Soc., 134 (36),* 14698-14701.

Furuyama, T., Ogura, Y., Yoza, K. & Kobayashi, N., (2012). Superazaporphyrins: Meso-Pentaazapentaphyrins and One of Their Low-Symmetry Derivatives. *Angew. Chem., 51,* 11110-11114.

Furuyama, T., Satoh, K., Kushiya, T. & Kobayashi, N., (2014). Design, Synthesis, and Properties of Phthalocyanine Complexes with Main-Group Elements Showing Main Absorption beyond 1000 nm, *J. Am. Chem. Soc., 136 (2),* 765-776.

Garip, E. Ö., Özçeşmeci, M., Nar, I., Özçeşmeci, İ. & Hamuryudan, E., (2018). Novel Phthalocyanines Containing Azo Chromophores; Synthesis, Characterization, Photophysical, and Electrochemical Properties, *J. Porphyrins Phthalocyanines, 22,* 198-206.

Gregory, P. M., (2000). Industrial Applications of Phthalocyanines, *J. Porphyrins Phthalocyanines*, *4*, 432–437.

Gürek, A. G. & Bekaroğlu, Ö. (1994). Octakis(a1kylthio)-Substituted Phthalocyanines and Their Interactions with Silver(I) and Palladium(II) Ions, *J. Chem. Soc. Dalton Trans., 84 (4),* 345-351.

Güzel, E., Günsel, A., Bilgiçli, A. T., Atmaca, G. Y., Erdoğmuş, A. & Yarasir, M. N., (2017). Synthesis and Photophysicochemical Properties of Novel Thiadiazole-Substituted Zinc (II), Gallium (III) and Silicon (IV) Phthalocyanines for Photodynamic Therapy. *Inorganica Chimica Acta, 467*, 169-176.

Hammond, R. B., Kubiak, Roberts, K. J., Docherty, R., Edmondson, M., & Gairns, R. J. (1996). X-Form Metal-Free Phthalocyanine: Crystal Structure Determination Using a Combination of High-Resolution X-Ray Powder Diffraction and Molecular Modelling Techniques. *J. Chem. Soc., Perkin Trans., 2*, 1527–1528.

Hao, E., Zhang, M., Wenbo, E., Kadish, K. M., Fronczek, F. R., Courtney, B. H. & Vicente, M. G. H., (2008). Synthesis and Spectroelectrochemistry of N-Cobaltacarborane Porphyrin Conjugates. *Bioconjugate Chem., 19*, 2171–2181.

Hatanaka, H. (1991). Boron-Neutron Capture Therapy for Tumors. In A. B. M. F. Karim, Edward R. LawsJr. (Eds.), *Glioma Principles and Practice in Neuro-Oncology* (pp.233-249) . New York : Springer, Berlin, Heidelberg.

Idowu, M. A., Xego, S., Arslanoglu, Y., Mark, J., Antunes, E. & Nyokong, T., (2018). Photophysicochemical Behavior and Antimicrobial Properties of Monocarboxy Mg (II) and Al (III) Phthalocyanine-Magnetite Conjugates. *Spectrochimica Acta Part A: Molecular and Biomolecular Spectroscopy*, *193*, 407-414.

Janczak, J., Kubiak, R., Richter, J. & Fuess, H., (1999). Bismuth Triple-decker Phthalocyanine: Synthesis and Structure. *Polyhedron, 18 (1999),* 2775–2780.

Joensuu, H., Kankaanranta, L., Seppälä, T., Auterinen, I., Kallio, M., Kulvik, ….. Savolainen, S., (2003). Boron Neutron Capture Therapy of Brain Tumours: Clinical Trials at The Finnish Facility Using Borophenylalanine, *J. Neuro-Oncol., 62*, 123–134.

Kahl, S. B. & Li, J. (1996). Synthesis and Characterization of a Boronated Metallophthalocyanine for Boron Neutron Capture Therapy, *Inorganic Chemistry, 35 (13),* 3878-3880.

Kalkan, A., Koca, A. & Bayır, Z. A. (2004). Unsymmetrical Phthalocyanines with Alkynyl Substituents, *Polyhedron, 23 (18),* 3155-3162.

Karadağ, S., Bozoğlu, C., Şener, M. K. & Koca, A., (2014). Synthesis and Electrochemical Properties of A Double-Decker Lutetium (III) Phthalocyanine Bearing Electropolymerizable Substituents on Non-Peripheral Positions, *Dyes and Pigments, 100*, 168-176.

Karaoğlu, H. R. P., Koca, A. & Koçak, M. B. (2013). The synthesis and electrochemistry of novel, symmetrical, octasubstituted phthalocyanines, *Synthetic Metals, 182*, 1-8.

Kennedy, J. C., Marcus, S. L. & Pottier, R. H. (1996). Photodynamic therapy (PDT) and photodiagnosis (PD) using endogenous photosensitization induced by 5-aminolevulinic acid (ALA): mechanisms and clinical results, *J Clin Laser Med Surg., 14 (5),* 289-304.

Kim, S. H. (2006). *Functional Dyes*. Amsterdam, The Netherlands: Elsevier.

Kobak, R. Z. U., Arı, M. U., Tekin, A. & Gül, A. (2015). Aggregation behavior in unsymmetrically substituted metal-free phthalocyanines, *Chemical Physics, 448,* 91-97.

Kobayashi, N., Nakajima, S., Ogata, H., & Fukuda, T., (2004). Synthesis, Spectroscopy, and Electrochemistry of Tetra-tert-butylated Tetraazaporphyrins, Phthalocyanines, Naphthalocyanines, and Anthracocyanines, together with Molecular Orbital Calculations. *Chem. Eur. J, 10,* 6294-6312.

Kobayashi, N., Ogata, H., Nonaka, N. & Luk'yanets, E. A., (2003). Effect of Peripheral Substitution on the Electronic Absorption and Fluorescence Spectra of Metal-Free and Zinc Phthalocyanines, *Chem. Eur. J., 9,* 5123-5134.

Kobayashi, N., Sasaki, N., Higashi, Y. & Osa, T., (1995). Regiospecific and Nonlinear Substituent Effects on the Electronic and Fluorescence Spectra of Phthalocyanines, *Inorg. Chem., 34 (7),* 1636-1637.

Kostka, M., Zimcik, P., Miletin, M., Klemera, P., Kopecky, K. & Musil, Z., (2006). Comparison of aggregation properties and photodynamic activity of phthalocyanines and azaphthalocyanines, *Journal of Photochemistry and Photobiology A: Chemistry, 178,* 16-25.

Kudrik, E. V., Nikolaev, I. U., Shaposhnikov, G. P., Usol'tseva, N. V. & Bykova, V. V. (2000). Synthetic Approaches to Asymmetric Phthalocyanines and Their Analogues, *Reviews and Accounts, 1,* 142-204.

Li, H., Fronczek, F. R. & Vicente, M. G. H., (2008). Synthesis and properties of cobaltacarborane-functionalized Zn(II)-phthalocyanines, *Tetrahedron Letters, 49,* 4828-4830.

Li, H., Fronczek, F. R. & Vicente, M. G. H., (2009). Cobaltacarborane–phthalocyanine conjugates: Syntheses and photophysical properties, *Journal of Organometallic Chemistry, 694,* 1607-1611.

Linstead, R. P. (1934). Phthalocyanines I. A new type of synthetic coloring matters, *J. Chem. Soc., 28,* 1016–1017.

Linstead, R. P. & Lowe, A. R. (1934). Phthalocyanines Part V. The Molecular Weight of Magnesium Phthalocyanine, *J. Chem. Soc., 28,* 1031–1033.

Lipscomb, W. H. (1993). The Boranes and Their Relatives. Forsén, S. (Ed.), in *Nobel Lectures, Chemistry 1971–1980* (pp. 224-245). Singapore: World Scientific Publishing Co.

Liu, Y. (2010). *Phthalocyanines for Photodynamic Therapy* (Doctoral dissertation).

Maree, S., Phillips, D. & Nyokong, T., (2002). Synthesis, Photophysical and Photochemical Studies of Germanium and Tin Phthalocyanine Complexes. *J. Porphyrins Phthalocyanines, 6,* 17-25.

Matlou, G. G., Kobayashi, N., Kimura, M., & Nyokong, T., (2017). Physicochemical Properties of Water Soluble Unsymmetrical Phthalocyanine-Folic Acid Conjugates. *Dyes and Pigments, 149,* 393-398.

Maya, E. M., Snow, A. W., Shirk, J. S., Pong, R. G. S., Flom, S. R. & Roberts, G. L, (2003). Synthesis, aggregation behavior and nonlinear absorption properties of lead phthalocyanines substituted with siloxane chains. *J. Mater. Chem., 13,* 1603-1613.

Mishima, Y., Ichihashi, M., Hatta, S., Honda, C., Yamamura, K., Nakagawa, T., Obara, H., Shirakawa, J., Hiratsuka, J., Taniyama, K., Tanaka, C. & Kanda, K., (1989). First Human Clinical Trial of Melanoma Neutron Capture. Diagnosis and Therapy, *Strahlenther.Onkol., 165 (2-3),* 251–254.

Moser, F. H. & Thomas, A. L. (1963). *Phthalocyanine Compounds*. New York: Reinhold Publ. Corp.

Moser, F. H. & Thomas, A. L., (1983). *The Phthalocyanines, Properties,* CRC. Boca Raton, Florida, 1-20.

Moss, R. L., (1990). Progress Towards Boron Neutron Capture Therapy at the High Flux Reactor Petten. Harling O. K., Bernard J. A., Zamenhof R. G. (Eds.), *Neutron Beam Design, Development, and Performance for Neutron Capture Therapy* (Vol. 54, pp. 169-183). Springer, Boston, MA: Basic Life Sciences.

Muranaka, A., Yonehara, M. & Uchiyama, M., (2010). Azulenocyanine: A New Family of Phthalocyanines with Intense Near-IR Absorption. *J. Am. Chem. Soc., 132 (23),* 7844-7845.

Nar, I., Atsay, A., Altındal, A. & Hamuryudan, E., (2018). *o*-Carborane, Ferrocene, and Phthalocyanine Triad for High-Mobility Organic Field-Effect Transistors, *Inorg. Chem., 57 (4),* 2199–2208.

Nar, I., Atsay, A., Gümrükçü, S., Karazehir, T. & Hamuryudan, E., (2018). Low-Symmetry Phthalocyanine Cobalt Bis(dicarbollide) Conjugate for Hydrogen Reduction, *Eur. J. Inorg. Chem., 34,* 3878–3882.

Nar, I., Bortolussi, S., Postuma, I., Atsay, A., Berksun, E., Viola, E., Ferrari, C., Cansolino, L., Ricciardi, G., Donzello, M. P. & Hamuryudan, E. (2019). A Phthalocyanine-ortho-Carborane Conjugate for Boron Neutron Capture Therapy: Synthesis, Physicochemical Properties, and *in vitro* Tests, *ChemPlusChem, 84 (4),* 345-351.

Nar, I., Gül, A., Sivaev, I. B. & Hamuryudan, E. (2015). Cobaltacarborane Functionalized Phthalocyanines: Synthesis, Photophysical, Electrochemical and Spectroelectrochemical Properties, *Synthetic Metals, 210,* 376–385.

Nemykin, V. N., Dudkin, S. V., Dumoulin, F., Hirel, C., Gürek, A. G. & Ahsen, V. (2014). Synthetic Approaches to Asymmetric Phthalocyanines and Their Analogues, *Reviews and Accounts, 1,* 142-204.

Nwaji, N., Dingiswayo, S., Mack, J. & Nyokong, T., (2018). Photophysical and Enhanced Nonlinear Optical Response in Asymmetric Benzothiazole Substituted Phthalocyanine Covalently Linked to Semiconductor Quantum Dots, *Spectrochimica Acta Part A: Molecular and Biomolecular Spectroscopy, 204*, 629–639.

Nyokong, T., (2007). Effects of Substituents on The Photochemical and Photophysical Properties of Main Group Metal Phthalocyanines. *Coordinatian Chemistry Reviews, 251(13-14)*, 1707-1722.

Ogbodu, R. O., Limson, J. L., Prinsloo, E. & Nyokong, T., (2015). Photophysical Properties and Photodynamic Therapy Effect of Zinc Phthalocyanine-Spermine-Single Walled Carbon Nanotube Conjugate on MCF-7 Breast Cancer Cell Line, *Synthetic Metals, 204,* 122–132.

Özçelik, Ş., Karaoğlan, G. K., Gümrükçü, G., Erdoğmuş, A. & Gül, A., (2014). Photophysical and Photochemical Properties of A Zinc Phthalocyanine With Four Diphenylborinic Ester Moieties. *Journal of Organometallic Chemistry, 769,* 17-23.

Özçeşmeci, İ., Burat, A. K., İpek, Y., Koca, A. & Bayır, Z. A. (2013). Synthesis, electrochemical and spectroelectrochemical properties of phthalocyanines having extended π-electrons conjugation, *Electrochimica Acta, 89,* 270-277.

Özçeşmeci, İ., Okur, A. İ. & Gül, A. (2007). New Phthalocyanines Bearing Tetra(hydroxyethylthio) Functionalities, *Dyes and Pigments, 75,* 761-765.

Özçeşmeci, İ., Özçeşmeci, M., Gül, A. & Hamuryudan E. (2016). Synthesis and Spectroscopic Investigation of Boronic Esters of Metal-Free Fluorinated and Non-Fluorinated Phthalocyanines. *Synthetic Metals, 222,* 344-350.

Özçeşmeci, M., Baş, S. S., Akkurt, B., Bolkent, Ş. & Hamuryudan E. (2020). Synthesis, Characterization and Staining Performance of Peripherally and Non-peripherally Substituted Metallophthalocyanines Bearing 1,3-Bis-(trimethylamino)-2-propoxy Groups. *New Journal of Chemistry, 44,* 7786-7794.

Özçeşmeci, M., Baş, S. S., Akkurt, B., Hamuryudan E. & Bolkent, Ş. (2018). Synthesis and Biological Uses of A3B Type Water-Soluble Phthalocyanine Alternate to Alcian Blue. *ChemistrySelect, 3,* 12805-12812.

Özkaya, A. R., Gürek, A. G., Gül, A. & Bekaroğlu, Ö. (1997). Electrochemical and spectral properties of octakis(hexylthio)-substituted phthalocyanines. *Polyhedron, 16 (11),* 1877-1883.

Patterson, M. S., Madsen, S. J. & Wilson, R. J., (1990). Experimental Tests of The Feasibility of Singlet Oxygen Luminescence Monitoring *in-vivo* During Photodynamic Therapy. *J. Photochem. Photobiol. B: Biol., 5*, 69-84.

Pietrangeli, D., Rosa, A., Pepe, A., Altieri, S., Bortolussi, S., Postuma, I., Protti, N., Ferrari, C., Cansolino, L., Clerici, A. M., Viola, E., Donzello, M. P. & Ricciardi, G. (2015). Water-soluble carboranyl-phthalocyanines for BNCT. Synthesis, characterization, and in vitro tests of the Zn(ii)-nido-carboranyl-hexylthiophthalocyanine, *Dalton Transactions, 44 (24)*, 11021-11028.

Pinelli, T., Zonta, A., Altieri, S., **Barni, S., Braghieri, A., Pedroni, P., Bruschi, P., Chiari, P., Ferrari, C. & Zonta, C.** (2002). TAOrMINA: From the First Idea to The Application to The Human Liver, *10th International Congress on Neutron Capture Therapy,* Essen, Germany, September 8-13.

Renner, M. W., Miura, M., Easson, M. W. & Vicente, M. G. H. (2006). Recent Progress in the Syntheses and Biological Evaluation of Boronated Porphyrins for Boron Neutron-Capture Therapy, *Anti-Cancer Agents in Medicinal Chemistry, 6 (2)*, 145-157.

Robertson, J. M., (1935). An X-Ray Study of the Structure of the Phthalocyanines. I. Metal-Free, Nickel, Copper and Platinum Compounds, *J. Chem. Soc.*, *29*, 615–621.

Robertson, J. M., (1936). An X-Ray Study of the Structure of the Phthalocyanines. Part II. Quantitative Structure Determination of Metal-Free Compound, *J. Chem. Soc.*, 1195–1209.

Robertson, J. M. & Woodward, I. (1937). An X-Ray Study of the Structure of the Phthalocyanines. Part III. Quantitative Structure Determination of Nickel Phthalocyanine, *J. Chem. Soc.*, 219–230.

Rosenthal, I. & Ben-Hur, E., (1995). Role of Oxygen in The Phototoxicity of Phthalocyanine. *Int. J. Radiat. Biol.*, *67*, 85-91.

Sakamoto, K. & Ohno-Okumura, E., (2009). Syntheses and Functional Properties of Phthalocyanines, *Materials, 2 (3)*, 1127–1179.

Saki, N., Akin, M., Atsay, A., Karaoglu, H. R. P. & Kocak, M. B., (2018). Synthesis and Characterization of Novel Quaternized 2, 3-(diethylmethylamino)phenoxy tetrasubstituted Indium and Gallium Phthalocyanines and Comparison of Their Antimicrobial and Antioxidant Properties with Different Phthalocyanines, *Inorganic Chemistry Communications, 95*, 122–129.

Sharman, W. M., Allen, C. M. & van Lier, J. E., (1999). Photodynamic Therapeutics: Basic Principles and Clinical Applications, *Drug Discov Today, 4 (11)*, 507-517.

Sharman, W. M. & van Lier, J. E., (2003). Phthalocyanines: Synthesis; Synthesis of Phthalocyanine Precursors, *In:* Kadish, K. M., Smith, K. M. & Guilard,R. (eds.), *The Porphyrin Handbook.*, New York: Academic Press.

Shmal'ko, A. V., Efremenko, A. V., Ignatova, A. A., , Sivaev, I. B., Feofanov, A. V., Hamuryudan, E., Gül, A., Kovalenko, L. V., Qi, S. & Bregadze, V. I. (2014). Synthesis and In Vitro Study of New Highly Boronated Phthalocyanine, *J. Porphyrins Phthalocyanines*, *18*, 1–7.

Sivaev, I. B. & Bregadze, V. I. (1999). Chemistry of Cobalt Bis(Dicarbollides). A Review, *Collect. Czech. Chem. Commun., 64,* 783-805.

Sorokin, A. B., (2013). Phthalocyanine Metal Complexes in Catalysis, *Chem. Rev., 113,* 8152–8191.

Szpak, S., Gabriel, C. J. & Driscoll, J. R., (1984). Li/$SOCl_2$ Battery Intercell Currents, *J. Electrochem. Soc., 131 (9),* 1996-2005.

Şen, B. N., Mert, H., Dinçer, H. & Koca, A., (2014). Synthesis and characterization of terminalalkynyl-substituted unsymmetrical zinc phthalocyanine conjugated with well-defined polymers, */ Dyes and Pigments, 100,* 1-10.

Taratula, O., Schumann, C., Naleway, M. A., Pang, A. J., Chon, K. J. & Taratula, O., (2013). A Multifunctional Theranostic Platform Based on Phthalocyanine-Loaded Dendrimer for Image-Guided Drug Delivery and Photodynamic Therapy, *Mol. Pharmaceutics, 10 (10),* 3946-3958.

Teixidor, F., Pedrajas, J., Rojo, I., Viñas, C., Kivekäs, R., Sillanpää, R., Sivaev, I., Bregadze, V. & Sjöberg, S. (2003). Chameleonic Capacity of [3,3'-$Co(1,2\text{-}C_2B_9H_{11})_2]^-$ in Coordination. Generation of the Highly Uncommon S(thioether)-Na Bond, *Organometallics, 22,* 3414-3423.

Tolbin, A. Yu, Tomilova, L. G. & Zefirov, N. S. (2007). Non-symmetrically Substituted Phthalocyanines: Synthesis and Structure Modification, *Russian Chemical Reviews, 76 (7),* 681-692.

Topal, S. Z., İşçi, Ü., Kumru, U., Atilla, D., Gürek, A. G., Hirel, C., Durmuş, M., Tommasino, J. B., Luneau, D., Berber, S., Dumoulin, F. & Ahsen, V. (2014). Modulation of the electronic and spectroscopic properties of Zn(ii) phthalocyanines by their substitution pattern, *Dalton Transactions, 43,* 6897-6908.

Tsaryova, O., Semioshkin, A., Wöhrle, D. & Bregadze, V. I. (2004). Synthesis of New Carboran-based Phthalocyanines and Study of Their Activities in the Photooxidation of Citronellol, *J. Porphyrins Phthalocyanines, 9,* 268-274.

Ukei, K., (1976). Electroconductive Properties of a One-Dimensional Conductor Lead Phthalocyanine. *J. Phys. Soc. Japan., 40,* 140–143.

Wang, A., Long, L. & Zhang, C., (2012). Synthesis of unsymmetrical phthalocyanines: a brief overview, *Tetrahedron, 68,* 2433-2451.

Wehrle, B. & Limbach, H. H., (1989). NMR Study of Environment Modulated Proton Tautomerism in Crystalline and Amorphous Phthalocyanine. *Chem. Phys., 136,* 223–247.

Wiesboeck, R. A. & Hawthorne, M. F. (1964). Dicarbaundecaborane (13) and Derivatives, *J. Amer. Chem. Soc., 86,* 1642-1643.

Wöhrle, D., Tsaryova, O., Semioshkin, A., Gabel, D. & Suvorova, O. (2013). Synthesis and photochemical properties of phthalocyanine zinc(II) complexes containing o-carborane units, *Journal of Organometallic Chemistry, 747,* 98-105.

Yamamoto, S., Zhang, A., Stillman, M. J., Kobayashi, N. & Kimura, M., (2016). Low-Symmetry Ω-Shaped Zinc Phthalocyanine Sensitizers having Panchromatic Light-Harvesting Property for Dye-Sensitized Solar Cells, *Chem. Eur. J.*, *22*, 1-10.

Zhang, Z., Kong, L., Xiong, Y., Luo, Y. & Li, J., (2014). The synthesis of Cu(II), Zn(II), and Co(II) Metalloporphyrins and Their Improvement to the Property of Li/$SOCl_2$ Battery, *J. Solid State Electrochem.*, *18 (12)*, 3471–3477.

APPENDICES

APPENDIX A: Spectra

APPENDIX A: Spectra

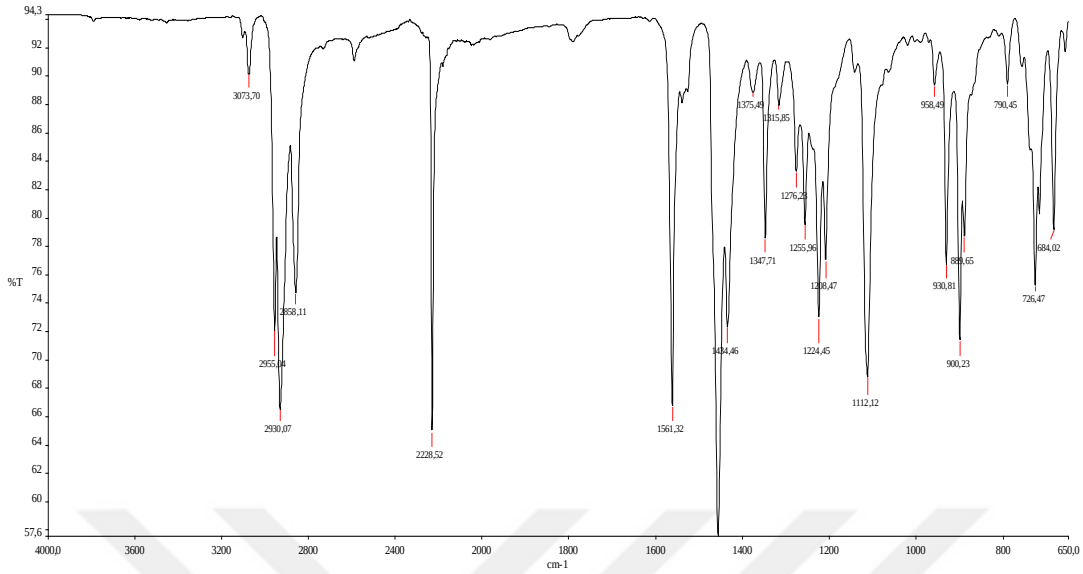

Figure A.1 : FT-IR spectrum of 4,5 Di(hexylthio) phthalonitrile (**1**).

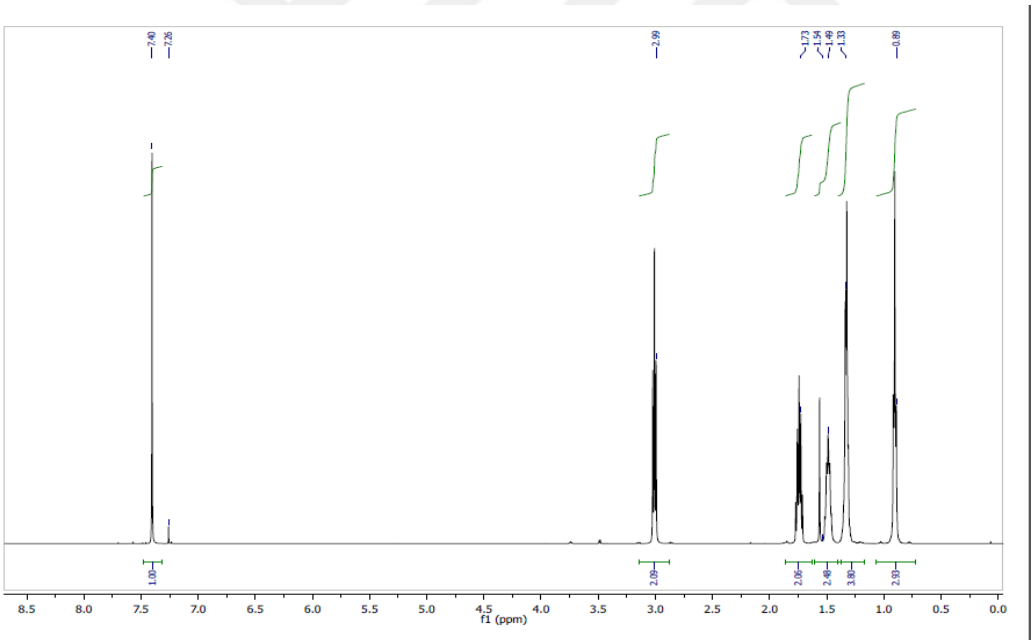

Figure A.2 : ^{1}H NMR spectrum of 4,5 Di(hexylthio) phthalonitrile (**1**).

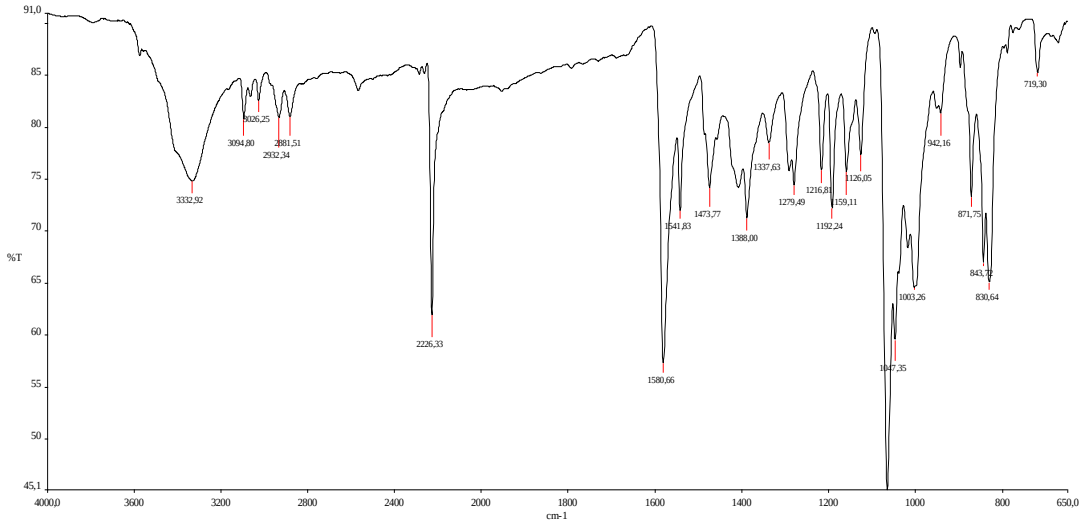

Figure A.3 : FT-IR spectrum of 4-[(2-hydroxyethyl)thio] phthalonitrile (**2**).

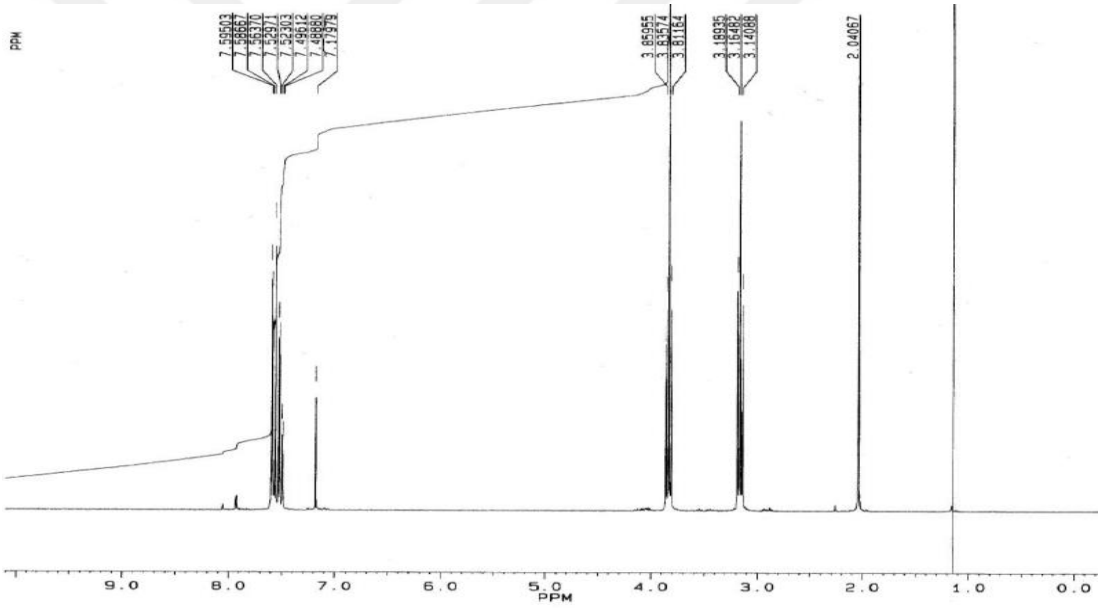

Figure A.4 : ^{1}H NMR spectrum of 4-[(2-hydroxyethyl)thio] phthalonitrile (**2**).

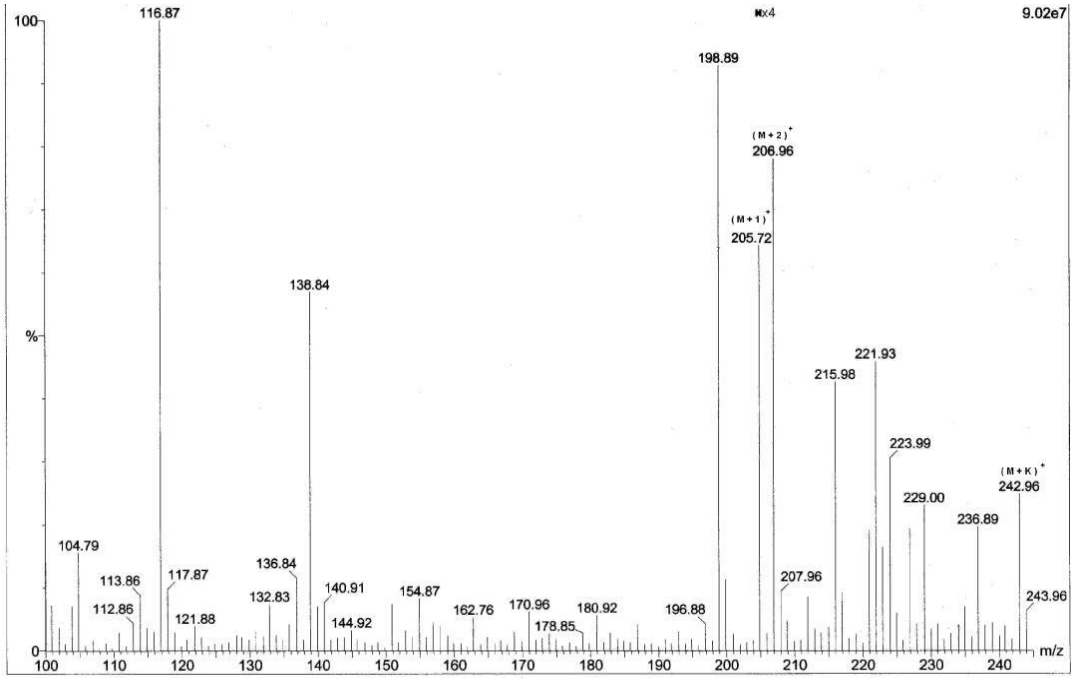

Figure A.5 : FAB-MASS spectrum of 4-[(2-hydroxyethyl)thio] phthalonitrile (**2**).

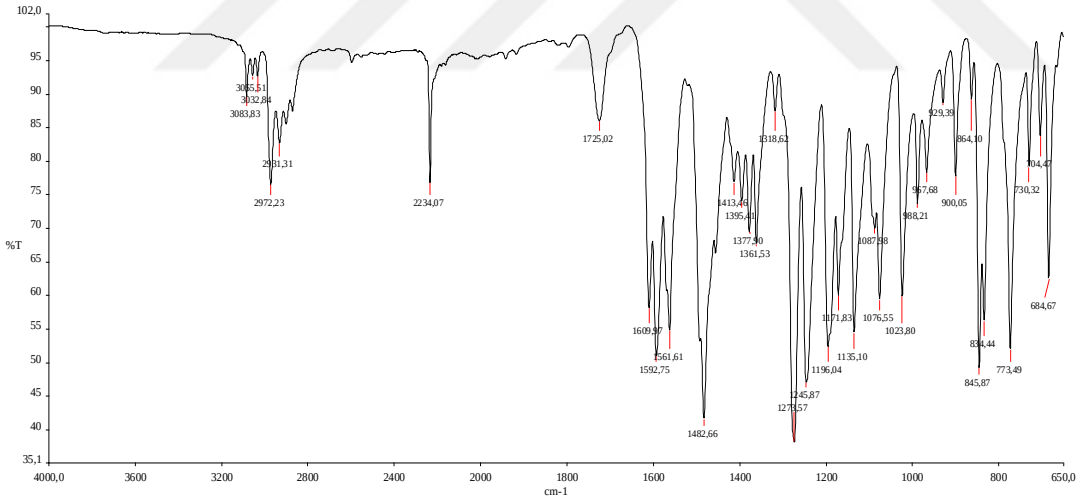

Figure A.6 : FT-IR spectrum of 4-[3-(diethylamino)phenoxy] phthalonitrile (**3**).

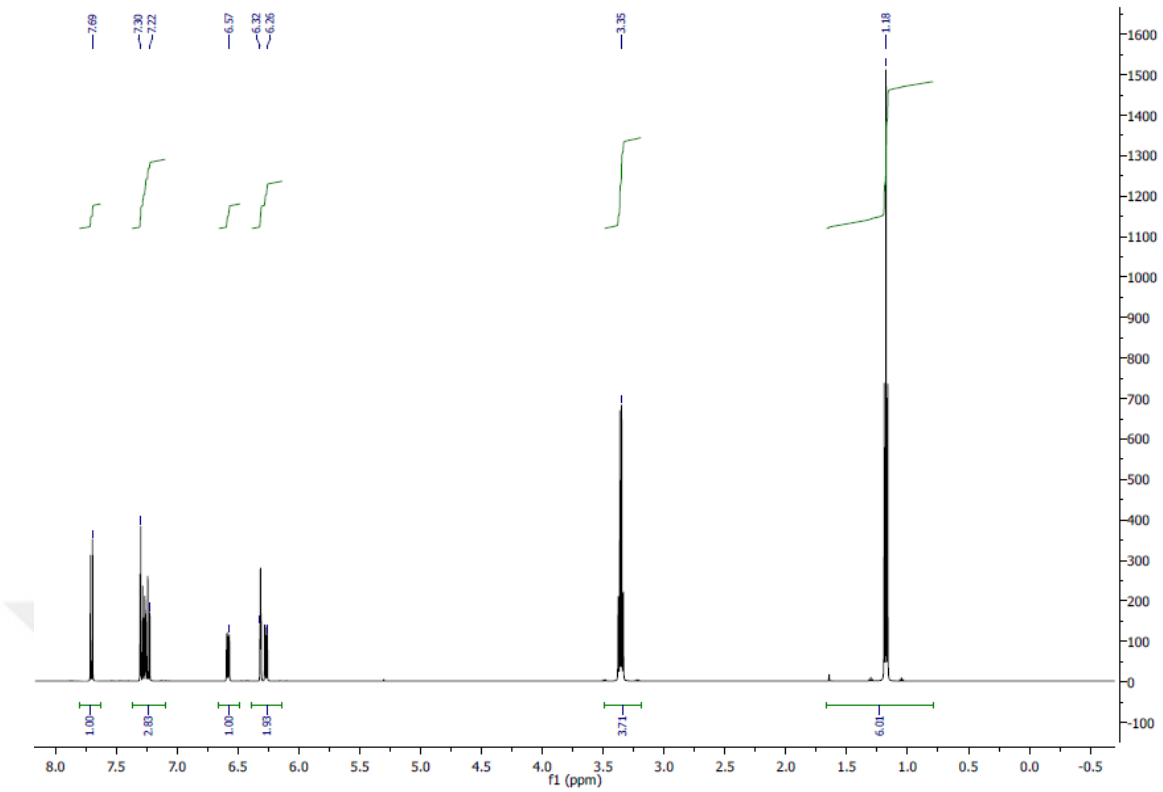

Figure A.7 : ^{1}H NMR spectrum of 4-[3-(diethylamino)phenoxy] phthalonitrile (**3**).

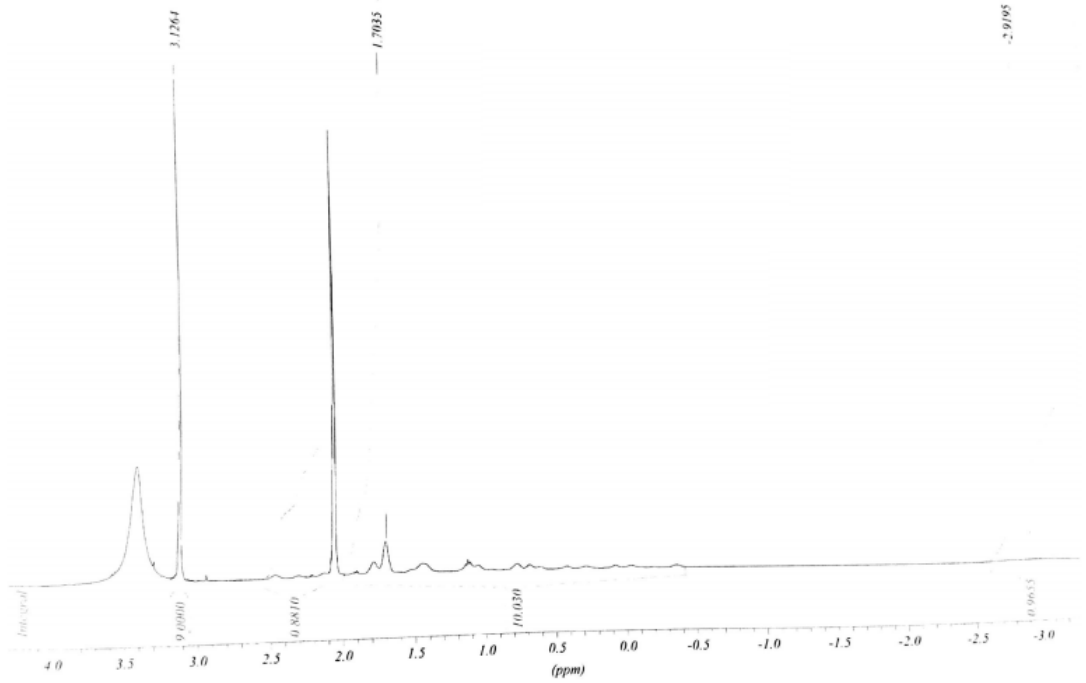

Figure A.8 : ^{1}H NMR spectrum of 7,8-dicarba-nido-undecaborate (**4**).

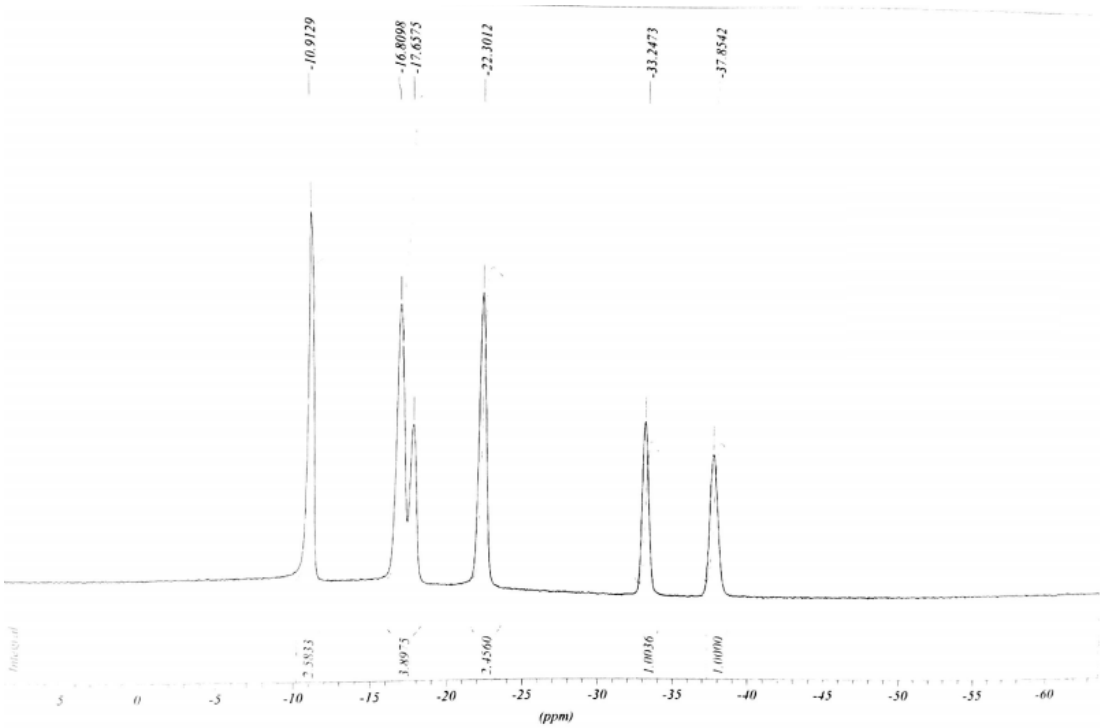

Figure A.9 : ^{11}B NMR spectrum of 7,8-dicarba-nido-undecaborate (**4**).

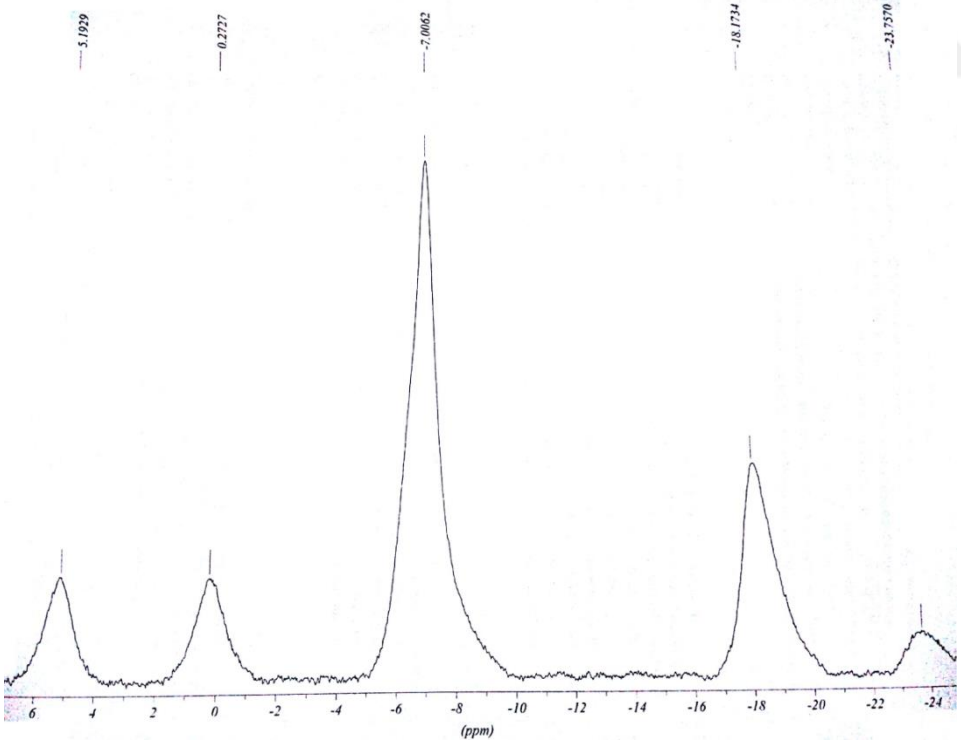

Figure A.10 : ^{11}B NMR spectrum of [3,3'-Co(1,2-$C_2B_9H_{11})_2]^-$ (**5**).

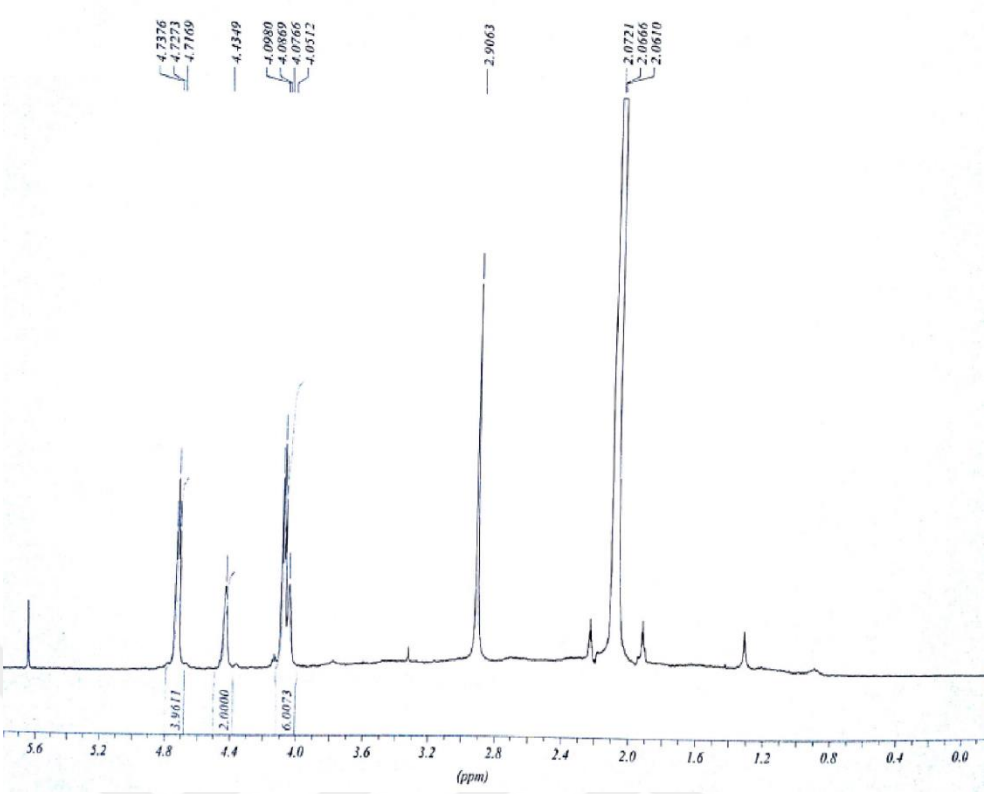

Figure A.11 : ^{1}H NMR spectrum of [3,3′-Co(8-$C_4H_8O_2$-1,2-$C_2B_9H_{10}$)(1′,2′-$C_2B_9H_{11}$)] (**6**).

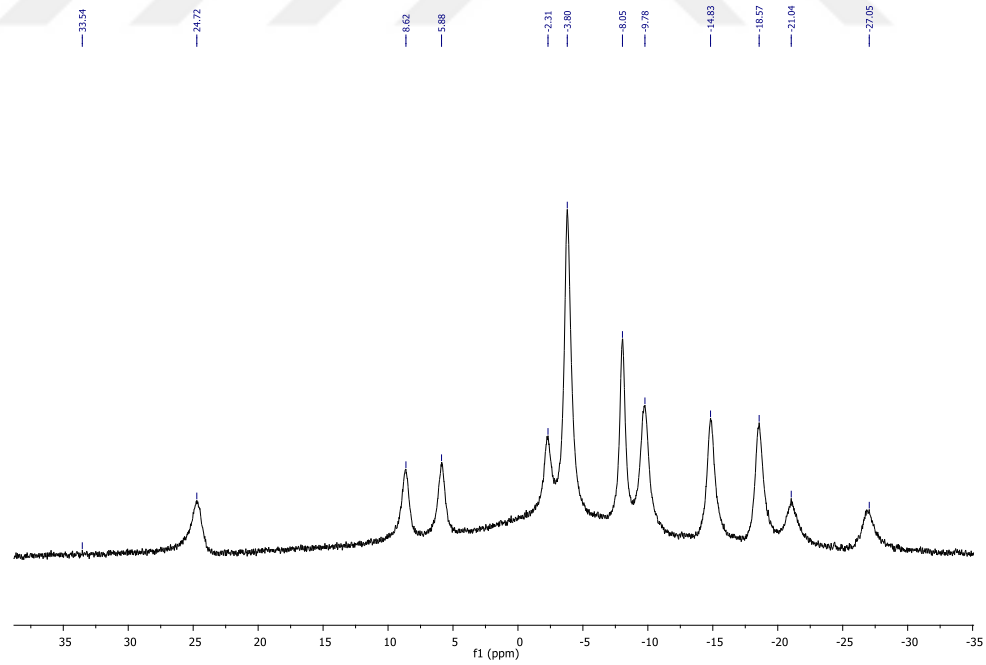

Figure A.12 : ^{11}B NMR spectrum of [3,3′-Co(8-$C_4H_8O_2$-1,2-$C_2B_9H_{10}$)(1′,2′-$C_2B_9H_{11}$)] (**6**).

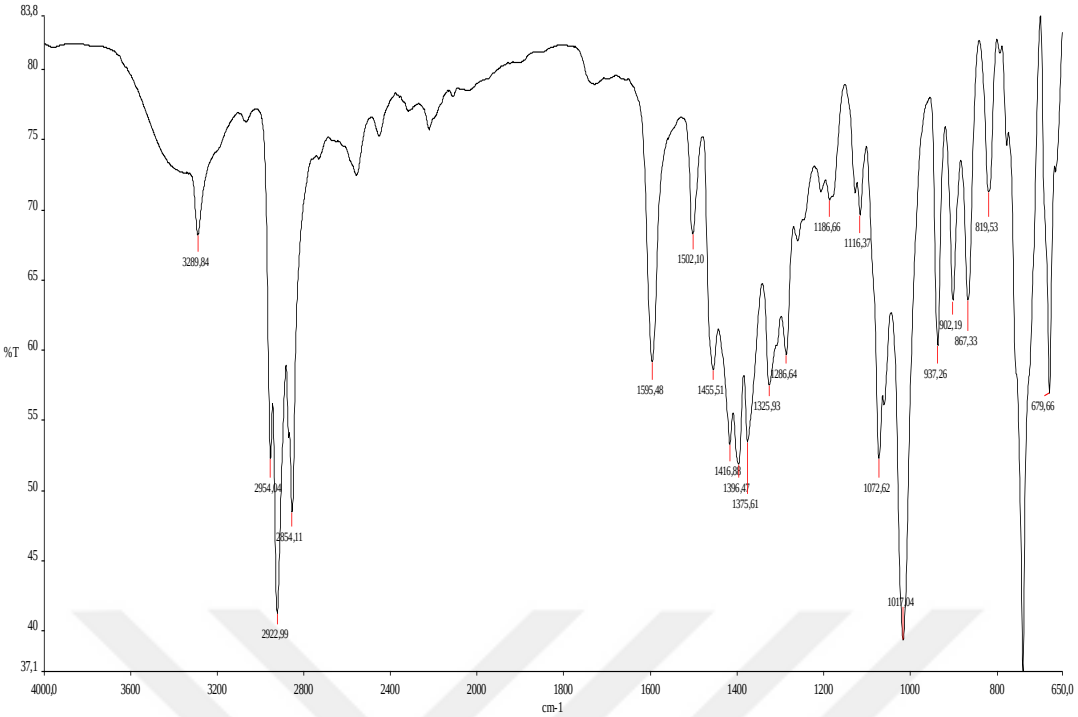

Figure A.13 : FT-IR spectrum of 2,3,9,10,16,17-hexakis(hexylthio)-23-hydroxyethylthiophthalocyanine (**7**).

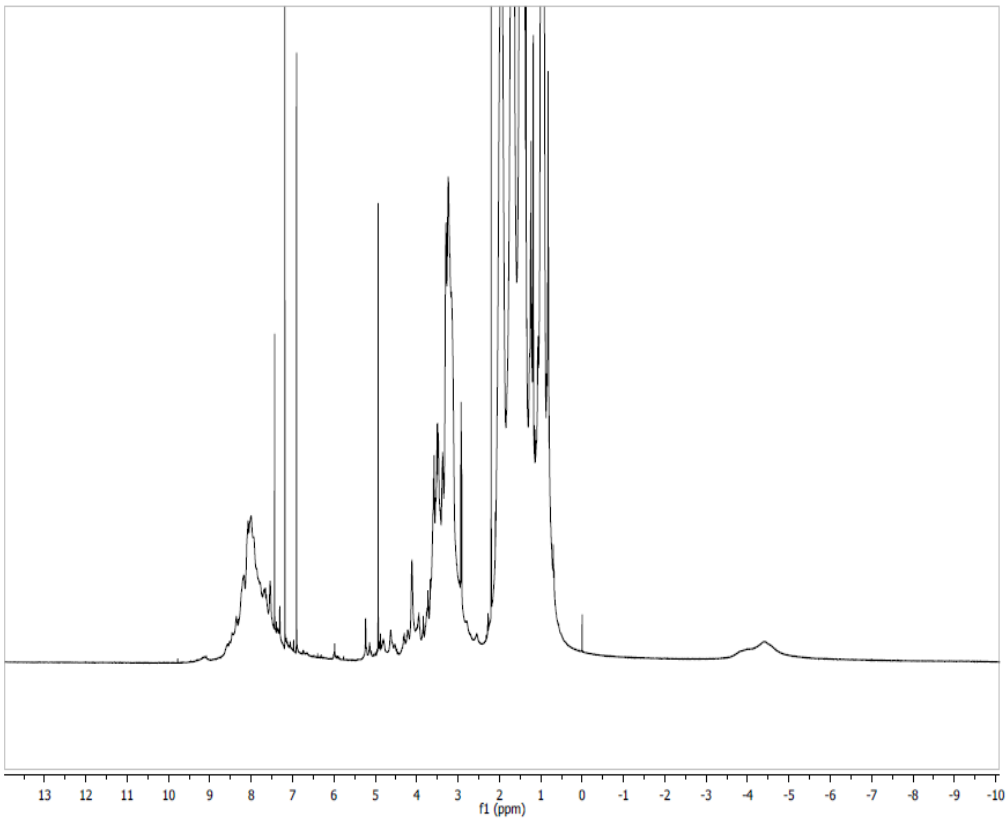

Figure A.14 : ^{1}H NMR spectrum of 2,3,9,10,16,17-hexakis(hexylthio)-23-hydroxyethylthiophthalocyanine (**7**).

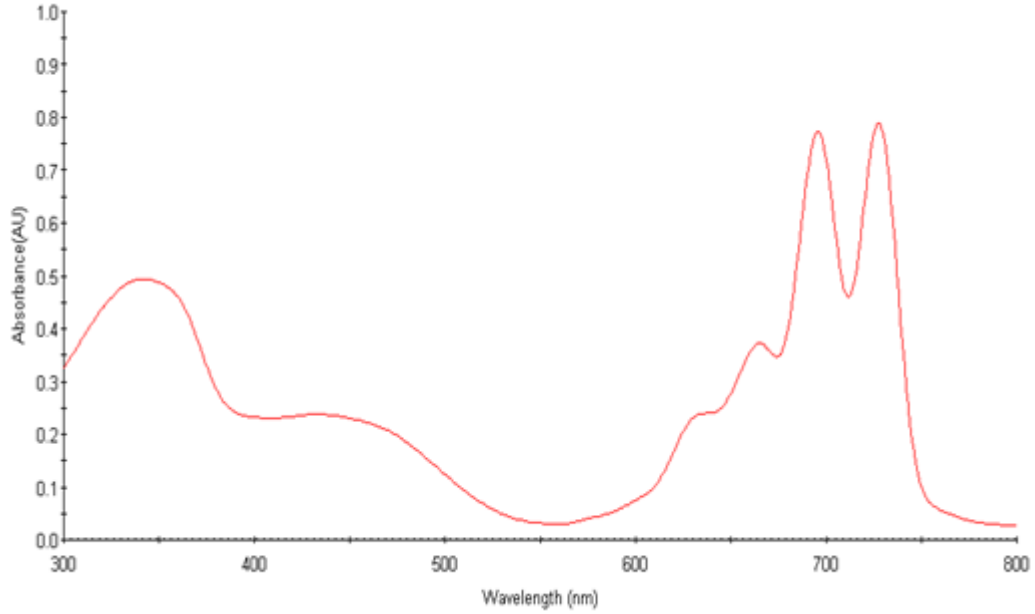

Figure A.15 : UV-vis spectrum of 2,3,9,10,16,17-hexakis(hexylthio)-23-hydroxyethylthiophthalocyanine (**7**).

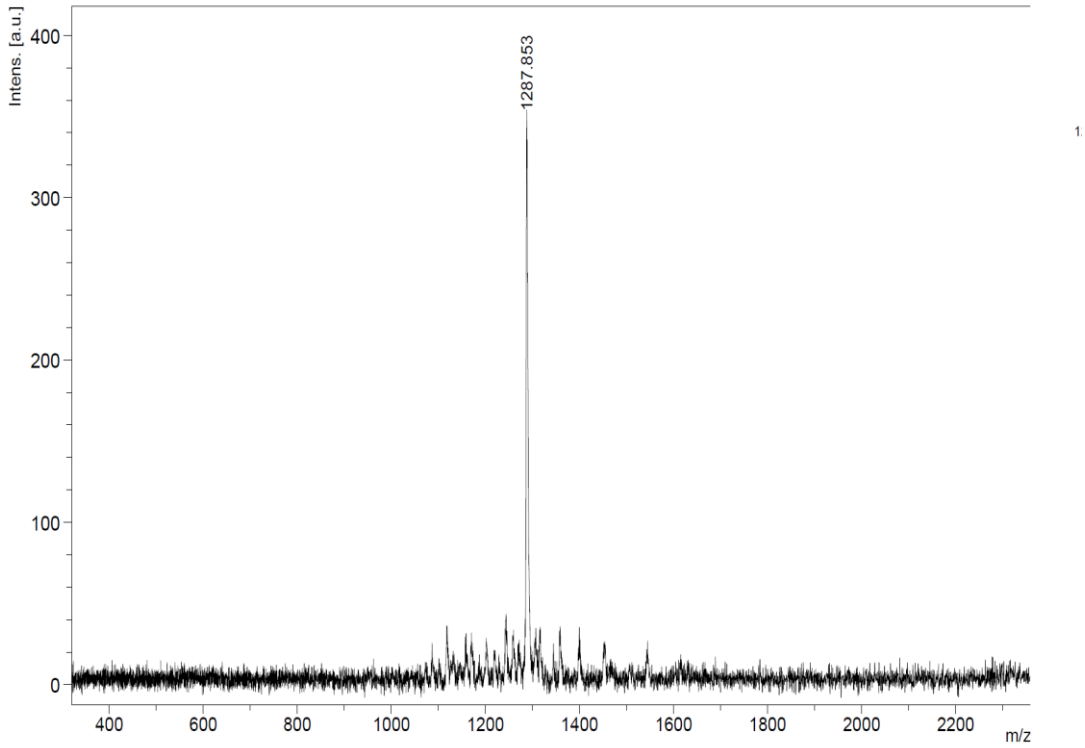

Figure A.16 : MALDI-TOF spectrum of 2,3,9,10,16,17-hexakis(hexylthio)-23-hydroxyethylthiophthalocyanine (**7**).

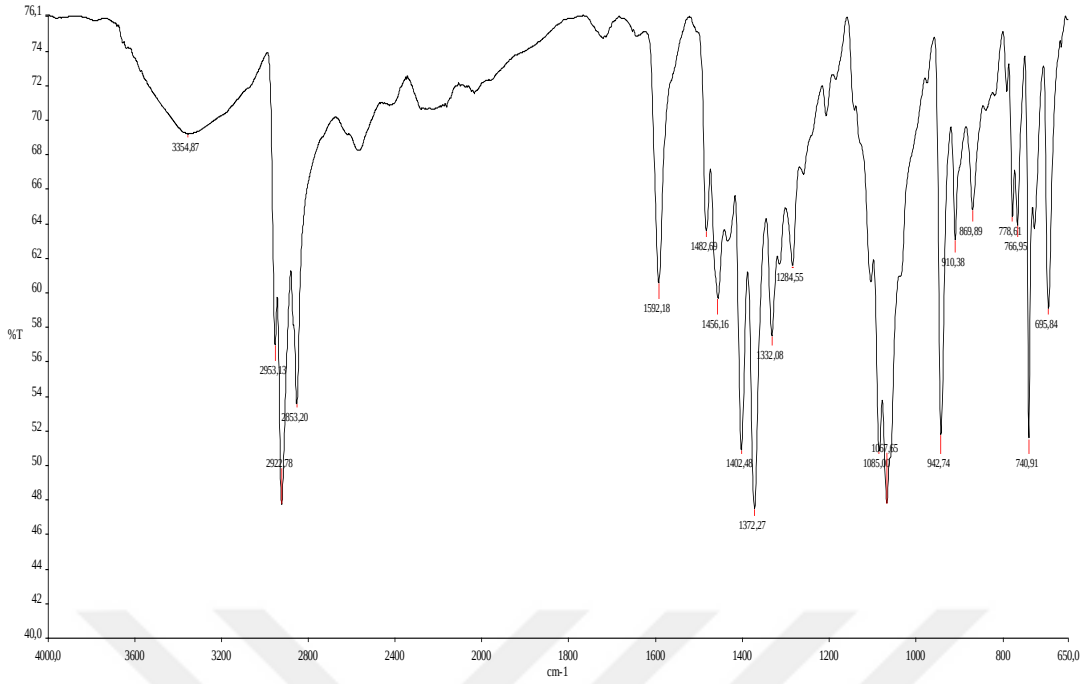

Figure A.17 : FT-IR spectrum of [2,3,9,10,16,17-hexakis(hexylthio)-23-hydroxyethylthiophthalocyaninato] zinc(II) (**8**).

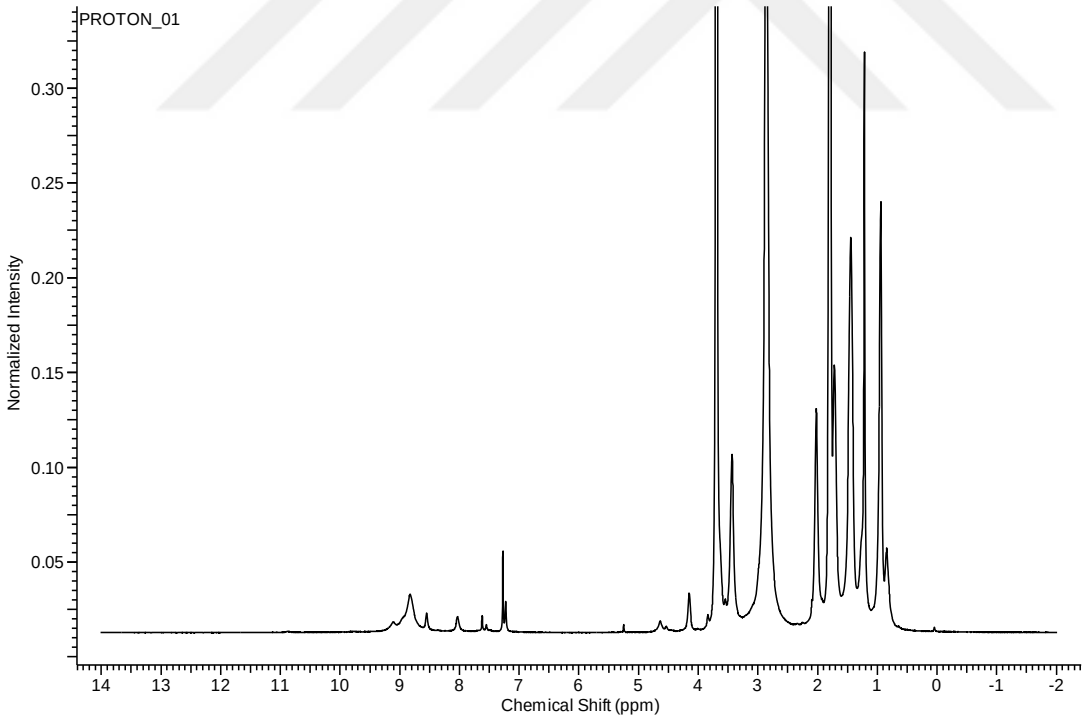

Figure A.18 : ^{1}H NMR spectrum of [2,3,9,10,16,17-hexakis(hexylthio)-23-hydroxyethylthiophthalocyaninato] zinc(II) (**8**).

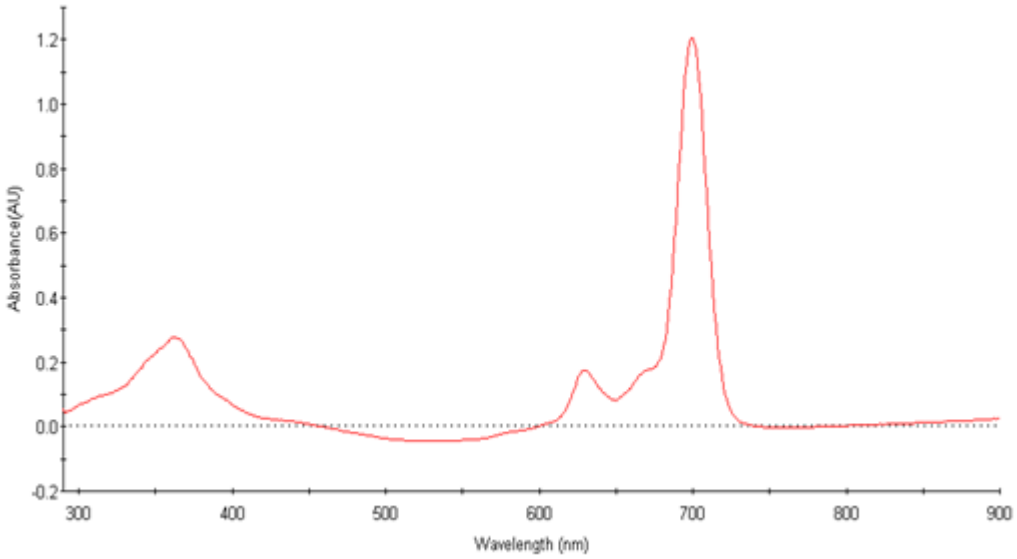

Figure A.19 : UV-vis spectrum of [2,3,9,10,16,17-hexakis(hexylthio)-23-hydroxyethylthiophthalocyaninato] zinc(II) (**8**).

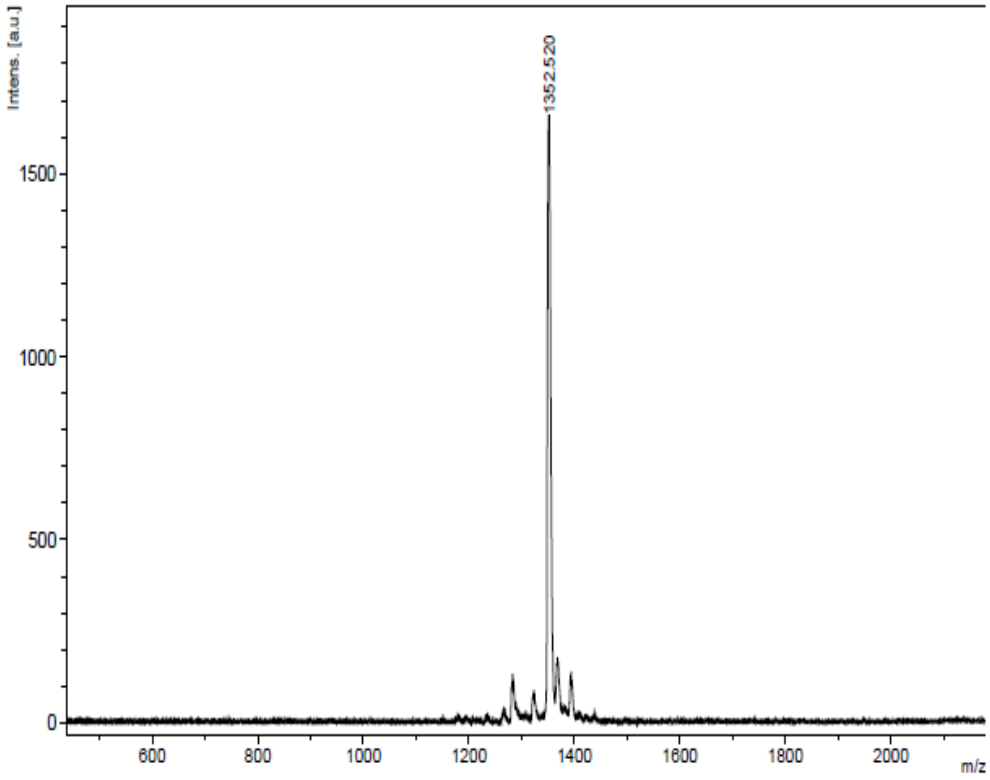

Figure A.20 : MALDI-TOF spectrum of [2,3,9,10,16,17-hexakis(hexylthio)-23-hydroxyethylthiophthalocyaninato] zinc(II) (**8**).

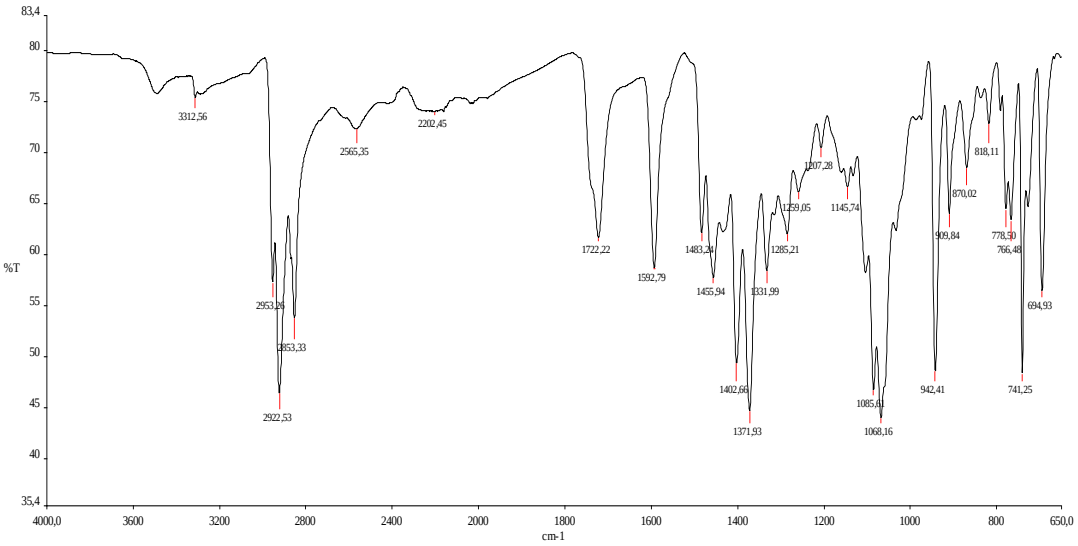

Figure A.21 : FT-IR spectrum of [2,3,9,10,16,17-hexakis(hexylthio)-23-1-pentynyloxyethylthiophthalocyaninato] zinc(II) (**9**).

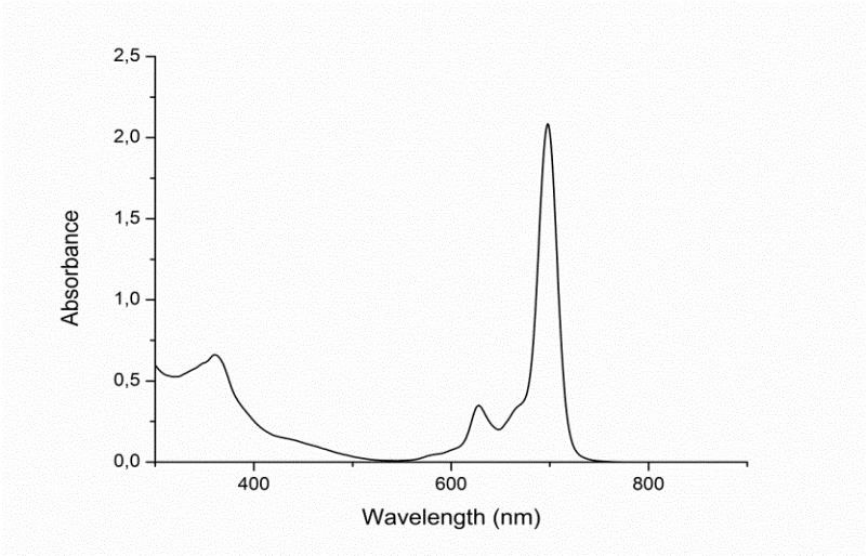

Figure A.22 : UV-vis spectrum of [2,3,9,10,16,17-hexakis(hexylthio)-23-1-pentynyloxyethylthiophthalocyaninato] zinc(II) (**9**).

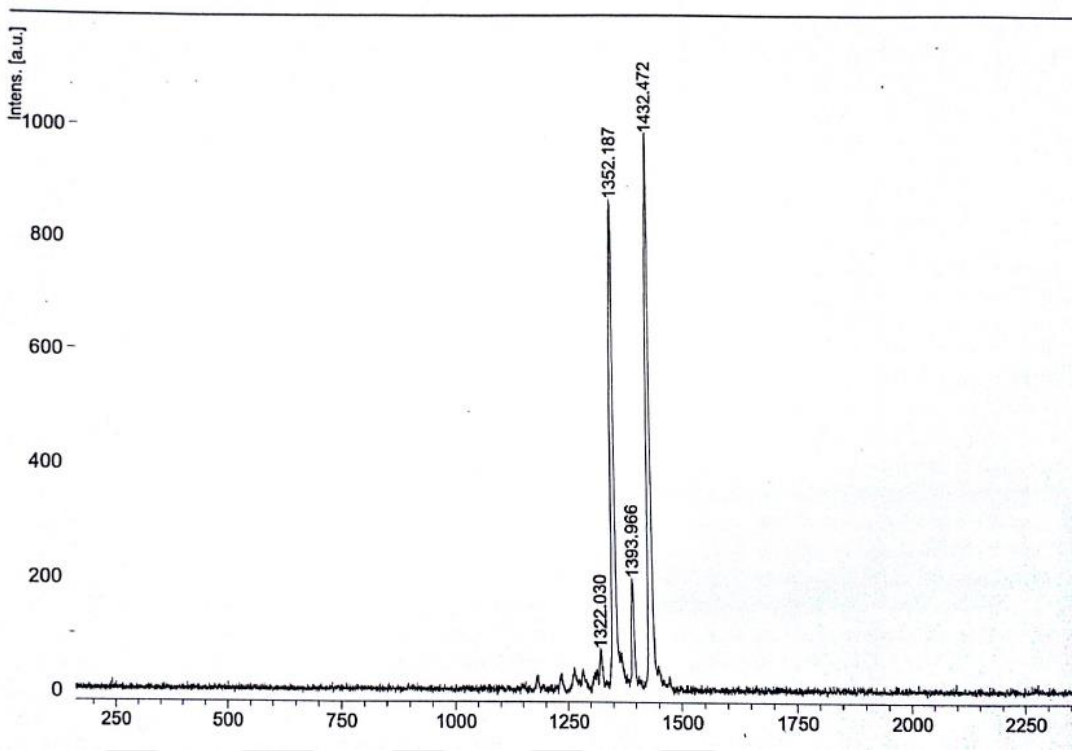

Figure A.23 : MALDI-TOF spectrum of [2,3,9,10,16,17-hexakis(hexylthio)-23-1-pentynyloxyethylthio phthalocyaninato] zinc(II) (**9**).

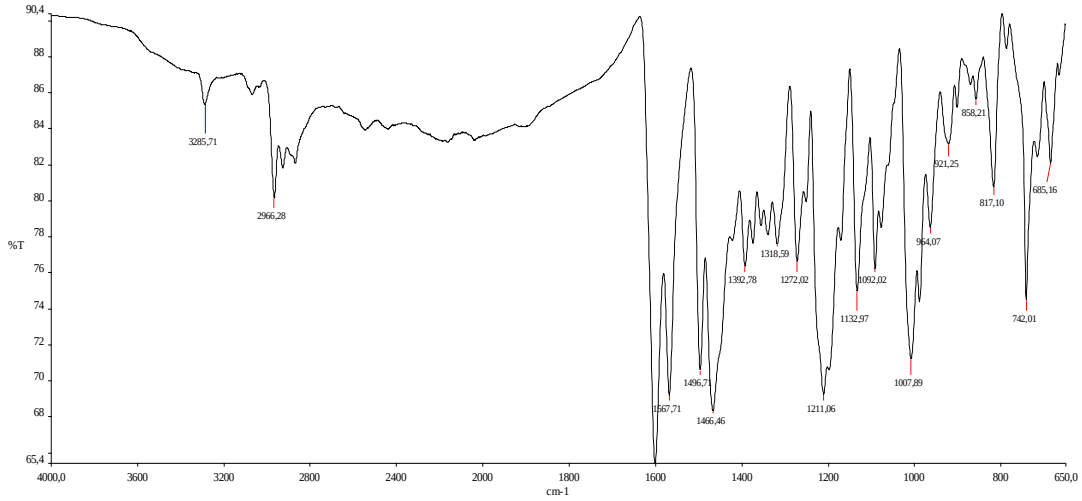

Figure A.24 : FT-IR spectrum of tris-9(10),16(17),23(24)[3-(diethylamino)phenoxy]-2-hydroxyethylthio phthalocyanine (**10**).

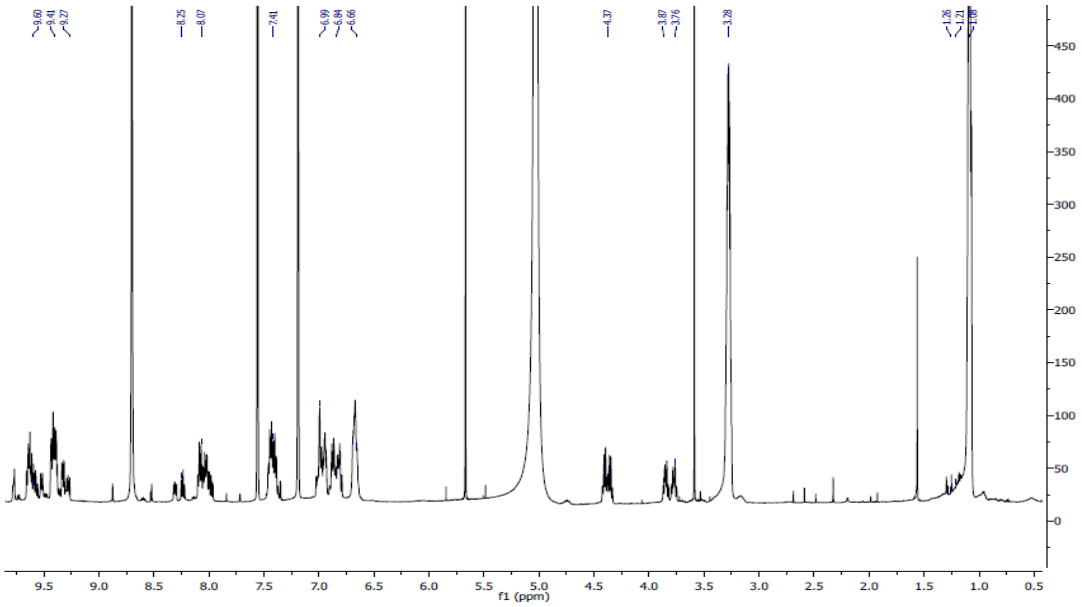

Figure A.25 : ^{1}H NMR spectrum of tris-9(10),16(17),23(24)[3-(diethylamino)phenoxy]-2-hydroxyethylthio phthalocyanine (**10**).

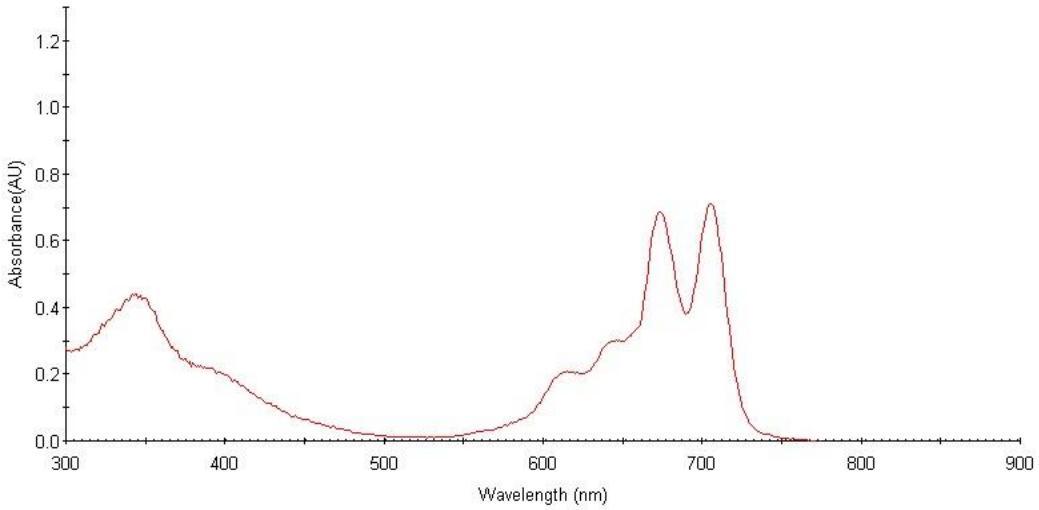

Figure A.26 : UV-vis spectrum of tris-9(10),16(17),23(24)[3-(diethylamino)phenoxy]-2-hydroxyethylthio phthalocyanine (**10**).

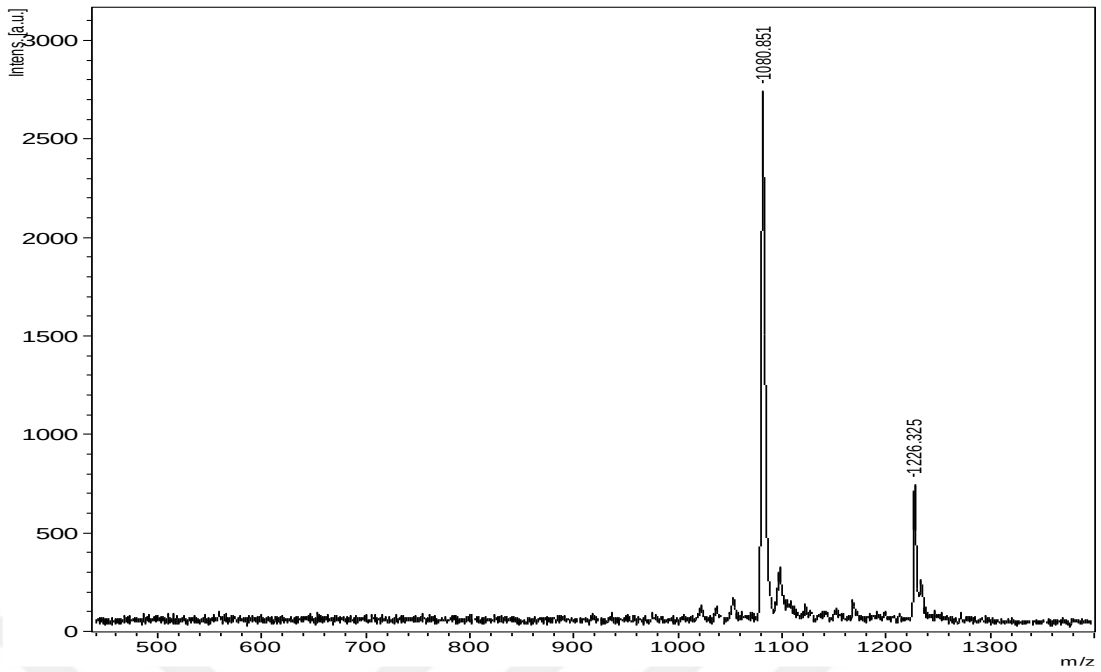

Figure A.27 : MALDI-TOF spectrum of tris-9(10),16(17),23(24)[3-(diethylamino)phenoxy]-2-hydroxyethylthiophthalocyanine (**10**).

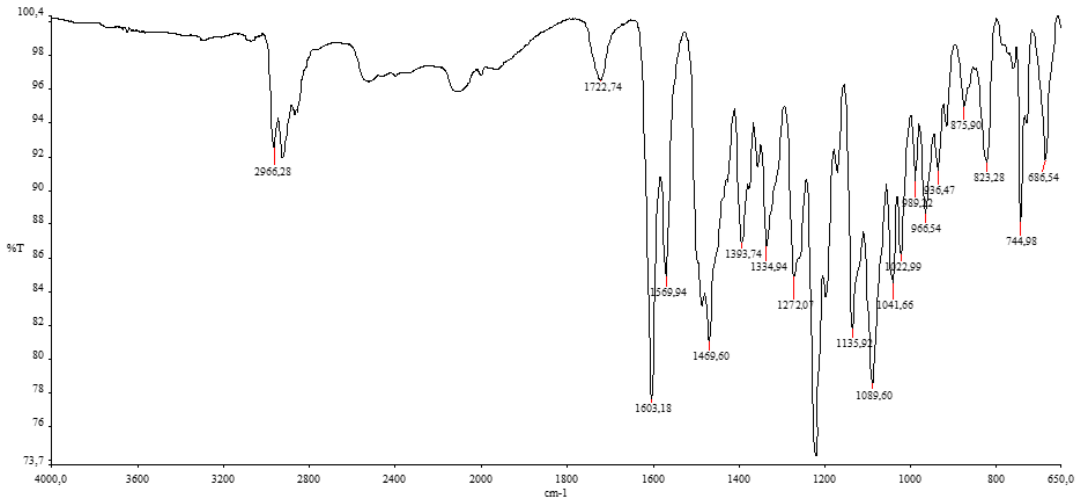

Figure A.28 : FT-IR spectrum of {tris-9(10),16(17),23(24)[3-(diethylamino)phenoxy]-2-hydroxyethylthio phthalocyaninato} zinc (II) (**11**).

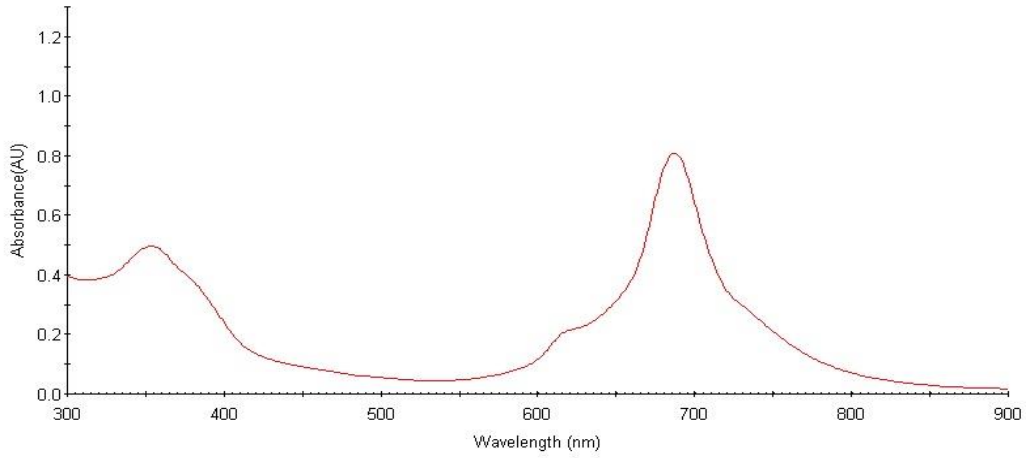

Figure A.29 : UV-vis spectrum of {tris-9(10),16(17),23(24)[3-(diethylamino)phenoxy]-2-hydroxyethylthio phthalocyaninato} zinc (II) (**11**).

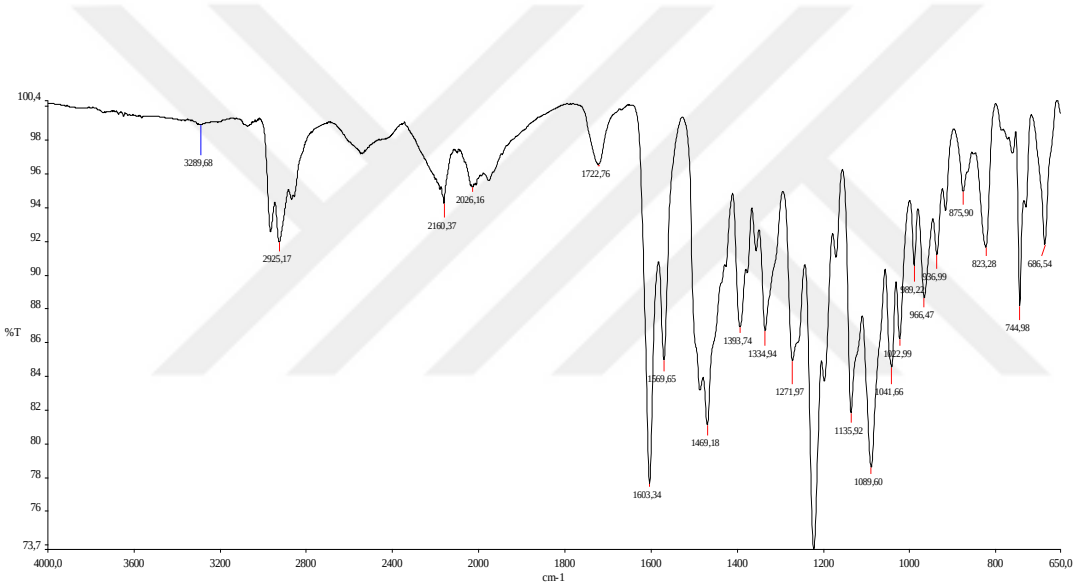

Figure A.30 : FT-IR spectrum of {tris-9(10),16(17),23(24)[3-(diethylamino)phenoxy]-2-1-propynloxyethylthio phthalocyaninato} zinc(II) (**12**).

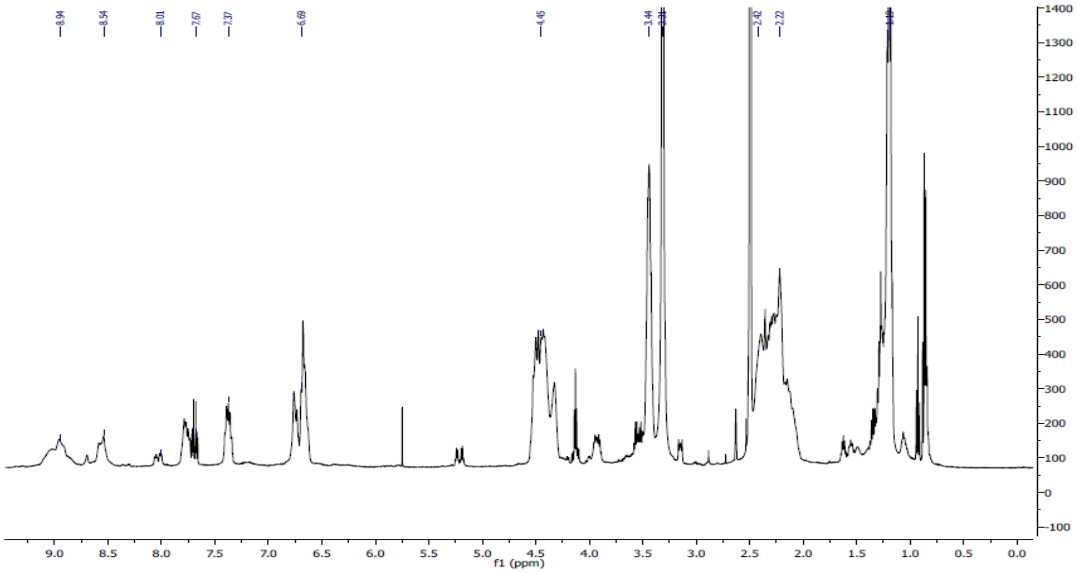

Figure A.31 : ^{1}H NMR spectrum of {tris-9(10),16(17),23(24)[3-(diethylamino)phenoxy]-2-1-propynloxyethylthio phthalocyaninato} zinc(II) (**12**).

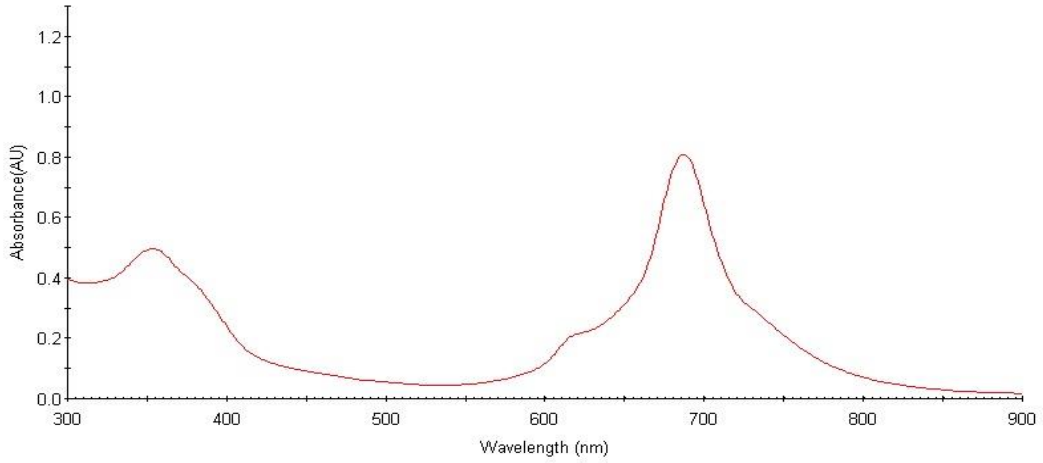

Figure A.32 : UV-vis spectrum of {tris-9(10),16(17),23(24)[3-(diethylamino)phenoxy]-2-1-propynloxyethylthio phthalocyaninato} zinc(II) (**12**).

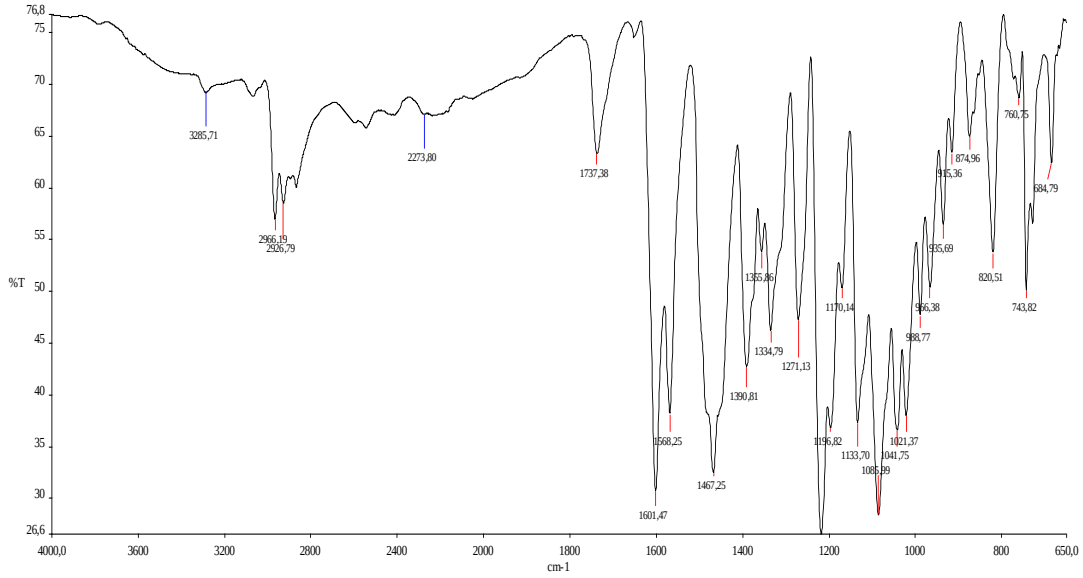

Figure A.33 : FT-IR spectrum of {tris-9(10),16(17),23(24)[3-(diethylamino)phenoxy]-2-1- pentynyloxyethylthio phthalocyaninato} zinc(II) (**13**).

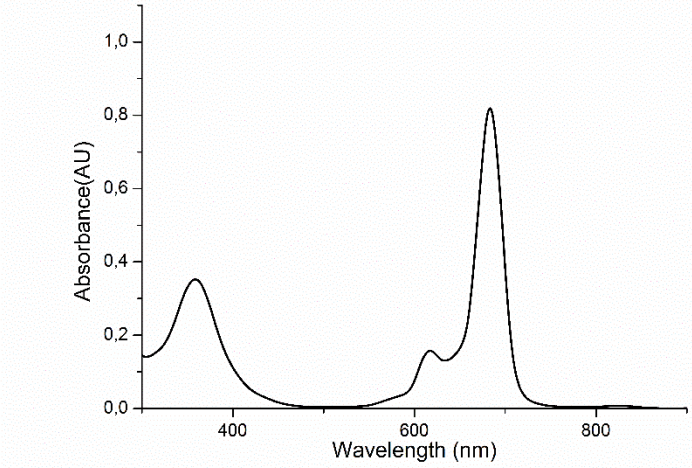

Figure A.34 : UV-vis spectrum of {tris-9(10),16(17),23(24)[3-(diethylamino)phenoxy]-2-1- pentynyloxyethylthio phthalocyaninato} zinc(II) (**13**).

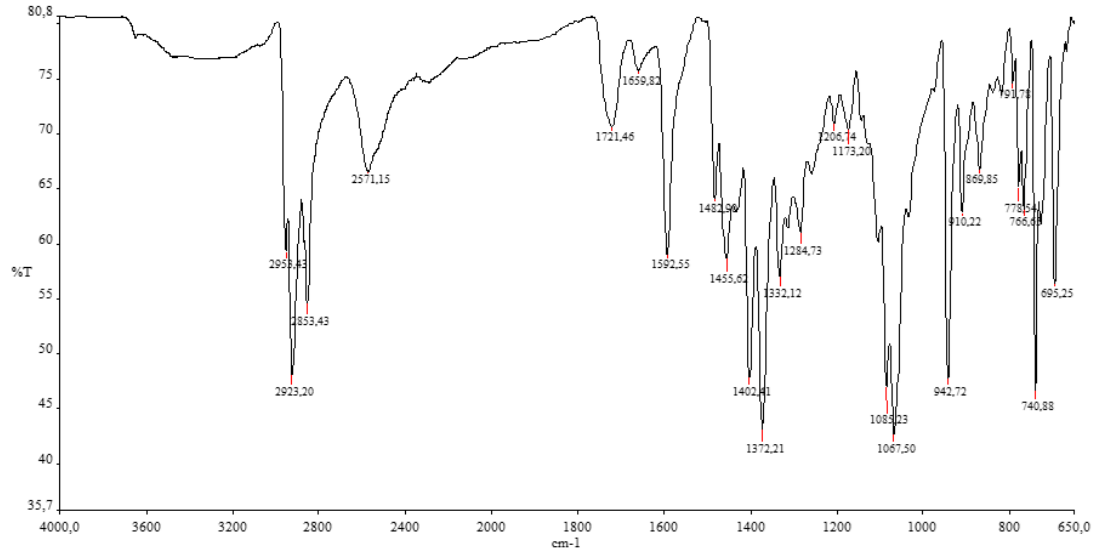

Figure A.35 : FT-IR spectrum of [2,3,9,10,16,17-Hexakis(hexylthio)-23-1-(o-carboranyl) propanoxyethylthio phthalocyaninato] (**14**).

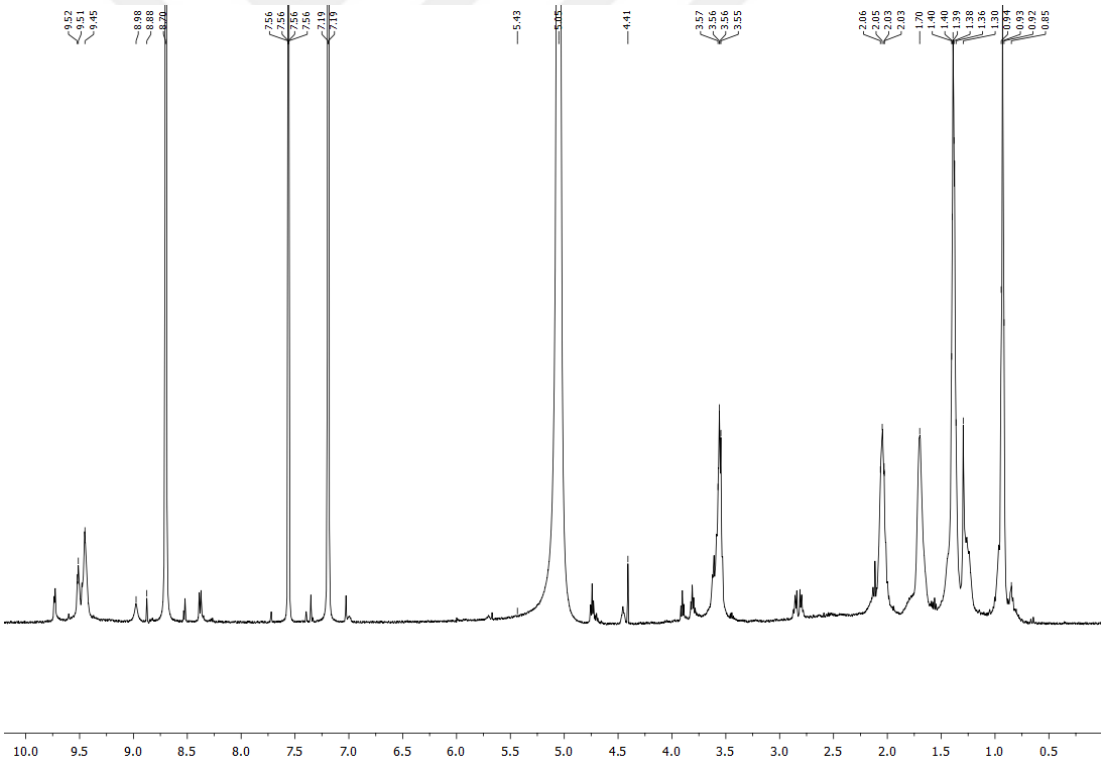

Figure A.36 : ^{1}H NMR spectrum of [2,3,9,10,16,17-Hexakis(hexylthio)-23-1-(o-carboranyl) propanoxyethylthio phthalocyaninato] (**14**).

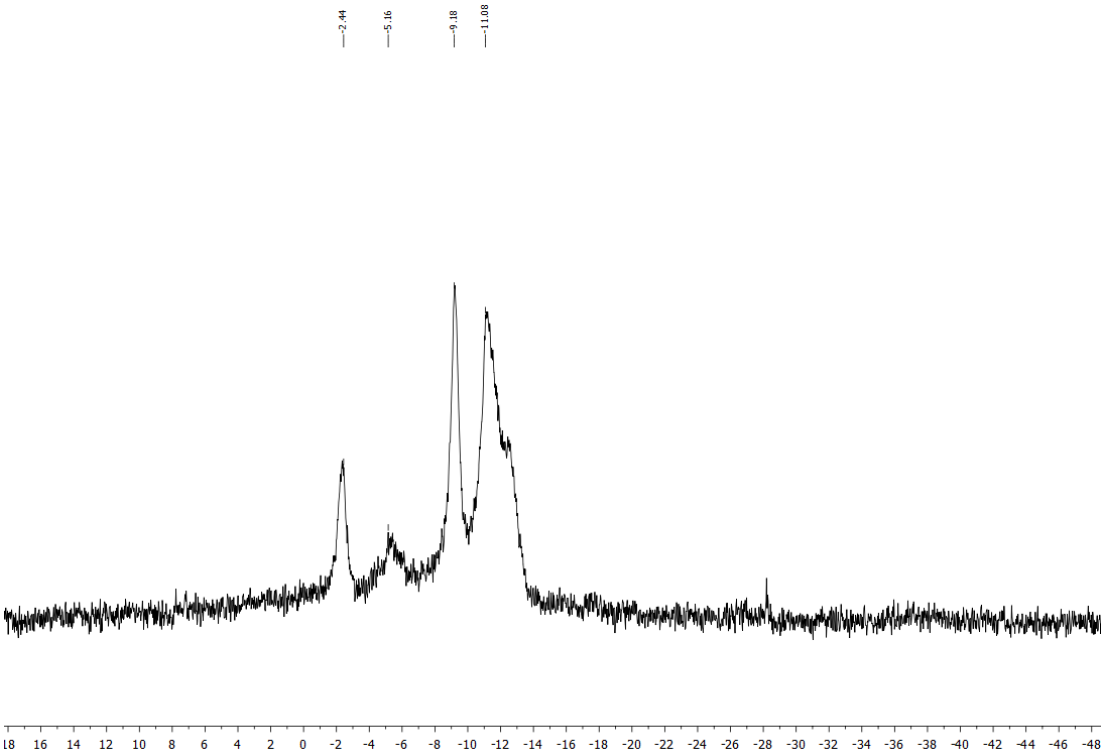

Figure A.37 : ^{11}B NMR spectrum of [2,3,9,10,16,17-Hexakis(hexylthio)-23-1-(o-carboranyl) propanoxyethylthio phthalocyaninato] (**14**).

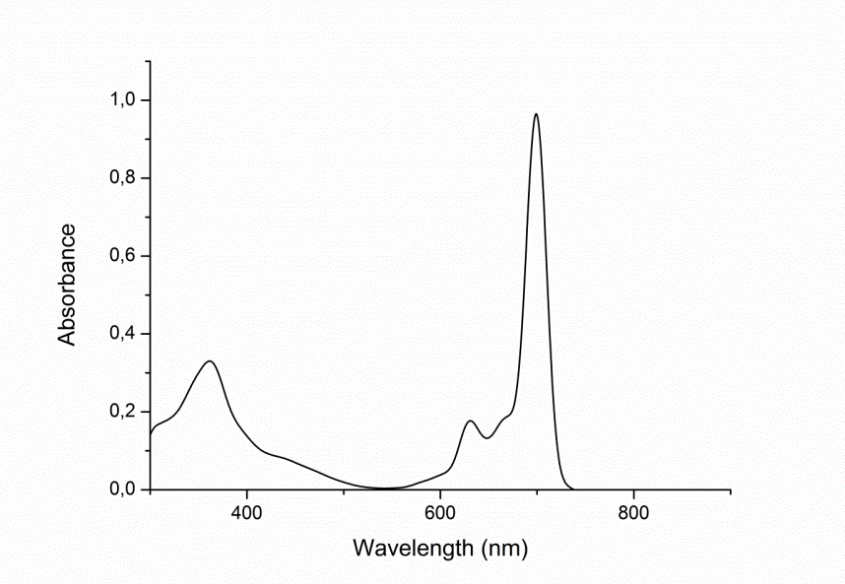

Figure A.38 : UV-vis spectrum of [2,3,9,10,16,17-Hexakis(hexylthio)-23-1-(o-carboranyl) propanoxyethylthio phthalocyaninato] (**14**).

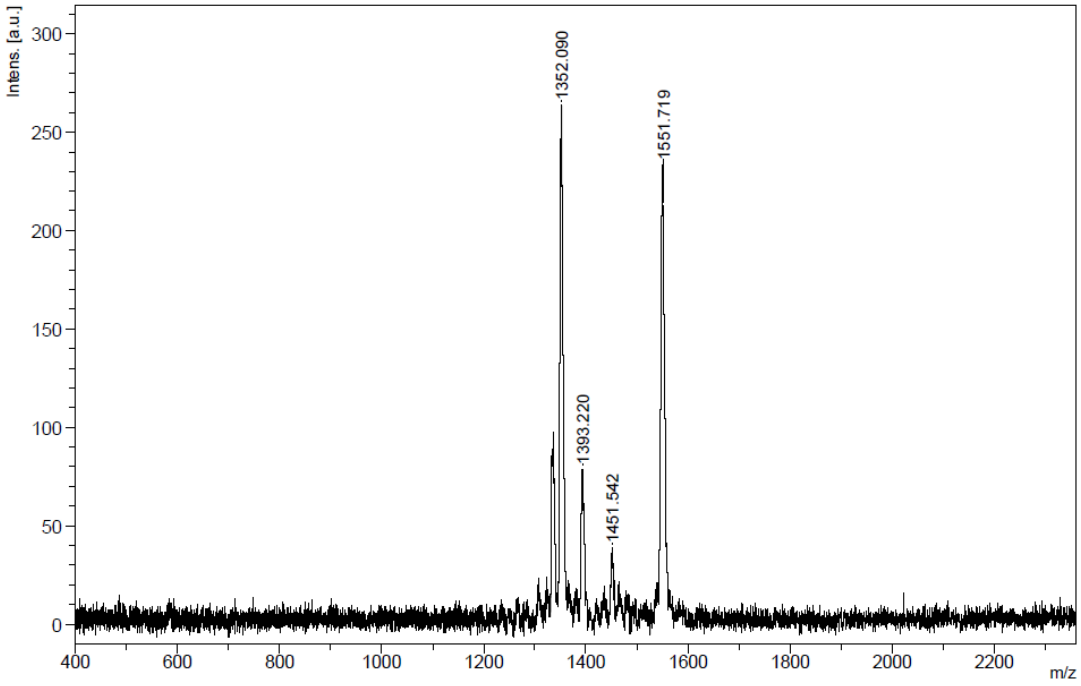

Figure A.39 : MALDI-TOF spectrum of [2,3,9,10,16,17-Hexakis(hexylthio)-23-1-(o-carboranyl) propanoxyethylthio phthalocyaninato] (**14**).

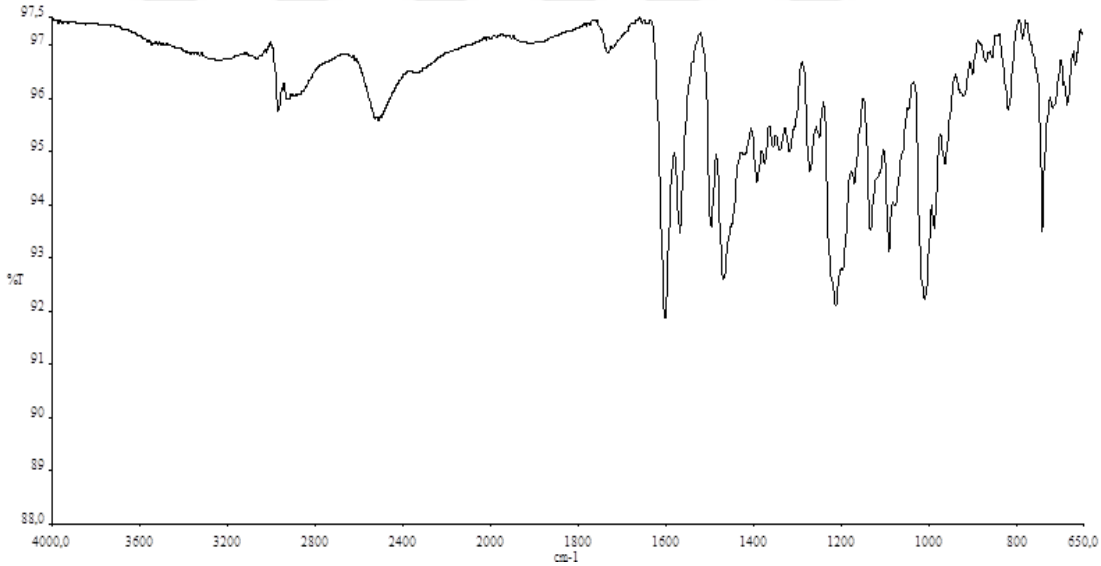

Figure A.40 : FT-IR spectrum of {tris-9(10),16(17),23(24)[3-(diethylamino)phenoxy]-2-1-(o-carboranyl) propanoxyethylthio phthalocyaninato} zinc(II) (**15**).

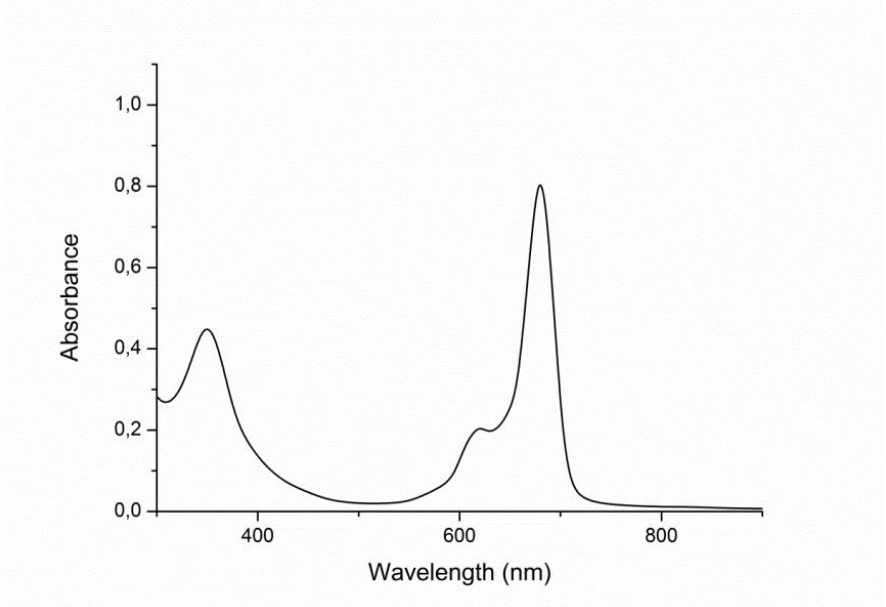

Figure A.41 : UV-vis spectrum of {tris-9(10),16(17),23(24)[3-(diethylamino)phenoxy]-2-1-(o-carboranyl) propanoxyethylthio phthalocyaninato} zinc(II) (**15**).

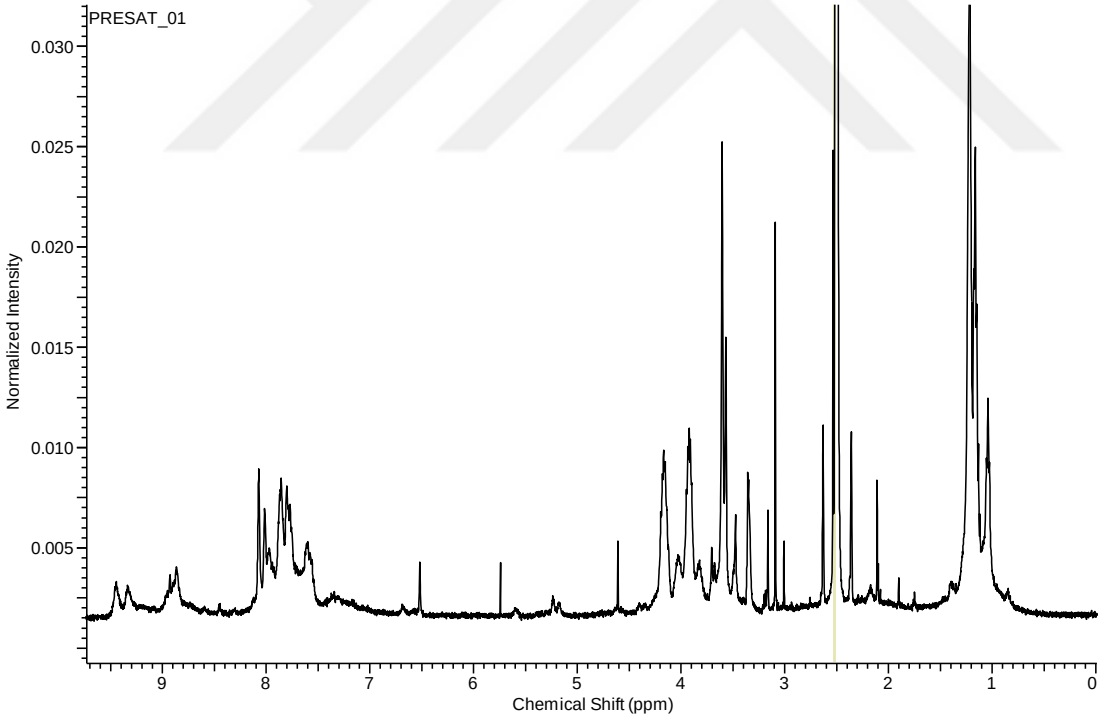

Figure A.42 : ^{1}H NMR spectrum of {tris-9(10),16(17),23(24)[3-(N, N, N diethylmethylammonium)phenoxy]-2-1-(o-carboranyl) propanoxyethylthio phthalocyaninato} zinc(II) triiodide (**16**).

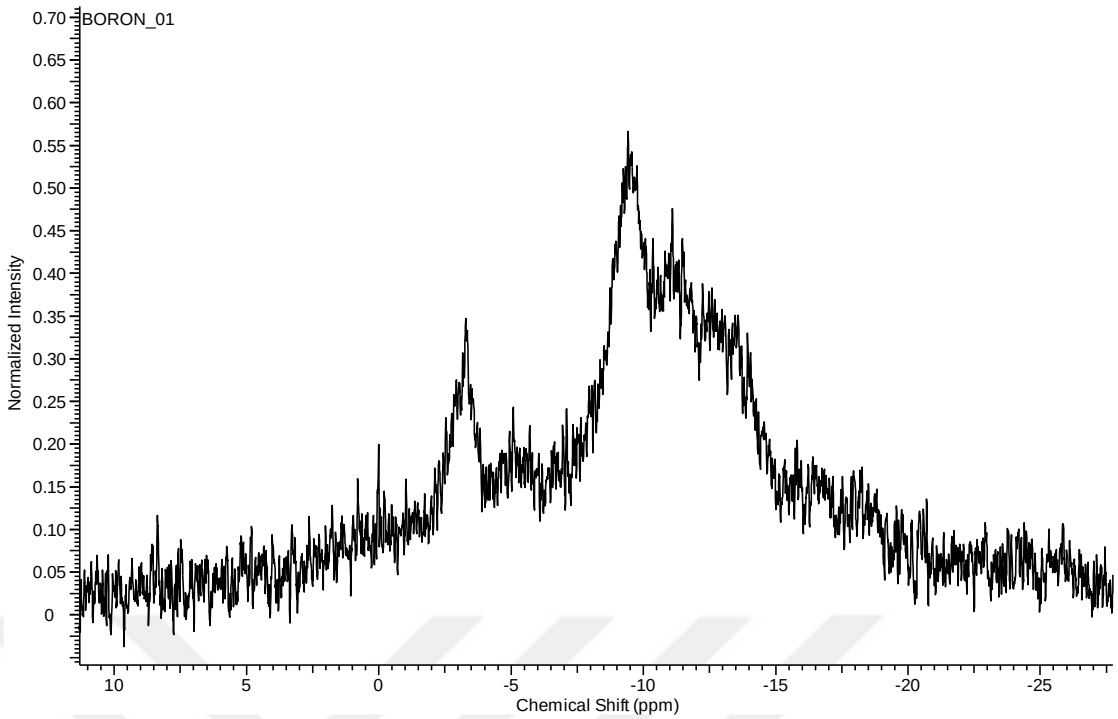

Figure A.43 : ^{11}B NMR spectrum of {tris-9(10),16(17),23(24)[3-(N, N, N diethylmethylammonium)phenoxy]-2-1-(o-carboranyl) propanoxyethylthio phthalocyaninato} zinc(II) triiodide (**16**).

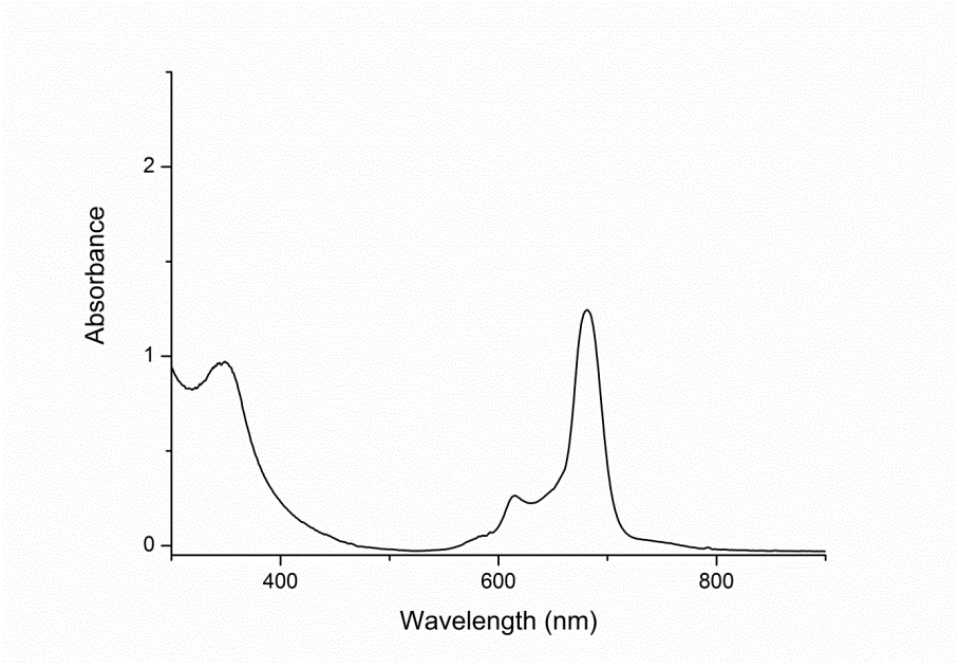

Figure A.44 : UV-vis spectrum of {tris-9(10),16(17),23(24)[3-(N, N, N diethylmethylammonium)phenoxy]-2-1-(o-carboranyl) propanoxyethylthio phthalocyaninato} zinc(II) triiodide (**16**).

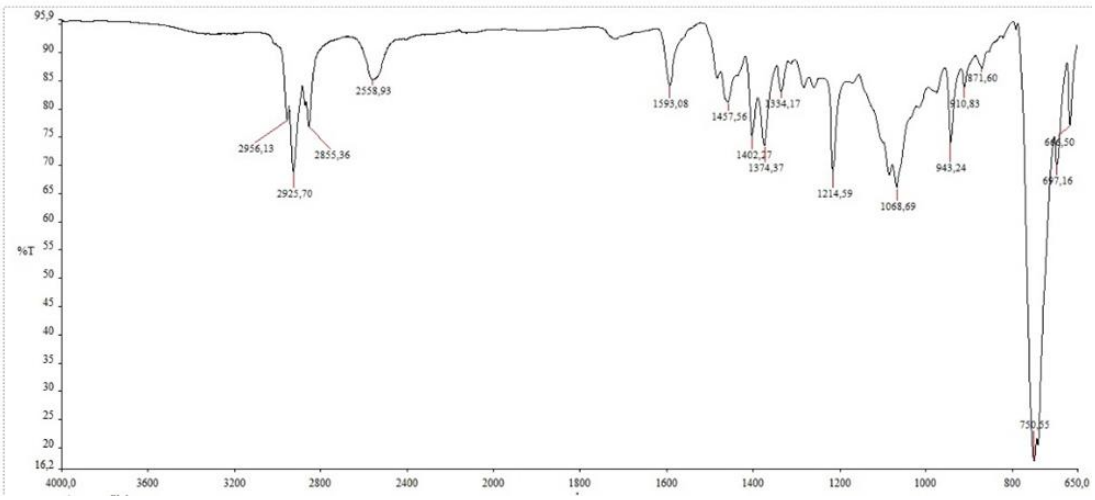

Figure A.45 : FT-IR spectrum of phthalocyanine (**17**).

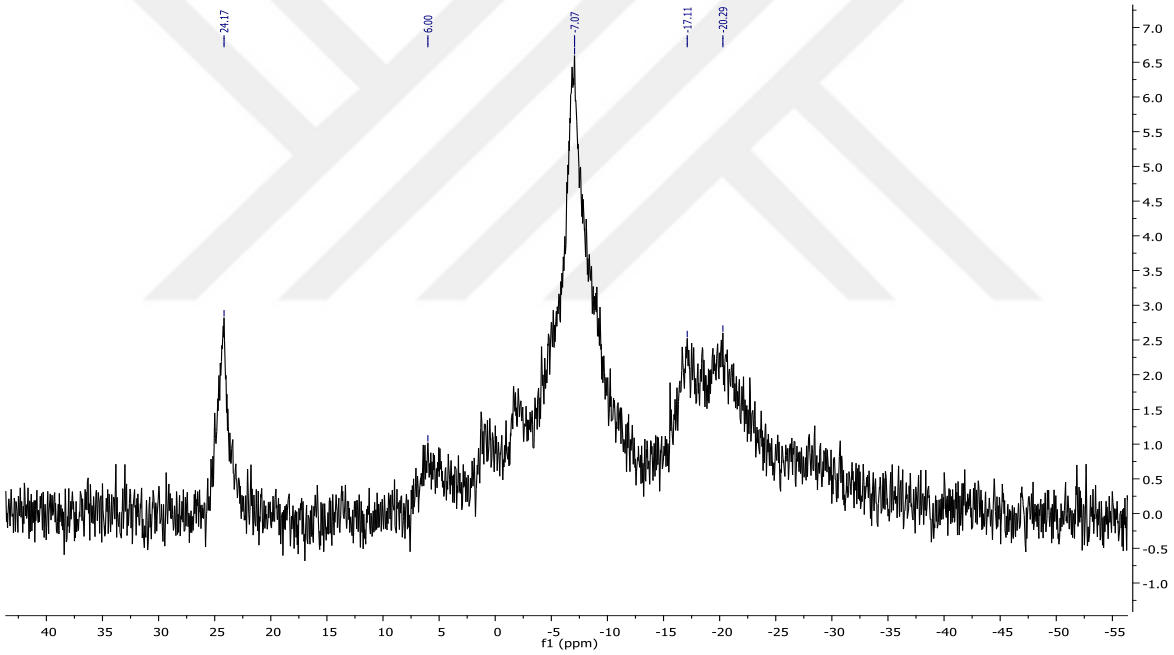

Figure A.46 : ^{11}B NMR spectrum of phthalocyanine (**17**).

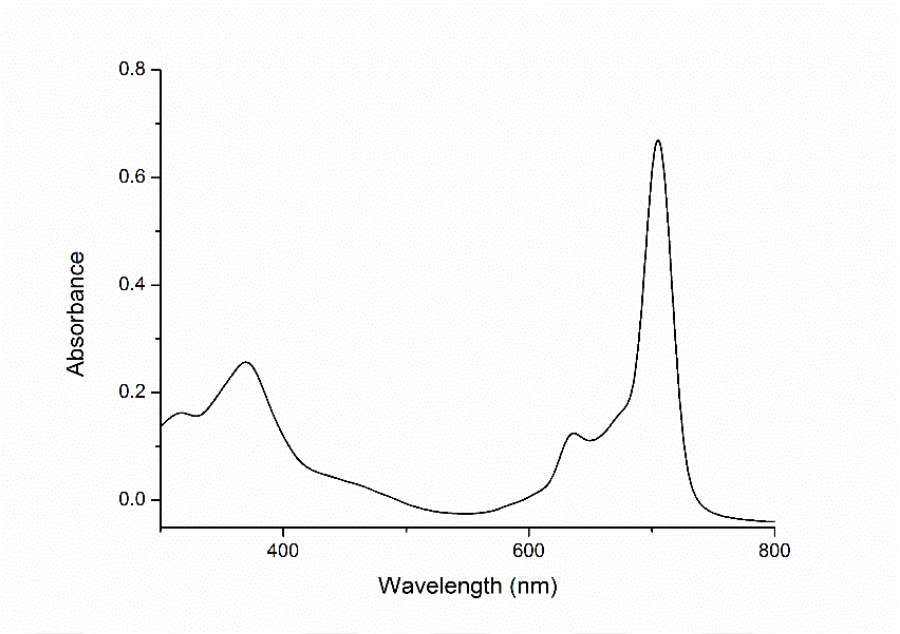

Figure A.47 : UV-vis spectrum of phthalocyanine (**17**).

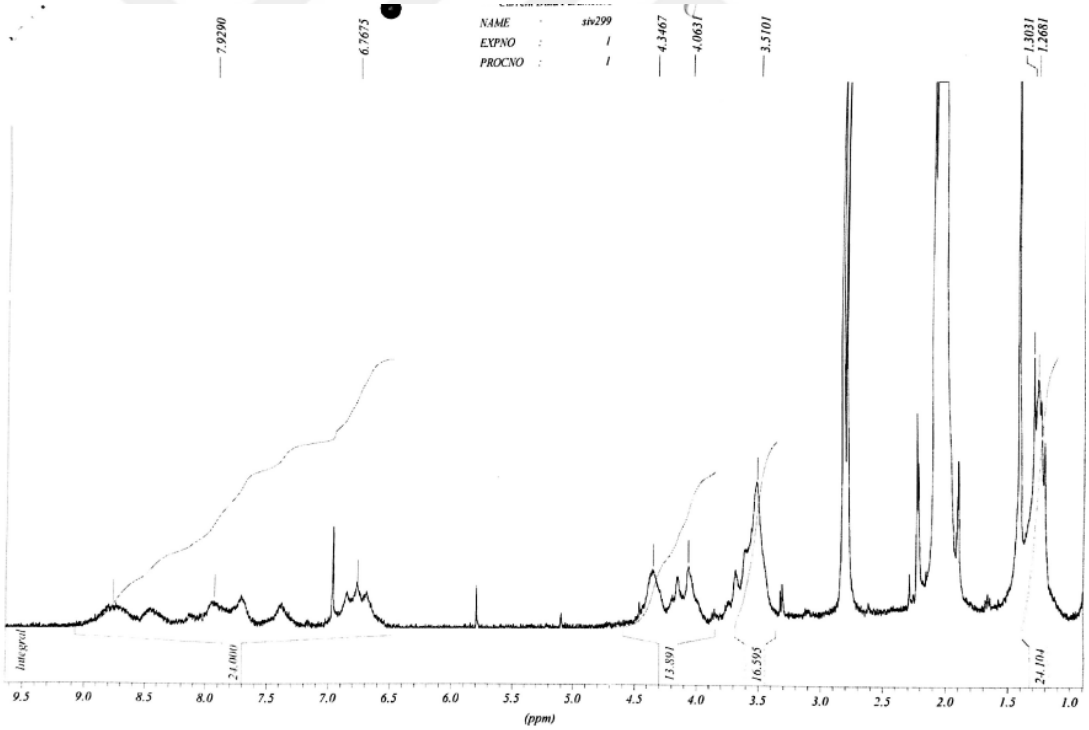

Figure A.48 : ^{1}H NMR spectrum of phthalocyanine (**18**).

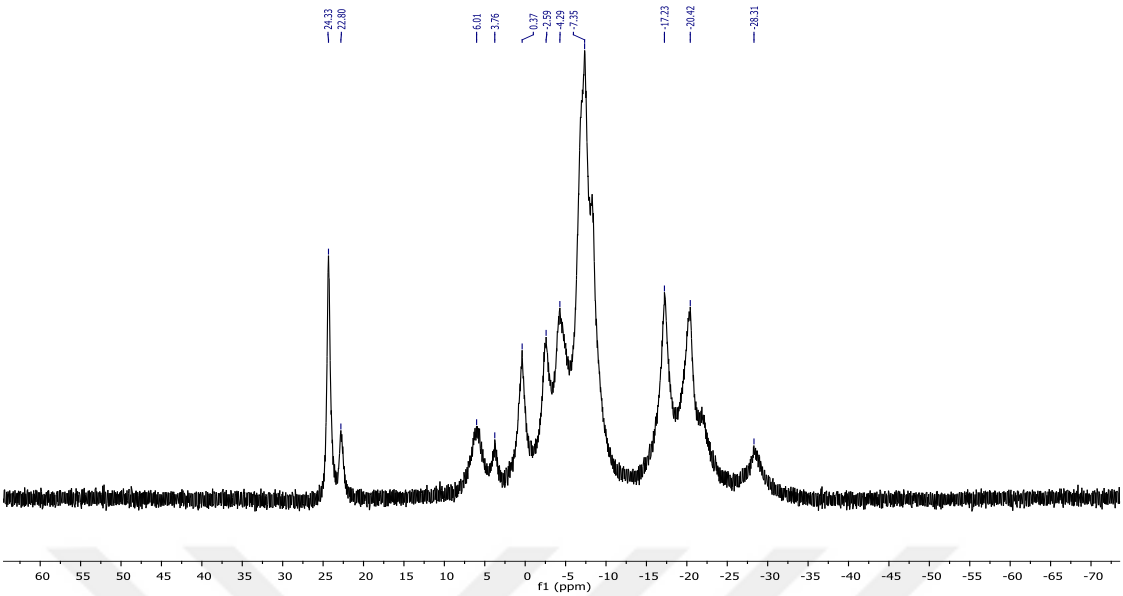

Figure A.49 : ^{11}B NMR spectrum of phthalocyanine (**18**).

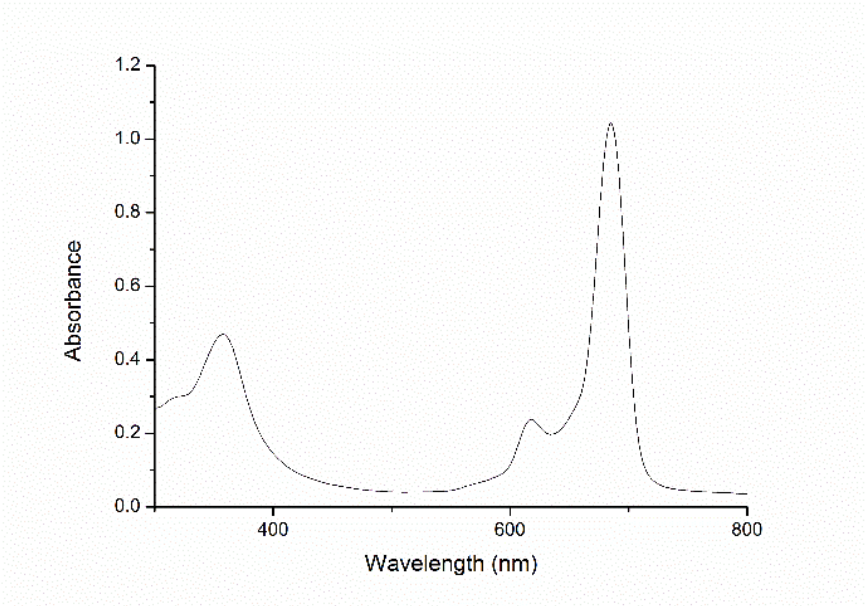

Figure A.50 : UV-vis spectrum of phthalocyanine (**18**).

CURRICULUM VITAE

Name Surname **:** Nilgün Özgür

EDUCATION **:**

- **B.Sc.** **:** 2011, ITU, Faculty of Science and Letters, Chemistry Department
- **M.Sc.** **:** 2012, ITU, Graduate School of Science, Engineering and Technology, Chemistry Department

PUBLICATIONS, PRESENTATIONS AND PATENTS ON THE THESIS:

- **Özgür, N.,** Nar, I., Gül, A. & Hamuryudan, E. 2015. A New Unsymmetrical Phthalocyanine With a Single *O*-Carborane Substituent, *Journal of Organometallic Chemistry*, 781, 53-58.
- **Özgür, N.,** Nar, I., and Hamuryudan, E. 2012: Synthesis of Hexythio and Hydroxyethylthio Substituted Unsymmetrical Phthalocyanines. International Congress - 7th Eurasian Meeting on Heterocyclic Chemistry, June 17-21, 2012 İstanbul, Turkey.
- **Özgür, N.,** Nar, I., and Hamuryudan, E. 2013: 3-(Diethylamino)phenoxy and Hydroxyethylthio Substituted Unsymmetrical Phthalocyanines. International Congress - 44th World Chemistry Congress, August 11-16, 2013 İstanbul, Turkey.
- **Özgür, N.,** Nar, I., and Hamuryudan, E. 2013: Novel o-Carborane Containing Unsymmetrical Phthalocyanine. International Congress - 44th World Chemistry Congress, August 11-16, 2013 İstanbul, Turkey.
- **Özgür, N.,** Nar, I., and Hamuryudan, E. 2014: Synthesis of Zn (II) Phthalocyanines Carrying Carboranyl Units as Promising BNCT Agents. International Congress - ICCP-8 International Conference on Porphyrins and Phthalocyanines, June 22-27, 2014 İstanbul, Turkey.
- Nar, I., **Özgür, N.,** and Hamuryudan, E. 2013: Synthesis and Characterization of Unsymmetrical Alkyne Functional Phthalocyanines. International Congress - 14th European Symposium on Organic Reactivity, September 01-06, 2013 Prag, Czech Republic.
- Nar, I., **Özgür, N.,** and Hamuryudan, E. 2014: Novel Carborane Functionalized Phthalocyanines. International Congress - ICCP-8 International Conference on Porphyrins and Phthalocyanines, June 22-27, 2014 İstanbul, Turkey.